Associazione MQC2
Istituto Italiano per gli Studi Filosofici

7-10 June, 2004

Palazzo Serra di Cassano - Via Monte di Dio 14, Napoli - Italy

con il patrocinio della Regione Campania

Macroscopic Quantum Coherence and Computing

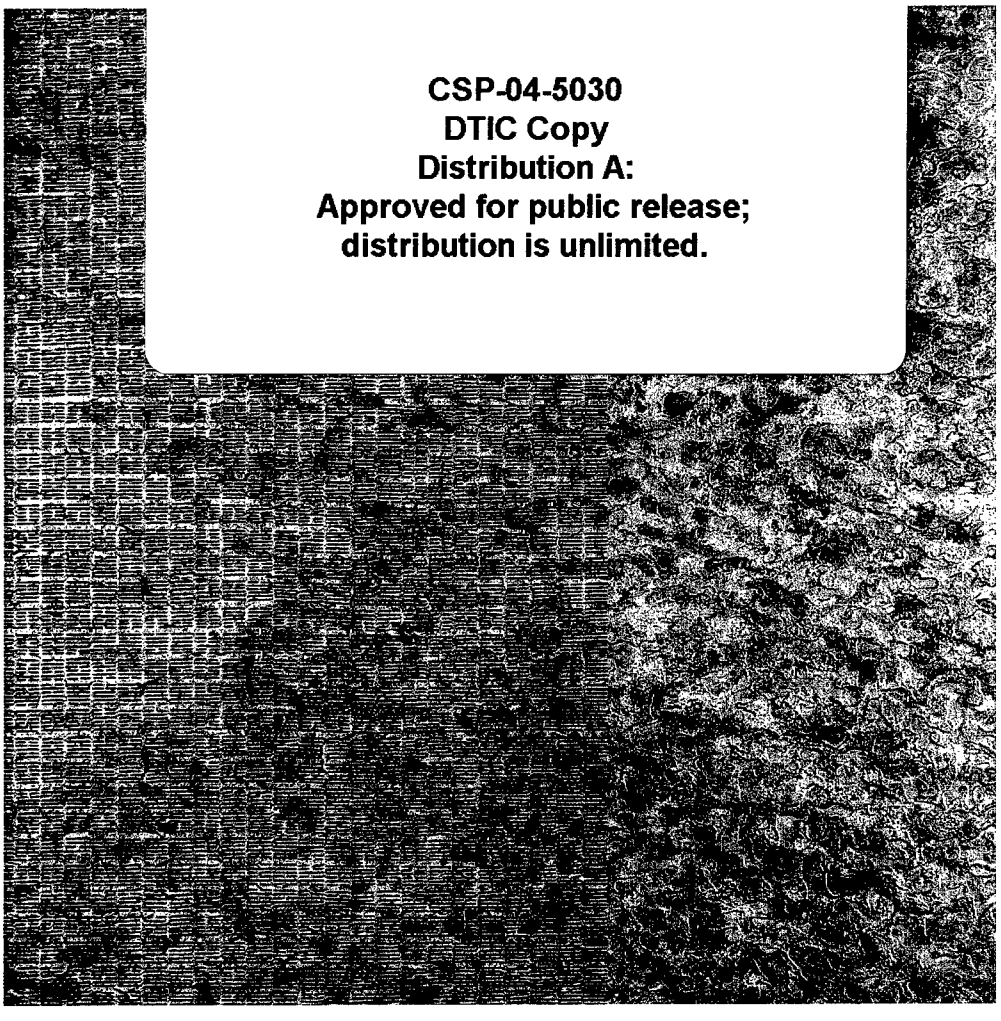

p. silvestrini: *la scala di torregaveta, 1994*

ABSTRACT BOOKLET

Istituto di Cibernetica "E. Caianiello", CNR
Seconda Università di Napoli

Asssociazione MQC2
Istituto Italiano per gli Studi Filosofici
Società Italiana Fisica

con il patrocinio della Regione Campania

IV INTERNATIONAL WORKSHOP ON

"Macroscopic Quantum Coherence and Computing"

MQC^2

Istituto Italiano per gli Studi Filosofici, Via Monte di Dio, 14 Napoli, Italy, 7-10 June, 2004

Chairman

P. Silvestrini *Seconda Università di Napoli, Italy*

Steering Committee:

P. Delsing *Chalmers University of Technology, Sweden*
C. Granata *Istituto di Cibernetica "E. Caianiello" CNR Italy*
Yu. Pashkin *RIKEN/NEC, Tsukuba, Japan*
B. Ruggiero *Istituto di Cibernetica "E. Caianiello" CNR, Italy*

Advisory Board:

M. Cirillo, Università di Roma "Tor Vergata", Italy
J. Clarke, Berkely University, USA
S. De Franceschi, Delft University of Technology, The Netherlands
D. Esteve, CEA-Saclay, France
A. J. Leggett, University of Illinois at Urbana-Champaign, USA
J. Lukens, SUNY at Stony Brook, NY-USA
Y. Ovchinnikov, Landau Institute Moskow, Russia
P. Sodano, Università di Perugia, Italy
L. Stodolsky, Max Planck Institute, Munich, Germany
J. S. Tsai, NEC/RIKEN, Tsukuba, Japan

REPORT DOCUMENTATION PAGE

Form Approved OMB No. 0704-0188

1. REPORT DATE *(DD-MM-YYYY)*	2. REPORT TYPE	3. DATES COVERED *(From – To)*
08-02-2005	Conference Proceedings	7 June 2004 - 10 June 2004

4. TITLE AND SUBTITLE

Macroscopic Quantum Coherence and Computing

5a. CONTRACT NUMBER
FA8655-04-1-5030

5b. GRANT NUMBER

5c. PROGRAM ELEMENT NUMBER

6. AUTHOR(S)

Conference Committee

5d. PROJECT NUMBER

5d. TASK NUMBER

5e. WORK UNIT NUMBER

7. PERFORMING ORGANIZATION NAME(S) AND ADDRESS(ES)

MQC2 - Associazione Macroscopic Quantum Coherence and Computing
Superconductivity Dept.
Via Campi Flegrei 34
Pozzuoli, Naples 80078-I
Italy

8. PERFORMING ORGANIZATION REPORT NUMBER

N/A

9. SPONSORING/MONITORING AGENCY NAME(S) AND ADDRESS(ES)

EOARD
PSC 802 BOX 14
FPO 09499-0014

10. SPONSOR/MONITOR'S ACRONYM(S)

11. SPONSOR/MONITOR'S REPORT NUMBER(S)
CSP 04-5030

12. DISTRIBUTION/AVAILABILITY STATEMENT

Approved for public release; distribution is unlimited.

13. SUPPLEMENTARY NOTES

14. ABSTRACT

The Final Proceedings for Macroscopic Quantum Coherence and Computing, 7 June 2004 - 10 June 2004

Quantum computing. Quantum phenomena in superconducting devices: phase-space and charge-space Nanodevices Dissipation and Decoherence in mesoscopic systems Macroscopic quantum coherence in physical systems, including: NMR, Nuclear Magnetic Resonance Quantum dots Ions Magnetic systems BEC, Bose Einstein Condensation

15. SUBJECT TERMS

EOARD, Quantum Computing, Superconductivity

16. SECURITY CLASSIFICATION OF:			17. LIMITATION OF ABSTRACT	18, NUMBER OF PAGES	19a. NAME OF RESPONSIBLE PERSON
a. REPORT	b. ABSTRACT	c. THIS PAGE			MICHAEL KJ MILLIGAN, Lt Col, USAF
UNCLAS	UNCLAS	UNCLAS	UL	97	19b. TELEPHONE NUMBER *(Include area code)* +44 (0)20 7514 4955

Aim of workshop

The aim of the workshop is to report on the recent theoretical and experimental results on the macroscopic quantum coherence of mesoscopic systems, as well as on solid state realization of qubits and quantum gates. Particular attention will be given to coherence effects in Josephson devices. Other physical systems, including quantum dots, optical, atomic, and molecular devices, exhibiting macroscopic quantum coherence, will also be discussed

in collaboration with:

Seconda Università di Napoli SUN, Italy
Consiglio Nazionale delle Ricerche CNR, Italy
NEC/RIKEN, Tsukuba, Japan
Chalmers University of Technology, Sweden
Istituto Nazionale Fisica della Materia- INFM
Istituto Nazionale di Fisica Nucleare-INFN
Università di Roma Tor Vergata, Italy
Università di Perugia, Italy
Air Liquide - Italia

We wish to thank the "*European Office of Aerospace Research and Development, Air Force Office of Scientific Research, United States Air Force Research laboratory*" for the contribution to the success of this conference

Local Committee:

V. Corato
S. Rombetto
R. Russo

MQC group - Istituto di Cibernetica "E. Caianiello" del CNR, Pozzuoli, Italy
and Seconda Università di Napoli, Aversa, Italy

Workshop Secretariat:

Anna Maria Mozzarella Hillard — *Associazione MQC2, Pozzuoli,Naples, Italy*
Maria Cristina Nisco — *Associazione MQC2, Pozzuoli,Naples, Italy*

phone: (+39 081) 8675269-5442852
fax: (+39 081) 8675128-5262

e-mail: am.mazzarella@cib.na.cnr.it
annamariahilliard@libero.it

web: http://www.mqc2.it

Speakers list

K.Arutyunov	University of Jyvaskyla, Finland
A. Berkley	University of Maryland, USA
P. Bertet	Delft University of Technology, The Netherlands
S. Chung	Western Michigan University, USA
J. Clarke	University of California, USA
V.Corato	SUN and IC "E. Caianiello" CNR, Italy
C. Cosmelli	Università di Roma "La Sapienza", Italy
T. Duty	Chalmers University of Technology, Sweden
D. Esteve	CEA-Saclay, France
M. Everitt	University of Sussex, UK
G. Falci	Università di Catania, Italy
R. Fazio	Scuola Normale Superiore, Italy
T. Fujisawa	NTT Atsugi, Japan
H.S. Goan	University of New South Wales, Australia
V. Golovach	University of Basel, The Switzerland
A. Granik	UOP, Stockton,USA
N. Grønbech- Jensen	University of California at Davis, USA
W. Guichard	Royal Institute of Technology, Stockholm, Sweden
T.Hakioglu	Bilkent University, Turkey
R.Hanson	University of Technology, Delft, The Netherlands
E. Il'ichev	1Institute for Physical High Technology, Germany
S.Komiyama	University of Tokyo, Japan
A. Konstadopoulou	University of Bradford, UK

J. Lantz	Chalmers University of Technology, Sweden
A. Maassen van den Brink	D-Wave Systems Inc., Vancouver, Canada
J. Mygind	Technical University of Denmark, Lyngby, DK
Yu. Pashkin	NEC/RIKEN, Tsukuba, Japan
E. Pazy	University of the Negev, Israel
J. Pekola	Helsinki University of Technology, Finland
T. Roscilde	University of Southern California, USA
R. Schäfer	Forschungszentrum Karlsruhe, Germany
F. Sciarrino	Università di Roma "La Sapienza", Italy
I. Siddiqi	Yale University, USA
R. Simmonds	NIST, USA
M. Sillanpää	Helsinki University of Technology, Finland
J. Sjöstrand	Stockholm University, Sweden
P. Sodano	Università di Perugia, Italy
R. M. Stevenson	Toshiba Research Europe Ltd., UK
P.B. Stiffell	University of Sussex, UK
V. Tognetti	Università di Firenze, Italy
A.V. Ustinov	Erlangen University, Germany
D.Vion	CEA-SACLAY, France
A. Vourdas	University of Bradford, UK
T. Yamamoto	NEC/RIKEN, Tsukuba, Japan
S.P. Yukon	Air Force Research Laboratory, MA, USA
A. Zorin	PTB, Brannschweig, Germany

Short Contributions

B. Bulka	Polish Academy of Sciences, Poland
P. Cappellaro	MIT Cambridge, USA
F. Chiarello	INFN - CNR, Roma, Italy
M.D. Kim	Seoul National University, Korea
N.V. Klenov	Moscow State University, Russia
B. Lovett	University of Oxford, UK
B. Militello	Università di Palermo, Italy
A. Naddeo	Università di Napoli "Federico II", Italy
M. Scala	Università di Palermo, Italy
J. Walter	Royal Institute of Technology, Stockholm, Sweden

INTERNATIONAL WORKSHOP ON
"MACROSCOPIC QUANTUM COHERENCE AND COMPUTING"
Istituto Italiano per gli Studi Filosofici, Via Monte di Dio 14, Napoli, Italy
7-10 June, 2004

PROGRAM

MONDAY - June 7, 2004

9.00 *Registration*
9.20 *Welcome Address*

Session I

9.30-10.15 J. CLARKE
Flux Qubits: Controllable Coupling, Single-shot Readout and Hot Electrons

10.15-10.50 Y. PASHKIN
Quantum Coherence and Entanglement of two Coupled Superconducting Charge Qubits

10.50-11.10 T. YAMAMOTO
Conditional Gate Operations in Superconducting Charge Qubits

Coffee Break

Session II

11.40-12.00 A. ZORIN
Josephson Charge-Phase Qubit with Radio Frequency Readout: Optimization of Coupling and Decoherence.

12.00-12.20 J. PEKOLA
Flux-assisted Adiabatic Single Island Cooper-pair Pump (Sluice)

12.20-12.40 M. SILLANPAA
Dynamics of the Inductive Single-Electron Transistor

12.40-13.00 V. CORATO
Macroscopic Quantum Tunneling in rf-SQUID Based Systems and Resonant Phenomena

LUNCH

Session III

14.40-15.00 A.V. USTINOV
Quantum Dissociation and Level Spectroscopy of a Vortex- Antivortex Molecule

15.00-15.20 N. GROENBECH-JENSEN
Anomalous Thermal Escape Statistics in Josephson Systems Perturbed by Microwaves

15.20-15.40 C. COSMELLI
Flux and Phase Qubits: Techniques of Operation

15.40-15.50 F. CHIARELLO
Realization and Characterization of a SQUID Flux Qubit with a Direct Readout Scheme

Coffee Break

Session IV

16.20-16.40 A. GRANIK
Transition from Quantum to Classical Information in a Superfluid and Holographic Reconstruction of the Entangled States

16.40-17.00 T. HAKIOGLU
Questioning the Validity of the Two Level Approximation

17.00–17.20 S. CHUNG
Size Dependence of the Superconductor-Insulator Transition in Josephson Junction Arrays

TUESDAY - June 8, 2004

Session V

9.00-9.45 A. BERKLEY
Phase Regime Josephson Junction Qubits

9.45-10.20 T. DUTY
Coherent Dynamics of a Josephson Charge Qubit

10.20-10.40 J. LANTZ
Josephson Junction Qqubit Network with Current-Controlled Interaction

10.40-11.00 A.MAASSEN VAN DEN BRINK
Continuous Monitoring of Rabi Oscillations in a Josephson Flux Qubit

Coffee Break

Session VI

11.30-11.50 S. YUKON
Josephson Junction Qubits with Symmetrized Couplings to a Resonant LC Bus

11.50-12.10 P. SODANO
Quantum Macroscopic Coherence in Josephson Networks with Non Conventional Architectures

12.10-12.30 R. FAZIO
Properties of Cooper Pair Shuttle

12.30-12.50 G. FALCI
Dynamical Suppression of Discrete Noise in Josephson Qubits

12.50-13.10 F. SCIARRINO
Optimal Quantum Machines by Linear and Non-linear Optics

LUNCH

Session VII

14.40-15.00 H. GOAN
Monte Carlo Method for a Superconducting Cooper-pair-box Charge Qubit Measured by a Single-electron Transistor

15.00-15.20 T. ROSCILDE
Entanglement in Quantum Critical Spin Systems in one and more Dimensions

15.20-15.30 N.V. KLENOV
Phase Second-Harmonic-Based Qubit

15.30-15.40 B. LOVETT
Selective Spin Coupling using a Single Excitation

Coffee Break

Session VIII

16.10-16.30 A. PAZY
On the Conversion of Ultracold Fermionic Atoms to Bosonic Molecules via Feshbach Resonances

16.30-16.50 R. SCHÄFER
Linear-Response Conductance of the Normal Conducting Single-electron Pump

16.50-17.00 P. CAPPELLARO
Entanglement Assisted Metrology

17.00-17.10 M. SCALA
Revealing Anisotropy in a Paul Trap through Berry Phase

WEDNESDAY - June 9, 2004

Session IX

9.00-9.45 I. SIDDIQI
Amplifying Quantum Signals with a Josephson Bifurcation Amplifier

9.45-10.05 P. BERTET
Coherent Dynamics of a Flux-Qubit Coupled to a Harmonic Oscillator

10.05-10.25 K. ARUTYUNOV
Quantum Tunneling Phenomena in Ultra-thin Superconducting Wires

10.25-10.40 J. SJOSTRAND
Modelling the Current Resolution of a Specific Josephson Junction System

10.40-10.50 J. WALTER
Binary Detection of Small Switching Currents

10.50-11.05 W. GUICHARD
Cooper Pair Transistor in a High Impedance Environment

Coffee Break

Session X

11.30-12.05 R.M. STEVENSON
Quantum Dots for Single Photon and Photon Pair Technology

12.05-12.25 V. GOLOVACH
Phonon-Induced Decay of the Electron Spin in Quantum Dots

12.25-12.45 R. HANSON
Single-shot Read-out of an Electron Spin Qubit

12.45-12.55 B. BULKA
Electronic Correlations in Transport through Molecules

LUNCH

Session XI

14.40-15.00 M. J.EVERITT
Macroscopic Quantum Superposition States, Squeezing and Entanglement in SQUID Rings

15.00-15.15 P.B. STIFFELL
Frequency Down Conversion and Entanglement between Electromagnetic Field Modes via a Mesoscopic SQUID Ring

15.15-15.35 A. VOURDAS
Photon-Induced Entanglement of Quantum Currents in Distant Mesoscopic SQUID Rings

15.35-15.50 A. KONSTADOPOULOU
Time Evolution of two Distant SQUID Rings Irradiated with Entangled Electromagnetic Field

15.50-16.05 E. IL'ICHEV
Application of the impedance measurement technique for investigation of quantum properties of superconducting structures.

Coffee Break

Session XII

16.30-16.50 V. TOGNETTI
Reentrant Behavior Associated with the Berezinskii Kosterlitz Thouless Transition in Josephson Junction Arrays and the Role of Dissipation

16.50-17.00 M. D. KIM
Persistent Currents in a Superconductor/normal Loop

17.00-17.10 A.NADDEO
Quantum Order in Josephson Junction Arrays

17.10-17.20 D. MILITELLO
Distilling Angular Momentum Schrödinger Cats in Trapped Ions

THURSDAY - June 10, 2004

Session XIII

9.00-9.45 T. FUJISAWA
Dynamics of Single-electron Charge and Spin in Semiconductor Quantum Dots

9.45-10.30 S. KOMIYAMA
Control of Nuclear Spins by Quantum Hall Edge Channels

Coffee Break

Session XIV

11.00 – 11.35 D. ESTEVE
NMR-like Control of a Quantum Bit Superconducting Circuit

11.35-11.55 D. VION
Analysis of Decoherence in a Quantum Bit Superconducting

11.55-12.15 R. W. SIMMONDS
Improvements to Josephson Phase Qubits

12.15-12.35 J. MYGIND
Non-hysteretic Positioner for Nano-Lithography and Cryogenic in Situ Adjustable Nano-Junctions

12:35 *Closing Remarks: J.CLARKE*

Flux qubits: controllable coupling, single-shot readout and hot electrons

John Clarke,[1] T. Hime,[1], S. Linzen,[1], B.L.T. Plourde,[1], P.A. Reichardt,[1], T.L. Robertson,[1] K.B. Whaley,[2], F.K. Wilhelm,[3], C.-E. Wu,[1], and J. Zhang[2]

Departments of [1]Physics and [2]Chemistry, University of California, Berkeley, CA 94720, USA
[3]Ludwig-Maximillians-Universität, 80333 München, Germany

The flux state of a three-junction qubit is measured with a dc Superconducting QUantum Interference Device. The qubit and SQUID are fabricated from evaporated aluminum films that are patterned using electron-beam lithography. The qubit encloses an area of 11280 μm^2, so that on-chip flux lines can be used to generate the necessary half-flux quantum of bias (Fig. 1); nonetheless, the geometrical inductance of the qubit is small compared with the kinetic inductance of the three junctions. The flux state of the qubit is determined by applying current pulses to the SQUID and adjusting the amplitude of the pulse to obtain a 50% switching probability. We discuss two aspects of the experiment: single-shot readout of the qubit with a SQUID in which each junction is shunted with a frequency-dependent impedance, and the role of hot electrons in the SQUID in reducing the relaxation time of the qubit. We begin, however, with a proposed scheme for varying the coupling between two flux qubits by adjusting the bias current of the readout SQUID in the zero-voltage state.

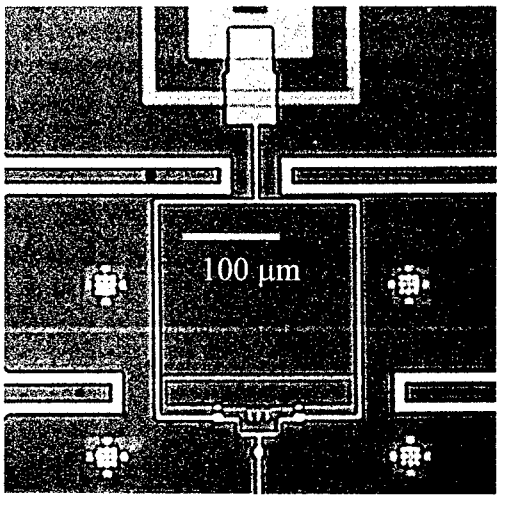

Fig. 1: SQUID and three-junction flux qubit. SQUID bias current and voltage leads at top and bottom of SQUID loop. Flux bias lines located at top and sides of SQUID loop. The Josephson tunnel junctions, located at the bottom of the SQUID and qubit loops, are typically 200 x 200 nm^2 and are formed with double-angle evaporation.

In order to entangle two flux qubits, it is highly desirable to be able to control their mutual inductance M. In particular, manipulations to achieve entanglement are much more straightforward if M can be reduced precisely to zero at specified times. This is not a trivial problem because of the inherent coupling of the two qubits even in the absence of external circuits. A scheme that enables one to vary the coupling and to reduce it to zero is shown in Fig. 2(a), in which two qubits are surrounded by a SQUID. The technique relies on the fact that the inverse dynamic inductance of a SQUID in the zero-voltage state can be either positive or negative. When a flux is applied to the SQUID, the flux generated by the induced supercurrent opposes applied flux in the first case, but supports it in the second. Thus, if there is a change in the current in (say) qubit 1, there will be a change in the flux in qubit 2 due to the mutual inductance between the qubits, and a second contribution that is mediated by the SQUID. This SQUID-mediated contribution can be made positive or negative simply by changing the magnitude of the bias current in the SQUID at an appropriate, fixed value of flux [Fig. 2(b)]; the SQUID remains in the zero-voltage state. Since the change in bias current required to control the inductive coupling of the two qubits is small, less than the critical current of the SQUID, it can be pulsed rapidly with existing technology. A set of

device parameters is proposed that is realistically achievable. This method enables one both to vary the mutual inductance between two qubits and to read their flux states with a single SQUID, simply by applying current pulses of appropriate magnitude. A scheme for a Controlled Not (CNOT) gate is suggested that involves only current pulses and precisely chosen microwave pulses (Fig. 3).

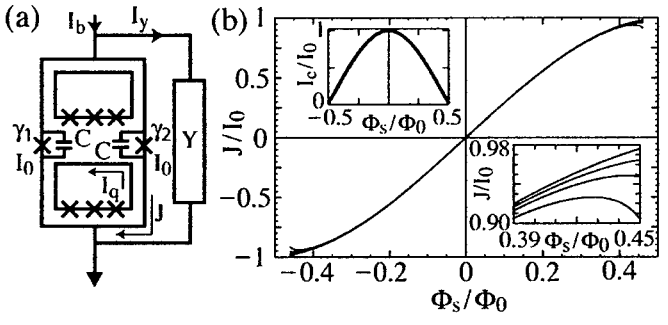

Fig. 2: (a) SQUID-based coupling scheme. The SQUID has inductance L and critical current I_c. The admittance Y represents the SQUID bias circuitry. **(b)** Response of SQUID circulating current J to applied flux Φ_s for $\beta_L = 2\,L\,I_0/\Phi_0 = 0.04$ and $I_b/I_c\,(0.45\,\Phi_0) = 0, 0.4, 0.6, 0.85$ (top to bottom). Lower right inset shows $J(\Phi_s)$ for same values of I_b near $\Phi_s = 0.45\,\Phi_0$. Upper left inset shows I_c versus Φ_s.

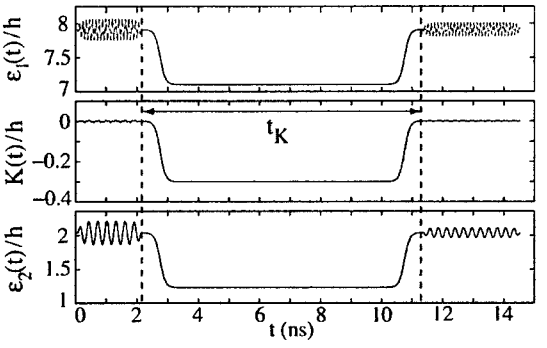

Fig .3: Pulse sequence for implementing CNOT gate. Energy scales in GHz. The bias current is pulsed to turn on the interaction in the central region. Total single-qubit energy bias $\varepsilon_i(t) = \varepsilon_i^0 + \varepsilon_i^m(t) + \delta\varepsilon_i(t)$, where ε_i^0 are the static qubit bias energies and $\varepsilon_{1,2}^m(t)$ are microwave pulses which produce single-qubit rotations in the decoupled configuration; crosstalk shift of $\varepsilon_i(t)$ due to bias current pulse, $\delta\varepsilon_i(t)$, along with modulation of coupling energy K(t) due to microwaves are shown.

The use of a dc SQUID with unshunted tunnel junctions has the advantage of creating low dissipation in the flux qubit but the disadvantage of a broad switching distribution due to the onset of macroscopic quantum tunneling (MQT) at low temperatures. Adding resistors across the junctions narrows the distribution but substantially increases dissipation in the qubit. We demonstrate that a resistor R in series with a capacitor C connected across each junction enables one to achieve single-shot readout while maintaining low dissipation in the qubit. The RC-time constant is chosen so that the reactance of the capacitor is small at the plasma frequency of the junctions, ~100 GHz, providing substantial damping that suppresses MQT. On the other hand, at the qubit frequency, ~1 GHz, the reactance of the capacitor is much greater than R, and the dissipation coupled to the qubit is low. Detailed calculations of the width of the switching distribution and of the qubit relaxation and dephasing rates due to the RC shunts are presented.

When the SQUID switches to the gap voltage $2\Delta/e$ (Δ is the energy gap of the Al films) following a measurement of its critical current, there is substantial dissipation. In spectroscopic measurements on a flux qubit, we have measured the relaxation of the microwave-induced peaks as a function of the delay time t between successive current pulses in the readout SQUID. We find that the relaxation rate increases dramatically as t is reduced. We explain this behavior in terms of a model in which hot electrons, generated when the SQUID switches to $2\Delta/e$, increase the subgap conductance of the tunnel junctions. This conductance increases the dissipation experienced by the flux qubit for a remarkably long time, ~1 ms, after the SQUID has been restored to its zero-voltage state.

This work was supported by AFOSR, ARO and NSF.

Quantum coherence and entanglement of two coupled superconducting charge qubits

Yu. A. Pashkin[1], T. Yamamoto[1,2], O. Astafiev[1], D. V. Averin[3], Y. Nakamura[1,2], T. Tilma[1,4], F. Nori[1,4] and J. S. Tsai[1,2]

[1] *The Institute of Physical and Chemical Research (RIKEN), Wako, Saitama 351-0198, Japan*
[2] *NEC Fundamental and Environmental Research Laboratories, Tsukuba, Ibaraki 305-8501, Japan*
[3] *SUNY at Stony Brook, Stony Brook, NY 11794-3800, USA*
[4] *University of Michigan, Ann Arbor, Michigan 48109-1120, USA*

We have studied quantum coherent dynamics of two coupled superconducting charge qubits[1]. Each qubit is based on a Cooper-pair box, a small superconducting island, coupled to a reservoir through a small Josephson junction. The qubits are electrostatically coupled to each other by a miniature on-chip capacitor formed by overlapping Al layers. The sample was fabricated by an angle evaporation of Al layers through a suspended mask formed by conventional electron-beam lithography.

In the charge regime when the charging energy of each qubit $E_{1,2}$ exceeds the Josephson energy$E_{J1,2}$, the Hamiltonian of the system can be reduced to the four-state Hamiltonian:

$$H = \sum_{n_1,n_2=0,1} E_{n_1 n_2} |n_1 n_2\rangle\langle n_1 n_2| - \frac{E_{J1}}{2} \sum_{n_2=0,1} (|0\rangle\langle 1| + |1\rangle\langle 0|) \otimes |n_2\rangle\langle n_2| - \frac{E_{J2}}{2} \sum_{n_1=0,1} |n_1\rangle\langle n_1| \otimes (|0\rangle\langle 1| + |1\rangle\langle 0|) \quad (1)$$

where $E_{n_1 n_2}$ is the electrostatic energy of the system corresponding to the charge configuration (n_1,n_2), and the four charge states $|00\rangle$, $|10\rangle$, $|01\rangle$ and $|11\rangle$ are used as a basis. Here the first and the second indices refer to the number of Cooper pairs in the first and the second qubit, respectively. By changing dc gate voltages we can control the initial state of the system. There is a special point in the energy diagram, that we call a double degeneracy point, where $E_{00} = E_{11}$ and $E_{10} = E_{01}$. By preparing the system in the $|00\rangle$ initial state and then bringing the system non-adiabatically to the double degeneracy point, we create conditions for coherent evolution of the system. Non-adiabatic shift of the system is done by a sharp control pulse applied to both qubits simultaneously. As a result of the evolution, the final state of the system is a superposition of all four charge states: $|\psi\rangle = c_1|00\rangle + c_2|10\rangle + c_3|01\rangle + c_4|11\rangle$, where the coefficients c_i depend on time and hence on the length of the control pulse. The problem can be solved analytically for a rectangular pulse shape. To readout each qubit, we attach a properly biased probe electrode to each Cooper pair box through a resistive tunnel junction. We then measure pulse induced probe currents I_1 and I_2 through the probes. Each current is proportional to the probability $p_{1,2}(1)$ of the corresponding qubit to be in state $|1\rangle$, i.e., $p_1(1) = c_2^2(t) + c_4^2(t)$ and $p_2(1) = c_3^2(t) + c_4^2(t)$. Thus, by measuring the probe currents we trace $p_{1,2}(1)$.

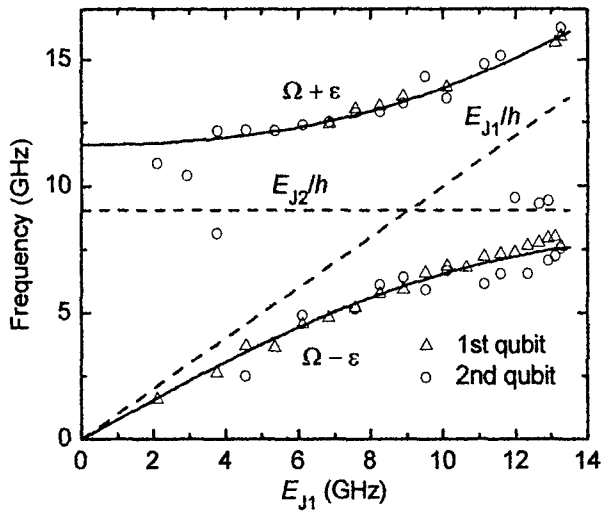

Fig. 1. Avoided level crossing of two coupled charge qubits.

The observed oscillations of I_1 and I_2 contained two frequency components in the spectrum, $\Omega + \varepsilon$ and $\Omega + \varepsilon$, that depend on the sample parameters and result in beatings. By tracing oscillations for different values of E_{J1}, we observed avoided level crossing in the energy spectrum as shown in Fig. 1. The observed beatings and avoided level crossing are direct evidence for the interaction between the qubits and in a remarkable quantitative agreement with the theoretical expectations.

Our experimental results show that the coherence time of the coupled qubit oscillations is a factor of four shorter compared to the case of single qubit oscillations. This fact is still to be understood. Nevertheless, even with short coherence time we were able to perform logic operation.

By adding one more pulse gate to the coupled qubit circuit we were able to address each qubit individually. This allowed us to demonstrate conditional gate operation, a prototype of the quantum C-NOT logic gate.

Our simulations[2] show that in the course of oscillations the qubits remain entangled most of the time.

[1]. Yu. A. Pashkin, T. Yamamoto, O. Astafiev, Y. Nakamura et al. *Nature* **421**, 823 (2003).
[2]. Yu. A. Pashkin, T. Tilma, D. V. Averin, O. Astafiev, T. Yamamoto et al. *IJQI* **1**, 421 (2003).

Conditional gate operation in superconducting charge qubits

T. Yamamoto[1,2], Yu. A. Pashkin[2], O. Astafiev[2], Y. Nakamura[1,2], and J. S. Tsai[1,2]

[1]*NEC Fundamental and Environmental Research Laboratories, Tsukuba, Ibaraki, Japan*
[2]*The Institute of Physical and Chemical Research (RIKEN), Wako, Saitama, Japan*

A variety of Josephson-junction-based qubits have recently been implemented with remarkable progress in coherence time and read-out scheme. These developments, together with its potential scalability, have renewed the position of this solid-state device as a strong candidate as a building block for the quantum computer. On the other hand, coupling multiple qubits to construct a logic gate is another important step toward the realization of quantum computer. In this talk, we introduce our experiments on conditional gate operations using coupled superconducting charge qubits[1].

Samples are fabricated by standard e-beam lithography and shadow evaporation technique. A scanning-electron micrograph of the device is shown in Fig. 1. Blight parts are made of Al. Two Cooper-pair boxes are electrostatically coupled by an on-chip capacitor which is shown in the dashed circle in the figure. The right qubit has SQUID geometry and we use this qubit as the control qubit and the left one as the target qubit. Two independent pulse gates allow us to address each qubit individually. The state of this two-qubit system is measured by currents through two probes.

The logic operation we tried to demonstrate is summarized as a classical truth table in Table 1. Target qubit is flipped only when the control qubit is in the |0> state. This operation was realized by utilizing the difference of the degeneracy condition between two pairs of the charge states, namely, |00>, |01> and |10>, |11>.

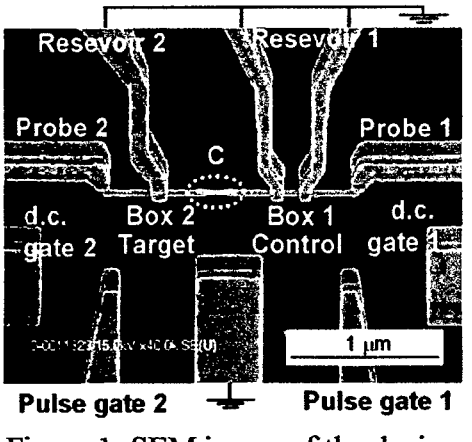

Figure 1: SEM image of the device.

Input		Output	
Control	Target	Control	Target
0	0	0	1
0	1	0	0
1	0	1	0
1	1	1	1

Table 1: Truth table for the conditional gate.

Figure 2(a) shows the pulse sequence, which we utilized in the experiment. It consists of the input preparation and the logic operation. The first pulse applied to the Pulse gate 1 creates the superposition state $\alpha|00\rangle+\beta|10\rangle$. This state should be transformed into the state $\alpha|01\rangle+\beta|10\rangle$, if the operation pulse, the second pulse applied to the Pulse gate 2, is described by Table 1. Figure 2(b) shows the output currents of the control and the target qubits under the application of this pulse sequence as a function of the Josephson energy of the control qubit E_{J1}. By changing E_{J1}, we can change the coefficients α and β, while keeping the pulse length constant. Observed anti-correlation between the magnitudes of the output currents is consistent with the above expectation, indicating that our operation pulse is properly working as a conditional gate.

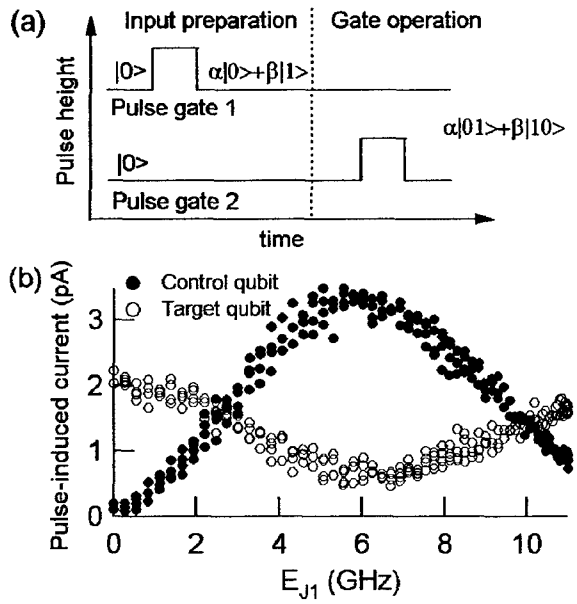

Figure 2: (a) The pulse sequence and (b) the output currents of the control and the target qubits.

[1] T. Yamamoto, Yu. A. Pashkin, O. Astafiev, Y. Nakamura and J. S. Tsai, Nature **425,** 941 (2003).

Josephson charge-phase qubit with radio frequency readout: optimization of coupling and decoherence

A. B. Zorin

Physikalisch-Technische Bundesanstalt, 38116 Braunschweig, Germany

The two-junction-SQUID configuration of the Cooper-pair-box qubit enables not only the control of Josephson coupling, but also a readout of the quantum states taking advantage of the phase degree of freedom. This readout can be realized by measuring either the persistent Josephson current circulating in the superconducting loop [1] or the Josephson inductance of the qubit junctions with small island in between, i.e. the single Cooper pair transistor, closed by this loop [2]. The Josephson inductance readout is performed by inducing small radio frequency oscillations of frequency ω in the loop and measuring the resonance frequency shift in a weakly coupled tank circuit. Although such measurement requires sufficiently long time, presumably $\gg Q/\omega$, where Q is the quality factor of the tank, the rate of decoherence caused by the setup is significantly reduced. This is achieved by appropriate choice of the operation point on the $\{q, \Phi\}$ plane, where q is the gate charge and Φ is the flux applied to the loop. Specifically, operation in the optimal (magic) points [1,3] makes the qubit much less sensitive to the charge and phase fluctuations and should even permit the single shot measurements. The problems of asymmetry in the junction parameters, quasiparticle tunneling and back action of the readout setup will be addressed in the talk.

[1] D. Vion, A. Aassime, A. Cottet, P. Joyez, H. Pothier, C. Urbina, D. Esteve and M.H. Devoret, *Science 296*, 886 (2002).
[2] A.B. Zorin, *Physica C 368*, 284 (2002).
[3] A.B. Zorin, arXive:cond-mat/0312225 .

Flux-assisted adiabatic single-island Cooper pair pump (sluice)

J. P. Pekola[1], A. O. Niskanen[1,2], J. M. Kivioja[1], and H. Seppä[2]

[1]*Low Temperature Laboratory, Helsinki University of Technology, POB 2200, FIN-02015 HUT, Finland*
[2]*VTT Information Technology, Microsensing, POB 1207, FIN-02044 VTT, Finland*

Fast and accurate pumping of charge in Josephson junction circuits poses a twofold problem. On one hand the speed is typically limited by the magnitude of Josephson coupling E_J due to Landau-Zener crossing, whereas errors due to supercurrent leakage and quantum interference effects increase with increasing E_J. Moreover, simultaneous suppression of the latter two is difficult due to their mutually orthogonal dependence on Josephson phase difference. To circumvent these apparent problems we propose and test an alternative device concept, the Cooper pair sluice, shown schematically in Fig. 1.

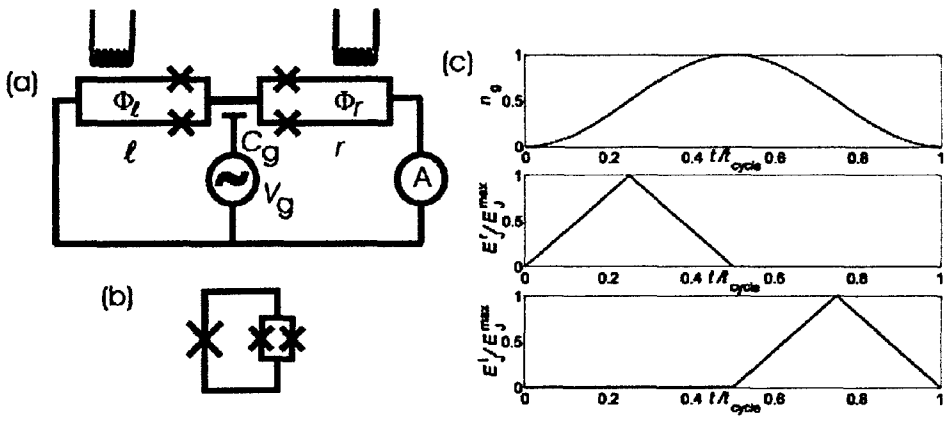

Figure 1. (a) Basic configuration of a Cooper pair sluice. (b) Three junction SQUIDs for better suppression of Josephson coupling. (c) Gate and flux cycles to pump one Cooper pair from right to left through the island.

The central idea of the sluice is to vary the Josephson couplings in time in order to allow fast charge transport when necessary but to suppress leakage contributions at other times. Therefore the sluice consists of two tunable mesoscopic junctions (DC-SQUIDs), with just one island in between [Fig. 1 (a)]. An example of an operating cycle is shown in Fig. 1 (c). Initially the system is in the neutral charge state with n_g (gate charge) and Josephson couplings E_{Jr} and E_{Jl} set to zero. Thereafter one of the Josephson couplings E_{Jr} is tuned adiabatically to maximum, and simultaneously n_g is ramped up also. In the middle of the cycle E_{Jr} has been turned off again. At this moment when $E_{Jr} = 0$ again, exactly one pair (or in general an integer number of pairs depending on the amplitude of n_g) has been brought from the right source to the central island. In the second half of the cycle the pair(s) is (are) taken out through the left SQUID in a similar fashion.

We demonstrate theoretically that it is possible to obtain a current as high as 0.1 nA at better than ppm accuracy using a sluice (and standard aluminium technology). We discuss the influence of imperfect suppression of the Josephson coupling and the finite operating frequency.

Figure 2 shows scanning electron micrograph of the SQUIDs and input coils of the sluice in (a) and a blow-up of the island region in (b). The tickmark in (b) is 1 μm long. The two-dimensional flux-modulation of the supercurrent through the sluice in (c) indicates better than 90 % suppression of Josephson couplings and only very weak cross-coupling between the SQUIDs and their input coils.

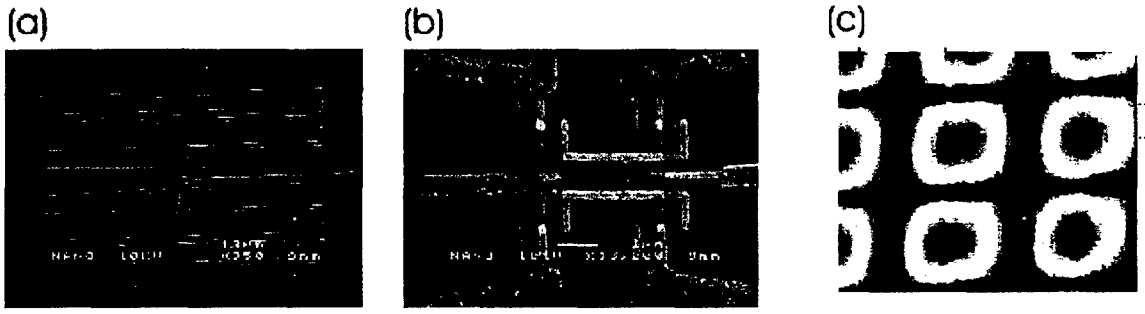

Figure 2. (a) and (b) show a fabricated sluice structure. Supercurrent through the sluice plotted against the two applied fluxes (i.e., currents in the input coils).

The first pumping measurements have demonstrated the operation of the device but still with non-optimal circuit parameters.

Dynamics of the Inductive Single-Electron Transistor

Mika Sillanpää, Leif Roschier, and Pertti Hakonen

Low Temperature Laboratory, Helsinki University of Technology, 02015 HUT, Finland

Electrometers based on Cooper pair tunneling are, in principle, dissipationless, and thus they are expected to exhibit only a small back action noise [1]. We have studied the dynamics of inductive single electron transistor (L-SET) which is one candidate for this kind of electrometry.

The L-SET consists of a superconducting SET (SSET) connected in parallel with a LC resonant circuit (See Fig. 1a). The SSET is described by the Hamiltonian is $(q - q_g)^2/2C_\Sigma - 2E_J\cos(\varphi/2)\cos(\theta)$. Here, q_g is the gate charge, φ is the phase difference across the whole device, assumed to be a classical variable due to an environment having impedance much smaller than $R_Q = h/(2e)^2 \sim 6.5$ kΩ, whereas θ, conjugate to the charge of the island q, experiences quantum effects. The lowest of the resulting bands $E_n(\varphi,q_g)$ has approximately sinusoidal energy $E_0(\varphi,q_g) \sim - E_0(q_g)\cos(\varphi)$ and thus, the SSET is effectively a gate-tunable single junction [2]. From our point of view the most important property of SSET is its Josephson inductance $L_J^{-1}(\varphi,q_g) = (2\pi/\Phi_0)^2\, \partial^2 E\,(\varphi,q_g)/\partial\,\varphi^2$, where $\Phi_0 = h/(2e)$ is the flux quantum. With a total shunting capacitance C, a SSET thus forms a harmonic oscillator with the plasma frequency $f_p = 1/(2\pi)\,(L_J\,C)^{-1/2}$ for small φ.

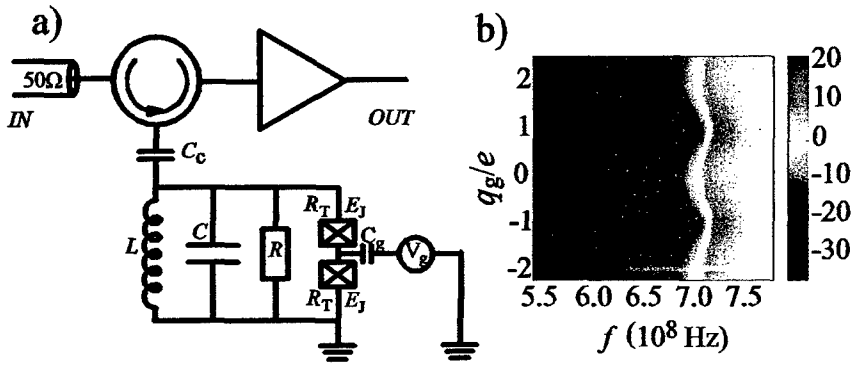

FIGURE 1. a) Schematics of experimental setup used in our measurements. The resonant frequency of the LC oscillator is 613 MHz. Coulomb energy of the SSET $E_C = 0.92$ K and the ratio $E_J / E_C = 1.7$. b) Variation of the phase of the reflected signal from the L-SET circuit using small, harmonic oscillation amplitudes in the tank circuit; the scale of variation in degrees is shown on the right.

Energy of the system of the SSET plus the LC oscillator is the sum of potential energy $E_n(\varphi,q_g) + \Phi^2/(2L)$, approximately $- E_0(q_g)\cos(\varphi) + [\Phi_0^2/(4\pi^2 L)]\,\varphi^2$ on the ground band, and kinetic energy $q^2/2C_\Sigma$. Here, Φ is the magnetic flux in the loop. Assuming the SSET stays at the lowest band, where $I \sim I_0 \sin(\varphi)$, classical dynamics of phase in the oscillator is thus analogous to a particle moving in a sinusoidally modulated parabolic potential. The dynamics is similar to that of the rf-SQUID [3], i.e., a single junction shunted with a loop inductance, except that since our loop is not fully superconducting, flux quantization or flux jumps do not exist. At small driving amplitude (linear regime), the phase particle experiences harmonic oscillations around $\varphi = 0$ at the frequency $f_p = 1/(2\pi)\,(L \,||\, L_J C)^{-1/2}$ which is controlled by gate-tuned L_J. This mode of operation, where

the L-SET works as a charge-to-frequency transducer, we call the "plasma oscillation mode".

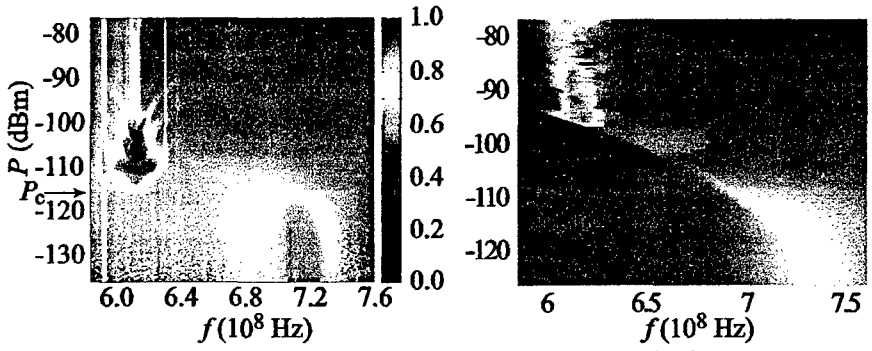

FIGURE 2. Measured frequency response of the reflection coefficient $|\Gamma|$ as a function of excitation power: data (left) and simulation (right) [4]. "Critical power" P_C is marked by the arrow. In order to guarantee convergence of the simulation, the calculations were performed using a slightly larger dissipation than present in the experiment.

At higher oscillation amplitude, in the "non-harmonic regime", the particle sees a different local curvature of the potential due to the cosφ term, thus changing the oscillation frequency. At very high amplitude, the cosine modulation becomes effectively averaged out. Thus, when increasing excitation, we expect a change of resonant frequency from f_p to $f_0 = 1/(2\pi)\ (LC)^{-1/2}$. This change of resonance frequency at a critical excitation power P_C is seen in experimental data of Fig.2. The dynamics of the L-SET, however, is still very sensitive to the q_g–induced variations of the cosine-potential when P is slightly above P_C.

Charge resolution was measured using both amplitude and phase read-out without any significant difference between these methods. In the plasma oscillation mode we got $s_q = 2.0 \cdot 10^{-3} e/\sqrt{\text{Hz}}$ at the maximum power $P_C \sim$ -116 dBm, corresponding to 20 fW dissipation in the whole resonator circuit. Note that due to Cooper pair tunneling, the power is not dissipated in the SSET island. In the non-harmonic mode, significantly better sensitivities were obtained: $s_q = 1.4 \cdot 10^{-4} e/\sqrt{\text{Hz}}$ was measured at -100 dBm. Due to a higher impedance mismatch, power dissipation can be kept below 20 fW in this case as well. The non-harmonic mode offers good possibilities to reach uncoupled energy sensitivity of $\varepsilon \sim \hbar$ using an optimized sample in the present configuration [4]. Our simulations indicate that by employing a sample with $R_{SET} = 35$ kΩ, $E_J = 0.45$ K and $L_J = 60$ nH, a resolution of $s_q \sim 1 \cdot 10^{-6} e/\sqrt{}$ can be reached.

Fruitful discussions with T. Heikkilä, G. Johansson, R. Lindell, H. Seppä, and J. Viljas are gratefully acknowledged. This work was supported by the Academy of Finland and by the Large Scale Installation Program ULTI-3 of the European Union.

[1] A. B. Zorin, *Phys. Rev. Lett.* **86**, 3388 (2001).
[2] A. Maassen van den Brink, L. J. Geerligs, and G. Schön, *Phys. Rev. Lett.* **67**, 3030 (1991).
[3] S. N. Erné, H.-D. Hahlbohm, and H. Lübbig, *J. Appl. Phys.* **47**, 5440 (1976).
[4] M. Sillanpää, L. Roschier, and P. Hakonen, to be published.

Macroscopic Quantum Tunneling in rf-SQUID based systems and resonant phenomena

V. Corato, S. Rombetto, and P. Silvestrini
Seconda Universita` di Napoli, Dipartimento di Ingegneria dell'Informazione, I-81031, Aversa, Italy and Istituto di Cibernetica "E. Caianiello" del CNR, I-80078 Pozzuoli, Italy

C. Granata, R. Russo, and B. Ruggiero
Istituto di Cibernetica "E. Caianiello" del CNR, I-80078 Pozzuoli, Italy

Yu. N. Ovchinnikov
Landau Institute for Theoretical Physics, Moscow, Russia

We present an experimental characterization in the quantum regime of Nb/AlO*x*/Nb Josephson devices. Josephson Junctions and fully integrated Josephson devices consisting of a rf SQUID coupled to a readout system based on a dc SQUID sensor have been measured. Data on the decay rate from the metastable states show evidence of Macroscopic Quantum Tunneling[1] with a very low dissipation level and a high insulation of the probes from the external environment.

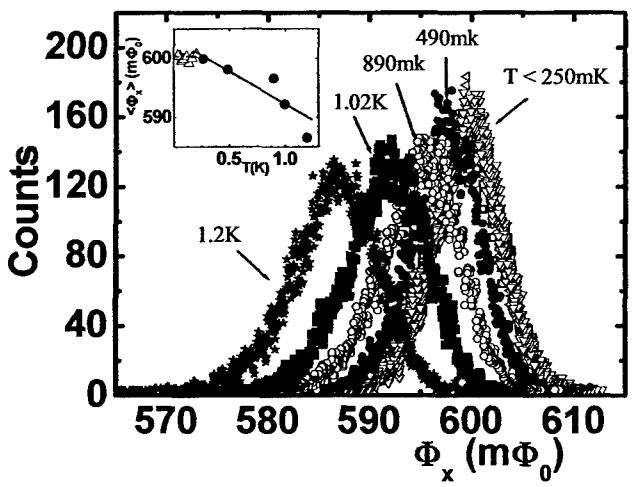

Figure 1 Experimental histograms of the switching flux distribution $P(\Phi_x)$ at different temperatures. The mean value of the flux distributions is reported in the inset as a function of T, together with the theoretical prediction in thermal (solid line) and quantum limit (dashed line). The rf SQUID parameters are L=80 pH, C=2.3 pF, I_c=9 μA, and β_L=2.

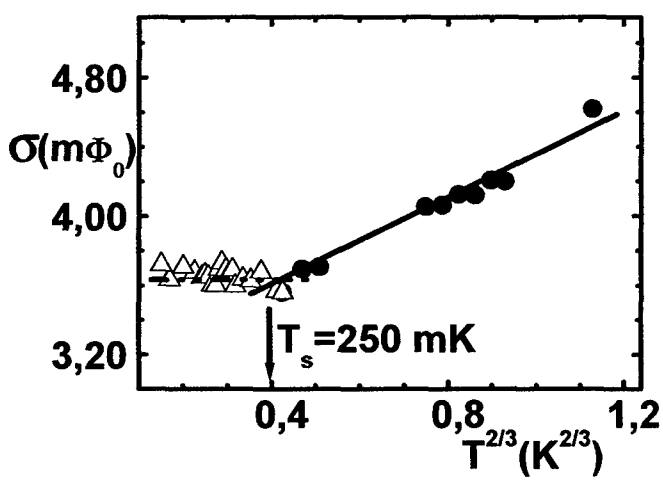

Figure 2. Data on the distribution width σ as function of $T^{2/3}$ is shown for the SQUID system. Experimental data in the thermal regime are compared with the theoretical prediction (dots and solid line) obtained for R=1 MΩ and C=2.3 pF. We also report the best fit line of the data in the quantum regime (triangles and dashed line). The interception of this line with the thermal curve gives an experimental extrapolation of the crossover temperature: T_S=250 mK.

Furthermore we consider the theoretical problem of resonant phenomena in the Macroscopic Quantum Tunneling for an rf-SQUID in presence of an external field[2]. The transition probability between energy levels is studied by varying the parameters of the potential describing the system in a way that the pumping level in the left potential well is close to some level in the right potential well. The dependence of transition probability from the external drive of the system shows two resonance peaks, the former connected with *resonance tunneling* and the latter with *resonance pumping*. Relative position of peaks depends on the pumping energy and on the potential parameters.

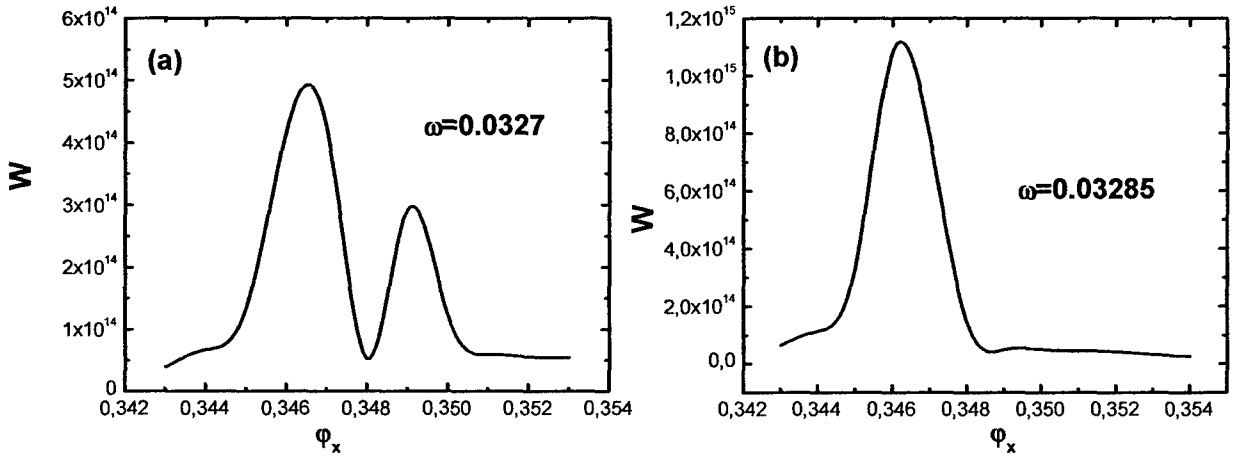

Figure 3. Transition probability W as function of the external magnetic flux φ_x. The curve is calculated for different values of the pumping frequency. The two peaks shown in a) and b) are connected with the effects of resonance tunneling between levels in different wells and the resonance pumping between levels in the same well. As predicted, the peaks due to the resonance pumping moves with the pumping frequency ω until it superimposes to the tunneling peak, as it is clear in Fig. 3b.

[1] D. B. Schwartz, B. Sen, C. N. Archie, and J. Lukens, Phys. Rev.Lett. **55**, 1547 (1985); S. Washburn, R. A. Webb, R. F. Voss and S. M. Faris , Phys. Rev. Lett. **54**, 2712 (1985); V. Corato, S. Rombetto, P. Silvestrini, C. Granata, R. Russo, and B. Ruggiero, Superc. Science Technol. **17**, S385-S338 (2004).

[2] A.I. Larkin, and Yu. N. Ovchinnikov, Phys. Rev. **B28**, 6281 (1983); A.I. Larkin, and Yu. N. Ovchinnikov, Sov. Phys. JEPT **60**, 1060 (1984); Yu.N. Ovchinnikov, P. Silvestrini, B. Ruggiero, and A. Barone, J. of Supercond. **5**, 481 (1992).

Quantum Dissociation and Level Spectroscopy of a Vortex-Antivortex Molecule

A. Kemp, M.V. Fistul, A. Lukashenko, Y. Koval, A. Wallraff[§], B.A. Malomed[*], and A.V. Ustinov

Physics Institute III, University of Erlangen-Nuremberg, D-91058 Erlangen, Germany
[§] Department of Applied Physics, Yale University, New Haven, CT 06520, USA
[*] Department of Interdisciplinary Science, Tel Aviv University, Tel-Aviv 69978, Israel

We report recent experiments that demonstrate quantum tunneling and energy level quantization of Josephson vortices at temperatures below 100 mK. A *single vortex* behaves as a macroscopic particle with a spatial extent of several micrometers which tunnels through a potential barrier created by a magnetic field applied to the annular Josephson junction [1]. We probe the quantum properties of this particle by investigating the statistics of a set of tunneling events. Measurements of vortex escape from a potential well in the presence of microwave radiation clearly indicate discrete energy levels of the vortex. Both the tunneling rate and the energy level separation can be tuned in experiment by varying the applied magnetic field.

The experiments on ultra-narrow annular long junction in the absence of initially trapped vortices allow for studying the properties of a vortex "molecule", consisting of a *bound state of vortex and antivortex* [2]. We find that a switching from the superconducting state to the resistive state occurs as the dissociation of this pinned vortex-antivortex pair. The interaction potential of the bound state is controlled by external magnetic field and dc bias current. The figure below shows our experimental data (dots) for the lowest energy level separation of vortex-antivortex bound state measured by microwave spectroscopy within 10-20 GHz frequency range. Solid line is the calculated vortex "molecule" level separation [2]; dashed line is the standard prediction of the lumped junction model. The inset schematically shows the sample geometry.

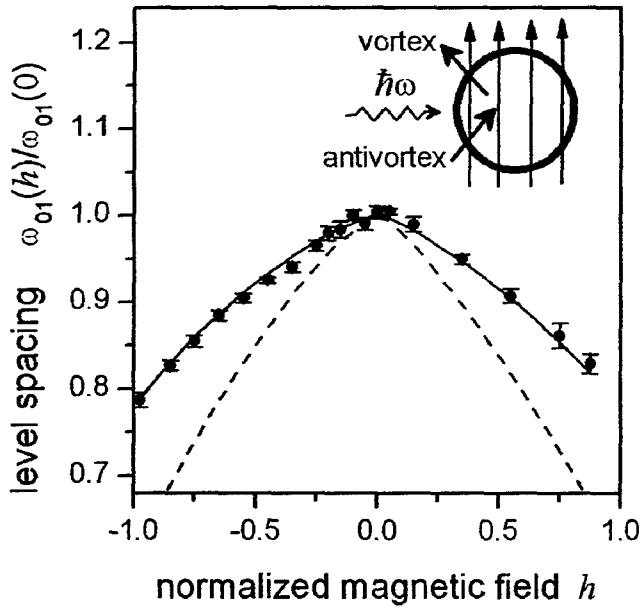

Engineering an energy profile for a vortex in a long Josephson junction opens an opportunity of designing vortex qubits. The energy profile for the vortex can be created, e.g., by making the junction of a particular geometrical shape and applying an external magnetic field [3]. Possible coupling schemes of vortex qubits [4] are feasible for creating and monitoring entanglement in multi-qubit circuits. Vortex qubits allow for a convenient state preparation and readout using superconducting Rapid Single Flux Quantum (RSFQ) circuitry [5].

[1] A. Wallraff et al., *Nature* **425**, 155 (2003)
[2] M.V. Fistul et al., *Phys. Rev. Lett.* **91**, 257004 (2003)
[3] A. Kemp, A. Wallraff and A. V. Ustinov, *Phys. Stat. Sol. (b)* **233**, 472 (2002)
[4] M.V. Fistul and A. V. Ustinov, *Phys. Rev. B* **68**, 132509 (2003)
[5] V.K. Kaplunenko and A.V. Ustinov, *Eur. Phys. J. B* **38**, 3 (2004)

Anomalous thermal escape statistics in Josephson systems perturbed by microwaves

Niels Grønbech-Jensen, Department of Applied Science (UC Davis)
M. Gabriella Castellano, IFN-CNR (Rome)
Carlo Cosmelli, Department of Physics (University of Rome "La Sapienza") Matteo Cirillo, Department of Physics (University of Rome "Tor Vergata")

We have investigated the statistical behavior of Josephson junctions with respect to their switching from the zero-voltage state when ac-perturbations are applied. The investigations are inspired by the experimental observations of anomalous switching distributions reported in for temperatures below the quantum transition temperature [1, 2]. These measurements have produced multi-peaked switching distributions when microwaves are applied to the system, and the results have been interpreted as a signature of intrinsic quantum energy levels excited by the external microwaves. Our work has been focused on the classical limit of the system, where thermal fluctuations dominate quantum uncertainties, and where the governing model equations of motion can be written as stochastic differential equations.

Extensive simulation results reveal [4, 5] that the entirely classical models can reproduce the multi-peaked switching distribution signatures observed experimentally in the low temperature limit. We have investigated both the small area Josephson junction and the magnetic field embedded long annular Josephson junction with a single trapped magnetic fluxon. The simulated current-voltage characteristics of the latter system can with good approximation be obtained from a simplified effective pendulum equation, and the characteristics of the small and long annular junctions are therefore very similar [3].

The essence of the system is summarized in Figure 1 (left), where ϕ is the quantum mechanical phase-difference between the superconductors of the junction. The escape is assisted by two components: 1) the thermal bath, and 2) forced oscillations from the ac-perturbation. We exemplify our investigations of the small area Josephson junction, modeled by a pendulum equation, through a set of switching distributions shown in Fig. 1. The middle plot shows the switching statistics for several different applied frequencies. The locations of the secondary (left) probability peak as a function of driving frequency, Ω, is shown on top along with the results of harmonic and anharmonic analysis of the intrinsic resonance as a function of bias current, η. As is well known, the linear resonance frequency of the system is a function of the bias, η. Thus, as the bias is swept (slowly) from low values toward the critical value, the resonance frequency of the system is tuned from the plasma frequency to zero. The classical interpretation of the anomalous switching statistics is that if the driving frequency (or a significant sub or super harmonic) is less than the plasma frequency, then multi-peaked switching distributions may arise by simple resonant coupling between the inherent system resonance and the external frequency, provided the ac-amplitude is tuned appropriately.

Similarly to the small area junction, we can demonstrate the same behavior for long annular junctions in a magnetic field and a single trapped fluxon. The system is

here modeled by the sine-Gordon equation. Figure 1 (right) shows anomalous switching distributions for the escape of the trapped fluxon in the magnetic field induced potential well. Again we observe anomalous multi-peaked switching distributions, generated by the ac-perturbation, and we verify the interpretation of the anomalous distributions as a direct result of a simple forced oscillation, which resonates near specific values of the bias current.

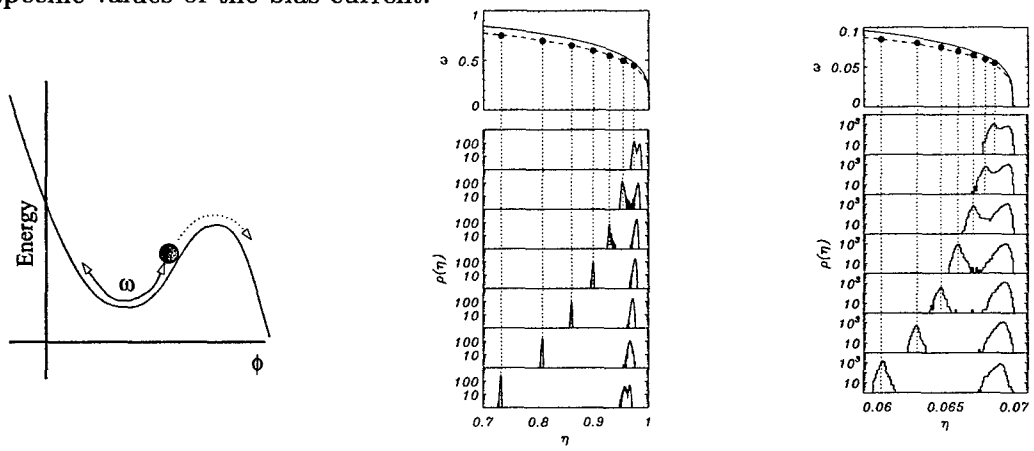

Figure 1: *(left) Sketch of the energetics of the system under consideration: an object is escaping a potential well due to a combination of forced oscillations and thermal fluctuations. (middle – see [4] for details) Escape distributions for different frequencies ω, applied to a pendulum model of a small area Josephson junction, as a function of bias current, η. Upper part shows the agreement with harmonic (solid) and anharmonic (dashed) analyses. (right – see [5] for details) Escape distributions for different frequencies ω, applied to a sine-Gordon model of a long annular Josephson junction with a single trapped fluxon, as a function of bias current, η. Upper part shows the agreement with harmonic (solid) and anharmonic (dashed) analyses.*

We will present comprehensive numerical simulations of the classical system, analytical perturbation results of the nonlinear equations to substantiate the data, and some comparisons to experimental measurements conducted at temperatures well above the quantum transition.

References

[1] J. M. Martinis, M. H. Devoret, and J. Clarke, Phys. Rev. Lett. **55**, 1543 (1985).

[2] A. Wallraff, A. Lukashenko, J. Lisenfeld, A. Kemp, M. V. Fistul, Y. Koval, and A. V. Ustinov, Nature **425**, 155 (2003).

[3] N. Grønbech-Jensen, Phys. Rev. B **45**, 7315 (1992).

[4] N. Grønbech-Jensen, M. G. Castellano, F. Chiarello, M. Cirillo, C. Cosmelli, L. Filippenko, R. Russo, G. Torrioli, *Microwave induced thermal escape in Josephson junctions*, cond-mat/0403245

[5] N. Grønbech-Jensen and M. Cirillo, *Ac-induced thermal vortex escape in magnetic field embedded long annular Josephson junctions*, Preprint (2004).

Flux and phase qubits: techniques of operation

C. Cosmelli

Dipartimento di Fisica, Università La Sapienza, 00185 Roma,italy
Istituto Nazionale di Fisica Nucleare, Roma

Recently, different types of qubits, all based on Josephson junctions, have been experimentally demonstrated. Flux [1,2], phase [3,4,5] and phase-charge [6] qubits have been operated as single devices, while charge qubits have also been used in an entangled couple, showing quantum-coherent behaviour [7] and operation as conditional gate [8]. Which one of the proposed qubits will be the most promising in view of the implementation in a practical quantum computer is still an open issue. The main points that concerns a feasible qubit system relay on the following features: the single qubit should have a long decoherence time, its writing and reading system must be simple, fast and should allow a one shot detectability with high efficiency. The single qubit, moreover, should allow a simple and switchable connection with one or more qubits to realize the core of a C-NOT gate.

In our talk we will present the system we have developed to realize single and coupled set of qubits. At present we have two systems that may operate as a phase and flux qubits. The flux qubit is an rf SQUID realized with standard Niobium trilayer technology, read by a hysteretic dc SQUID working as a one shot detector of the rf SQUID flux states. The hysteretic dc SQUID may operate also as a phase qubits, driven by short pulses of microwaves. On this system we made a set of measurements to show induced oscillations between the first two energy levels of the dc SQUID.

A third scheme to implement a flux qubit, where the reading system is integrated with the qubit has been realized and tested. We will present the main idea underlying the qubit design and some preliminary test on the system, showing the correct behaviour of the proposed device.

To realize an efficient coupling between flux qubits we have proposed and realized a switchable coupling making use of the variable inductance of a hysteretic dc SQUID driven by short pulses of current. This coupling transformer looks, at the moment, one of the most efficient schemes to implement a flux based c-not gate.

References

[1] J.R. Friedman, V. Patel, W. Chen, S. K. Tolpygo, and J. E. Lukens, *Nature* **406,** 43 (2000).

[2] I.Chiorescu, Y.Nakamura, C.J.P.M.Harmans, J.E.Mooij, *Science* **299** (2003) 1869.

[3] J. M. Martinis, S. Nam and J Aumentado, *Phys. Rev. Lett.* **89**, 518 (2002)

[4] Y. Yu, S. Han, X. Chu, and Z. Wang, *Science* **296** , 889 (2002).

[5] C. Cosmelli, M. G. Castellano, F. Chiarello, G. D. Palazzi, S. Poletto, R. Leoni, M. Di Bucchianico, G. Torrioli, *Sup. Science and Techn.* ,**16**, 1337 (2003).

[6] D. Vion, A. Aassime, A. Cottet, P. Joyez, H. Pothier, C. Urbina, D. Esteve, M. H. Devoret, *Science* **296** (2002) 886.

[7] Yu. A. Pashkin, T. Yamamoto, O. Astafiev, Y. Nakamura, D. V. Averin & J. S. Tsai, *Nature* **423** (2003) 823.

[8] T. Yamamoto, Y. A. Pashkin, O. Astafiev, Y. Nakamura, and J.S. Tsai, *Nature* **425**, 941 (2003).

Realization and characterization of a SQUID flux qubit with a direct readout scheme

M. G. Castellano, F. Chiarello, R. Leoni, F. Mattioli, S. Poletto, D. Simeone, G. Torrioli
Istituto di Fotonica e Nanotecnologie – CNR, via Cineto Romano 42, 00156 Roma, e INFN, Sez. Roma
E-mail: chiarello@ifn.cnr.it

C. Cosmelli
Università di Roma "La Sapienza" e INFN, P.le A. Moro 2, 00185 Roma

P. Carelli
Università dell'Aquila e INFN, Monteluco di Roio, 67040 L'Aquila

Superconducting devices based on the Josephson effect have proved to be promising candidates for the implementation of quantum computing. After a demonstrative phase, concerning the capability to implement and couple Josephson qubits [1-8], the actual efforts concern the design and realization of new optimised elements with small decoherence, efficient readout, simple and complete coherent manipulation, integration and coupling of more qubits. In this direction, we introduce a flux qubit based on a fully gradiometric double rf SQUID, with a readout scheme based on the direct injection of current in a large junction in the SQUID loop. The device has been realized, and we present a preliminary experimental characterization at 4.2 K showing the capability to perform an efficient flux state readout.

The qubit is essentially an rf SQUID with the superconducting loop interrupted by a very small inductance hysteretic dc SQUID [9]. The system is described by the magnetic flux threading the large loop, with a potential shaped as a double well (if the externally applied flux is near a half flux quantum, and for appropriate constructive parameters). The distinct flux states in the two minima can be used as computational states "0", "1". The flux applied to the large loop controls the potential symmetry, and can be used to prepare the system in one of the two flux states, and to manipulate the relative phase between them during the computation. The flux applied to the small loop controls the potential barrier height, allowing the freezing or the "rotation" between the flux states [10]. The manipulation can be performed by means of non-adiabatic changes, realized for example by using Rapid Single Flux Quantum Logic elements [11, 12]. Our device is designed in order to have a gradiometric configuration for both the small and the large loops. This has the double advantage to protect the qubit against magnetic noise, and to allow the device self-bias: if a single flux quantum (or an odd number of flux quanta) is trapped in the gradiometric large loop, the qubit is automatically biased near the symmetric condition, required for the computation. The readout scheme is similar to that used for the Quantronium charge-phase qubit [4], and consists in a large junction inserted in the qubit loop. A current pulse directly applied to this junction can induce a transition to the voltage state for a critical value that strongly depends on the qubit flux state. This allows an effective one-shot qubit state readout.

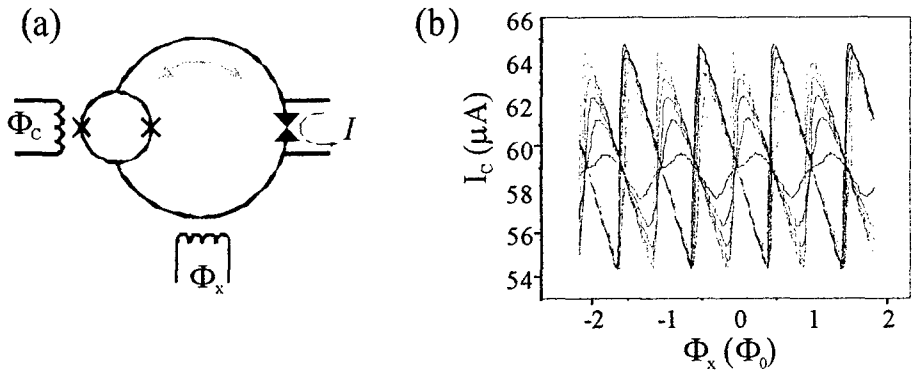

In the above figure are shown: (a) the simplified scheme of the considered flux qubit (for simplicity it is not considered the gradiometric configuration); (b) the plot of the readout critical current I_C for different fluxes Φ_x applied to the large loop (horizontal axis), measured at 4.2 K. The different curves correspond to different fluxes applied to the small control loop (Φ_C), related to different barrier height and distances between minima. Since the measured spread of the critical current due to thermal noise is below 1 μA, the one-shot readout can be performed also at 4.2 K with a very high efficiency.

Bibliography

[1] J. R. Friedman, V. Patel, W. Chen, S. K. Tolpygo, and J. E. Lukens, *Nature 406*, 43 (2000).
[2] J. M. Martinis, S. Nam, and J. Aumentado, *Phys. rev. Lett. 89*, 518 (2002).
[3] Y. Yu, S. Han, X. Chu, S. Chu, and Z. Wang, *Science 296*, 889 (2002).
[4] D. Vion, A. Aassime, A. Cottet, P. Joyez, H. Pothier, C. Urbina, D. Esteve, and M. H. Devoret, *Science 296*, 886 (2002).
[5] I. Chiorescu, Y. Nakamura, C. J. P. Ma. Harmans, and J. E. Mooij, *Science 299*, 1869 (2003).
[6] Y. A. Pashkin, T. Yamamoto, O. Astafiev, Y. Nakamura, D. V. Averin, and J. S. Tsai, *Nature 423*, 823 (2003).
[7] T. Yamamoto, Y. A. Pashkin, O. Astafiev, Y. Nakamura, and J. S. Tsai, *Nature 425*, 941 (2003).
[8] C. Cosmelli, P. Carelli, M. G. Castellano, F. Chiarello, G. Diambrini Palazzi, R. Leoni, G. Torrioli, *Superconductor Science and Technology 16*, 1337 (2003).
[9] S. Han, J. Lapointe, and J. E. Lukens, *Phys. Rev. Lett. 63*, 1712 (1989).
[10] M. G. Castellano, *Fortschr. Phys. 51*, 288 (2003).
[11] R. C. Rey-de-Castro, M. F. Bocko, A. M. Herr, C. A. Mancini, M. J. Feldman, *IEEE Trans. Appl. Sup. 11*, 1014 (2001).
[12] V. K. Semenov and D. V. Averin, *IEEE Trans. Appl. Sup. 13*, 960 (2003).

Transition from Quantum to Classical Information in a Superfluid and Holographic Reconstruction of the Entangled States.

A.Granik

Physics Dept., UOP, Stockton,CA 95211(USA) and G.Chapline , LLNL, Livermore, CA 94330, (USA)

We show that in general the transition from the classical to quantum behavior depends on the probing length scale,and occurs for microscopic length scales, except when the interactions between the particles are very weak. This transition explains why, on macroscopic length scales, physics is described by classical equations.
In particular, the smooth transition from localized quantum mechanical information to classical waves may allow one to holographically reconstruct entangled quantum states.

Questioning the validity of the Two Level Approximation

T. Hakioğlu and Kerim Savran

Department of Physics, Bilkent University, Bilkent, 06533, Ankara, Turkey

We examine the effect of multilevels on decoherence and dephasing properties of a quantum system consisting of a non-ideal two level subspace, identified as the qubit and a finite set of higher energy levels above this qubit subspace. The whole system is under interaction with an environmental bath through a Caldeira-Leggett type coupling. The model that we use is an rf-SQUID in the macroscopic quantum coherence regime and coupled inductively to a flux noise characterized by an environmental spectrum. The model interaction can generate dipole couplings between the qubit subspace and a high number of excitation levels. The decoherence properties of the qubit subspace is examined numerically using the master equation formalism of the system's reduced density matrix. We numerically examine the relaxation and dephasing times as the environmental frequency spectrum, the environmental temperature, and the multilevel system parameters are varied. We observe that, these time scales receive contribution from all available energies in the noise spectrum (even well above the system's energy scales) stressing the dominant role played by the non-resonant (virtual) transitions. The relaxation and dephasing times calculated, strongly depend on the number of active levels. Under the influence of these effects, the validity of the two level approximation is restricted not by the temperature but by the dipole couplings as well as the availability of the environmental modes at low temperatures.

To stress the importance of the non-resonant transitions, we use other model spectral profiles and study the effect of the central frequency, the width and the total spectral area on the decoherence times. We find that, due to the strong influence of the non-resonant transitions, the spectral parameters affect the decoherence times only through the dependence on the spectral area. In this regard the weight of the resonant contributions is negligible as compared to that of the entire noise spectrum.

The credibility of our results depends on the accuracy of the Born approximation in the short time evolution. In this regard, it is crucial that the approximation holds in the range of the numerical data. This has been also confirmed by checking the renormalization of the noise spectrum at the RPA level.

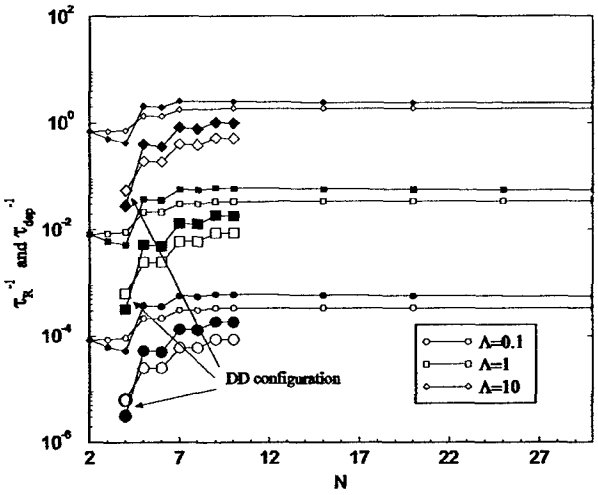

Figure 1. Relaxation and dephasing rates against the number of levels for different spectral widths at T=0. The open and solid symbols refer to dephasing and relaxation times respectively.

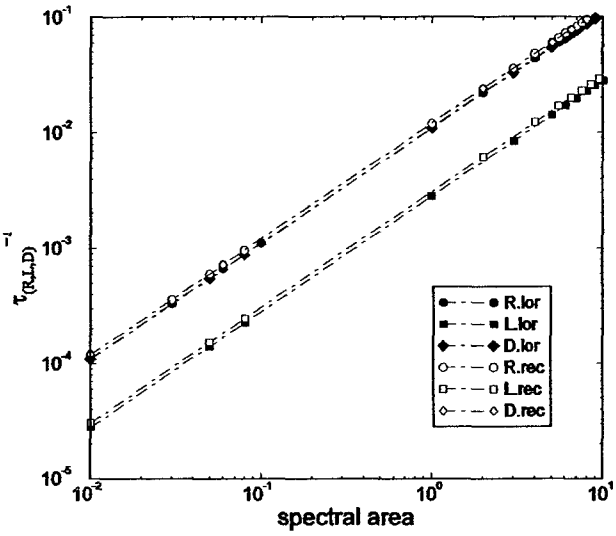

Figure 2. Decoherence times for rectangular and Lorentzian spectra

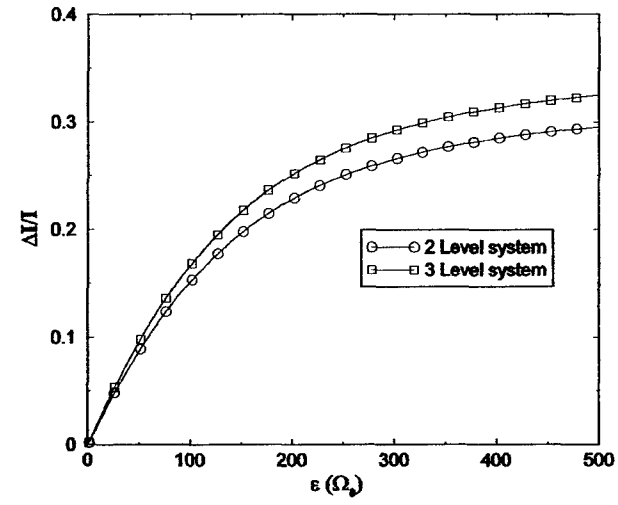

Figure 3. Renormalization of the noise spectrum at the RPA level

References:

[1] A.O. Caldeira, A.J.Leggett, Phys.Rev. Lett. , 46, 211 (1981)

[2] T. Hakioğlu, K. Savran, *Decoherence and dephasing in multilevel systems interacting with thermal environment* cond-mat/0311136 (2003)

Size dependence of the superconductor-insulator transition in Josephson junction arrays

Sung Chung

Department of Physics, Western Michigan University, Kalamazoo, Michigan 49008, USA

The superconductor-insulator (SI) transition in a single Josephson junction (JJ) and JJ arrays in one and two dimensional geometry have been extensively studied. Experimentally observed phase diagrams in the E_J/E_C - g plane show two features [1-5]. Here E_J, E_C and $g=R_Q/R_S$ are, respectively, the Josephson energy, capacitive Coulomb energy of the superconducting islands, and the Ohmic shunt resistance in units of the quantum resistance, $R_Q=h/4e^2$. One is dissipative transition controlled by g and the other is quantum phase transition controlled by E_J/E_C. Here our focus is on the E_J/E_C axis at g=0 where the critical E_J/E_C~3 for a single JJ and ~0.3 for the 48x40 JJ arrays. This order of magnitude difference was argued to be an evidence of cooperative phenomena and the phase boundary in the 48x40 JJ arrays a true phase boundary.

The theoretically irrefutable treatment of the fully 2D quantum mechanical and strongly correlated systems near the phase boundary is an ever-lasing challenge. One simplification is to neglect the quantum fluctuation due to the capacitive Coulomb energy and assume that the single parameter in the resulting 2D XY model E_J/T where T is temperature may play the role of E_J/E_C at T=0. The difference between the fully quantum mechanical JJ and the classical 2D XY model is that the former undergoes a quantum phase transition (QPT) whereas the latter a classical phase transition (CPT). The qualitative resemblance nevertheless lies in the fact that both undergo the Berezinskii-Kosterlitz-Thouless (BKT) transition. More importantly, the strong size dependence seems to be rather universal in two dimension. In fact, while the 2D XY model has been studied extensively in the past, there are two noteworthy development recently concerning the strong size dependence. One is in the context of the planar magnets. It is well-known that in spite of the fact that the BKT transition describing the SI transition is infinite order, in a dozen of planar magnets, the magnetization appears like in the 2-nd order transition with a universal magnetization exponent ~0.23. Bramwell and Holdsworth [6] used renormalization group, Monte Carlo and finite-size scaling to show that the transition looks like 2-nd order with Tc~1.08 for 10^3 spins and ~1.02 for 10^4 spins, which are fairly modified from Tc=0.892 believed to be exact for the infinite system. The size dependence is significant, reflecting the peculiar singularity of the correlation length in the BKT transition. The other development is the transfer-matrix density-matrix-renormalization-group (TM-DMRG) method by the present author [7]. Using the Roomany-Wyld finite-size scaling, without any unknown parameters, nor relying on the BKT-RG, we found that Tc=1.07 for 2000-3000 spins in agreement with [6].

To account for the strong size dependence in the critical E_J/E_C~E_J/T, we need to go one step further and look for a signature of the SI transition as a function of the system size. Note that the 2D XY model is, under Villain approximation, equivalent to the 1D quantum sine-Gordon (SG) model, with the correspondence $E_J/E_C \sim 1/\beta^2$ [8],

$$H = \sum_{i=1}^{L} \{ -\frac{\beta^2}{2} \frac{d^2}{d\phi_i^2} + \frac{1}{2\beta^2} (\phi_i - \phi_{i+1})^2 + \frac{1}{\beta^2} (1 + \cos\phi_i) \}$$

The ground state of the SG Hamiltonian can be analyzed by DMRG. We have found that there is a spontaneous symmetry breaking (SSB) of the ground state as a function of the system size [9]. The identification of the BKT transition as a SSB is then demonstrated by combining DMRG with the Roomany-Wyld finite-size scaling. Fig.1 is the ground state phase diagram in the β^2-L plane. With increase of the size, $E_J/E_C \propto 1/\beta^2$ decreases like $\beta^2(L=5)/\beta^2(L=50) \sim 0.1$ which is consistent with the experimental findings.

After this is done, it is now clear that we can accurately analyze the size dependences of (1) the QPT in the JJ chain with on-site Coulomb fluctuation and (2) the CPT in the 2D XY model for the JJ arrays with relatively large superconducting islands. We will report on the size dependence of the superfluid densities of these systems.

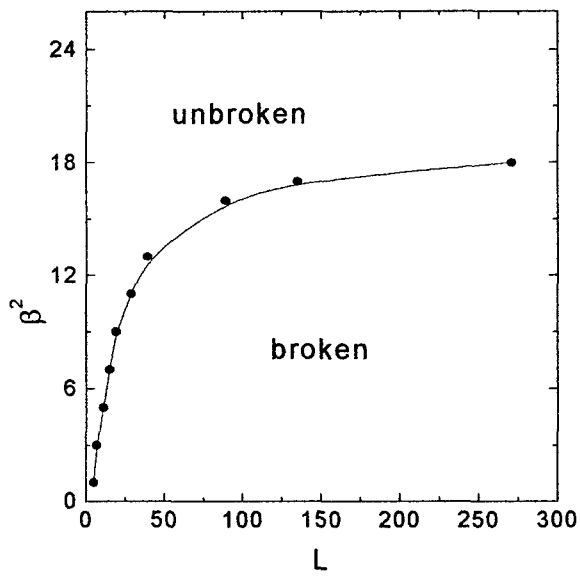

FIG.1 The ground-state phase diagram in the β^2-L plane

[1] J.S. Penttilä, Ü. Parts, P.J. Hakonen, M.A. Paalanen and E.B. Sonin, Phys. Rev. Lett. 82, 1004(1999).
[2] E.Chow, P.Delsing and D.B.Haviland, Phys. Rev. Lett. 81, 204(1998).
[3] R. Yagi, S. Kobayashi and Y. Otuka, J. Phys. Soc. Japan 66, 3722(1997).
[4] H.S.J. van der Zant, W.J. Elion, L.J. Geerligs and J.E. Mooij, Phys. Rev. B 54, 10081(1996).
[5] T. Yamaguchi, R. Yagi, A. Kanda, and S. Kobayashi, Phys. Rev. Lett. 85, 1974(2000).
[6] S.T. Bramwell and P.C.W. Holdsworth, J. Phys. : Condens. Matt. 5, L53(1993)
[7] S.G. Chung, Phys. Rev. B 60, 11761(1999).
[8] C. Itzykson and J.-M. Drouffe, *Statistical Field Theory* (Cambridge University Press, New York, 1989).
[9] S.G. Chung, Phys. Rev. E 62, 3262(2000); K. Korea Phys. Soc. 37, 134(2000), and preprint

Phase regime Josephson junction qubits

Andrew J. Berkley[1], Hanhee Paik[2], Huizhong Xu[2], Sudeep Dutta[2], J. Robert Anderson[2], Christopher J. Lobb[2], and Frederick C. Wellstood[2]

[1] *D-Wave Systems Inc., 320-1985 West Broadway, Vancouver BC, Canada V6J4Y3*
[2] *University of Maryland, College Park, MD 20742 USA*

Isolated large area Josephson junctions can be used as qubits for quantum computation [1-3]. Readout of the junction can be performed by allowing the system to tunnel to the voltage state. Single qubit gate operations are performed by capacitively coupling short microwave pulses into the junction bias current. These pulses must be carefully designed so as to achieve purely σ_x or σ_y operations. The large capacitance of the Josephson junctions, typically a few pF, allows for the use of capacitive inter-qubit coupling [4,5]. While fixed physical capacitors can be used to couple junctions, a tunable capacitance coupling scheme not only simplifies gates, but also reduces perturbation of one qubit by the tunneling of the other qubit to the voltage state. In this talk, I will discuss challenges in implementing single and two qubit gates and a tunable capacitor coupling scheme based on a Cooper pair box.

The microwave pulses for single qubit gate operations can be generated by room temperature electronics. Ideal single qubit gate pulses have a roughly Gaussian envelope and fixed phase and have durations of several nanoseconds [6]. To generate these pulses one needs full vector control of the microwave source, that is control in both amplitude and phase. Errors introduced in the pulse phase by the amplitude modulation, as typically occurs in most pulse modulators, results in single gate operations that can be described as sequenced application of σ_x then σ_y then σ_x on the qubit. Without proper control, this results in effectively a reduced modulation amplitude during Rabi oscillations. Also, since the microwave drive pulses are in the strong drive regime, the rotating wave approximation no longer applies [7] and the envelope of the microwave pulse must be synchronized to the microwave phase with jitter of less than 10 ps for typical qubit parameters and desired gate fidelities. Generating these desired microwave pulses is possible using state of the art electronics.

In the case of fixed capacitive coupling, two qubit operations can be performed by non-adiabatically biasing the qubits to tune the energy level spacing of one qubit into resonance with a second qubit. These bias manipulation pulses must maintain the high signal to noise ratio of the bias current while simultaneously having a high bandwidth. After manipulation, readout of one of the qubits by allowing it to tunnel to the voltage state results in a burst of current to any qubit coupled to it. I will briefly describe an experiment that measures the resulting correlated switching between the two qubits for the case of fixed capacitive coupling This effect can be reduced by using a tunable capacitor between the qubits that can be turned off during measurement.

A tunable capacitor can be implemented by using a Cooper pair box (CPB). The capacitance of a typical CPB for this application can be tuned from 0 fF to roughly 50 fF through gate voltage control. For the simplest version of the tunable capacitor to work, one must avoid resonant interactions between the qubit and the CPB so as to keep

the CPB in the ground state. This can be achieved by designing the Josephson coupling energy E_j, of the CPB to be higher than the energy spacing of the qubit, or by only limiting the gate voltage to the regime where the CPB energy spacing is more than the qubit energy spacing. One must also keep the charging energy E_c, larger than E_j to maintain a large on/off ratio of capacitance. This tunable capacitor scheme can potentially be combined with a bus bar to allow coupling between non-nearest neighbors.

[1] R. C. Ramos, M. A. Gubrud, A. J. Berkley, J. R. Anderson, C. J. Lobb, and F. C. Wellstood, *IEEE Trans Appl Supr 11*, 998 (2001)

[2] J. M. Martinis, S. Nam, J. Aumentado, and C. Urbina, *Phys Rev Lett 89,* 117901 (2002)

[3] Y. Yu, S. Han, X. Chu, S. Chu, and Z. Wang, *Science 296*, 886 (2002)

[4] F. W. Strauch, P. R. Johnson, A. J. Dragt, C. J. Lobb, J. R. Anderson, F. C. Wellstood, *Phys Rev Lett 91*, 167005 (2003)

[5] A. J. Berkley, H. Xu, R.C. Ramos, M.A. Gubrud, F.W. Strauch, P.R. Johnson, J.R. Anderson, A.J. Dragt, C.J. Lobb, and F.C. Wellstood, *Science 300*, 1548 (2003)

[6] M. Steffan, J. M. Martinis, and I. Chuang *Phys Rev B 68*, 224518 (2003)

[7] P. Pradhan, G. Cardoso, M. S. Shariar quant-ph/0402122

Experimental Studies of a Josephson Charge Qubit with RF-SET read-out.

Tim Duty, Kevin Bladh, David Gunnarsson, and Per Delsing

Department of Microtechnology and Nanoscience
Chalmers University of Technology
41296 Göteborg, Sweden

In order to experimentally realize a superconducting charge qubit, one must overcome several challenging problems. The first, which is surprisingly subtle and difficult, involves producing Cooper-pair-boxes with robust even-parity states. One must then optimize the readout while simultaneously minimizing its back-action on the qubit. Finally, the mechanisms of decoherence in Josephson junction qubits must be understood if we are to scale up to many qubits. We must identify both the sources of dephasing and relaxation, and how they couple to the qubit. Although there is much to learn from the mature field of spin physics, superconducting qubits are fundamentally different in that they are mesoscopic objects, the noise is very asymmetric, and measurements are not made on ensembles.

We present experimental studies of a Josephson charge qubit (Cooper-pair-box) that uses radio-frequency, single-electron-transistor (RF-SET) readout. We describe the evolution of our sample fabrication process that led to robust even-parity boxes with SET's that can be operated in the sub-gap regime in a manner that minimizes the backaction. Fast DC pulses are used to manipulate the qubit and coherent oscillations with a high fidelity are consistently observed. The reduction from 100% is understood as an adiabatic effect of the finite pulse rise-time. Measurements of dephasing for the full range of gate charge and on time scales extending to the sub-nanosecond regime have been made. These allow us to attribute the main source of dephasing to fluctuations that couple predominantly to charge.

Measured relaxation times vary considerably and can be smaller than what is expected from either the Ohmic control circuitry or extrapolation of the known 1/f spectrum to GHz frequencies. Investigations of various relaxation processes as well as backaction due to the SET are also presented.

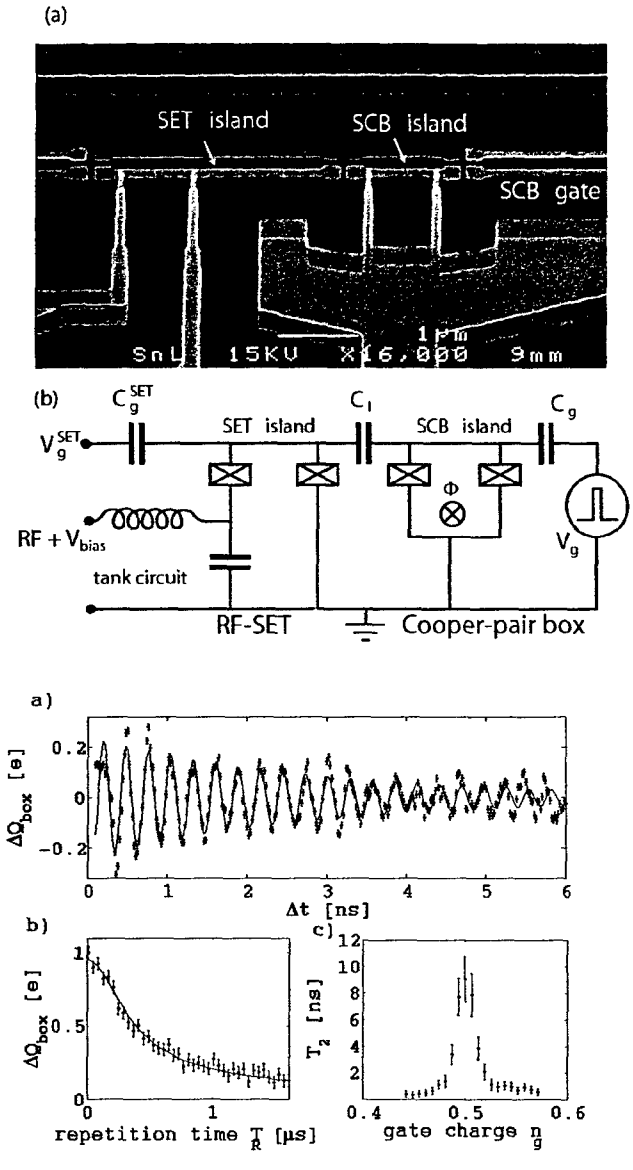

T. Duty, D. Gunnarsson, K. Bladh, and Per Delsing
Phys. Rev. B. **69**, 140503 (2004).

Josephson junction qubit network with current-controlled interaction

J.Lantz, M. Wallquist, V.S. Shumeiko, and G. Wendin
Department of Microtechnology and Nanoscience, Applied Quantum Physics Laboratory Chalmers University of Technology, SE-41296 Gothenburg, Sweden.

After several years of great experimental achievements on Josephson junction (JJ) qubits [2-4], coupling of qubits is now becoming feasible. A few challenging experiments with coupled JJ-qubits have been reported [5]. However, so far experiments on coupled JJ qubits have been performed without direct physical control of the qubit-qubit coupling.
We present a new solution for controllable physical qubit-qubit coupling [1]. The network has the following properties: (a) nearest-neighbour qubit-qubit coupling controlled by external bias current, (b) qubits parked at the degeneracy points, also during qubit-qubit interaction, (c) separate knobs for controlling individual qubits and qubit-qubit coupling, (d) scalability. An important feature is that the network is easily fabricated, and is in line with current mainstream experiments.

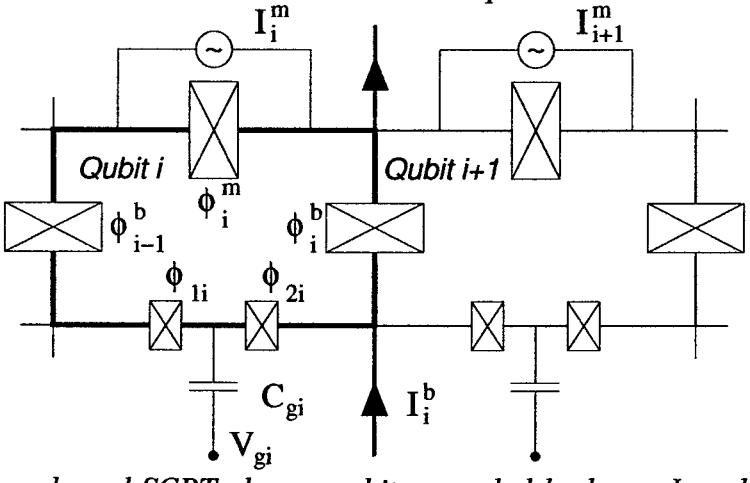

Network of loop-shaped SCPT charge qubits, coupled by large Josephson junctions. The interaction of the qubits (i) and (i+1) is controlled by the current bias I_{bi} or by simultaneous current biasing of readout junctions. Individual qubits are controlled by voltage gates, $n_{gi}=C_{gi}V_{gi}$. The Josephson energies of the coupling JJs, E_J^b, and the readout JJs, E_J^m, are much larger than the charging energies, $E_J^{b(m)} >> E_C^{b(m)}$.

The network under consideration consists of a chain of charge qubits - Single Cooper Pair Transistors (SCPT) - with loop-shaped electrodes coupled together by current biased coupling JJs at the loop intersections. The loop design creates an (inductive) interface to the qubit by means of circulating currents [4]. We employ these current states in the qubit loops to create controllable coupling of neighbouring qubits. Left without any external current biasing of the coupling and readout JJs, the network acts as a quantum memory of independent qubits (neglecting a weak residual interaction [1]). When a bias current is sent through the coupling JJ, the current-current interaction between the neighbouring qubits is switched on and increases with increasing bias current. Moreover, if both of the readout JJs of the same qubits are biased well below threshold, again there is nearest-neighbour coupling via the circulating currents. However, if one of the readout JJs is current biased, this only affects that particular qubit and allows readout of individual qubits. Thus the bias currents serve as the interaction control knobs. The loop inductances are assumed to be

sufficiently small to neglect qubit-qubit coupling via induced magnetic flux, as well as undesirable qubit coupling to the magnetic environment. In addition, we assume negligible capacitive coupling between the islands, which are well shielded by the injection leads.

The qubit network dynamics in the charge qubit regime $E_C >> E_J$ is described by the Hamiltonian

$$H = \sum_{i=1}^{N} [\frac{E_{Ci}}{2}(1-n_{gi})\sigma_{zi} - E_{Ji}\cos\bar{\theta}_i\sigma_{xi} + \eta_i\sigma_{xi}\sigma_{x(i+1)}] + \sum_{i\neq j}\kappa_{ij}\sigma_{xi}\sigma_{xj},$$

which consists of the individual qubits, where $\bar{\theta}_i$ is the mean phase difference induced by current bias in the coupling and readout JJs, the controllable interaction, and finally a weak residual coupling. The residual coupling effectively connects all the qubits, but is a factor $\hbar\omega_p / E_J^b << 1$, where ω_p is the coupling JJ plasma frequency, smaller than the maximum controllable coupling.

In order to couple exclusively the qubits (i) and (i+1) one should apply a current bias I_i^b, while $I_{i\pm1}^b = 0$. In this case the qubit coupling amplitude is given by the equation

$$\eta_i = \frac{E_{Ji}E_{J(i+1)}}{4E_J^b\cos\bar{\phi}_i^b}\sin^2\frac{\bar{\phi}_i^b}{2}.$$

The coupling is quadratic, $\sim(I_i^b / I_c^b)^2$, for small currents and diverges when the current approaches the critical current I_c^b. An alternative way to switch on the qubit interaction is to apply current bias (below the critical current) simultaneously to two neighbouring readout JJs, which will give a similar but weaker interaction.

By applying current bias pulses with controlled amplitude and duration it is possible to perform quantum gates on the qubit network, eg. control-NOT and cNOT-SWAP gates. Readout can be performed either using the readout JJ:s [6] or by measuring the charge on the qubit islands [7].

Finally we emphasize that the present analysis and design is equally relevant in the region of $E_C \sim E_J$, characterizing the "Quantronium" [4].

In conclusion, the present scheme provides a realistic solution for easy local control of the physical coupling of charge qubits via current biasing of coupling Josephson junctions or, alternatively, pairs of readout junctions. The design is in line with experimental mainstream development of charge qubit circuits and can easily be fabricated and tested experimentally. The tunable coupling of the qubit chain allows easy implementation of CNOT and CNOT-SWAP operations.

Acknowledgment - We thank Y. Nakamura, D. Esteve, R. Fazio and P. Delsing for helpful discussions. This work has been supported by the EU IST-FET-SQUBIT project, the Swedish Research Council, and the Swedish Foundation for Strategic Research.

[1] J.Lantz, et al., submitted to Phys. Rev. Lett.; cond-mat/0403285.
[2] Y. Nakamura, Yu.A. Pashkin and J.S. Tsai, Nature 398, 786 (1999).
[3] I. Chiorescu, Y. Nakamura and C.J.P.M. Harmans, J.E. Mooij, Science 299, 1869 (2003)
[4] D. Vion et al., Science 296, 886 (2002).
[5] Yu.A. Pashkin et al., Nature 421, 823 (2003).
[6] I. Siddiqi et al., submitted to Phys. Rev. Lett.; condmat/0312553 and condmat/0312623.
[7] A. Assime et al., Phys. Rev. Lett. 86, 3376 (2001).

Continuous Monitoring of Rabi Oscillations in a Josephson Flux Qubit

E. Il'ichev,[1] N. Oukhanski,[1] A. Izmalkov,[1,2] Th. Wagner,[1] M. Grajcar,[3,4] H.-G. Meyer,[1] A.Yu. Smirnov,[5] Alec Maassen van den Brink,[5] M.H.S. Amin,[5] and A.M. Zagoskin[5,6]

[1]*Institute for Physical High Technology, Jena, Germany*
[2]*Moscow Engineering Physics Institute (State University), Russia*
[3]*Department of Solid State Physics, Comenius University, Bratislava, Slovakia*
[4]*Friedrich Schiller University, Institute of Solid State Physics, Jena, Germany*
[5]*D-Wave Systems Inc., Vancouver, Canada*
[6]*Physics & Astronomy Dept., The University of British Columbia, Vancouver, Canada*

Under resonant irradiation, a quantum system can undergo Rabi oscillations in time, a signature of quantum coherence. We have seen evidence for such oscillations [1] in a continuously observed three-Josephson-junction flux qubit [2]—a macroscopic, SQUID-type device consisting of a small superconducting ring including the three junctions, in which the states correspond to the two possible directions of circulating supercurrent.

In any discussion of quantum phenomena, prominent attention must be given to the readout method. Our qubit is coupled to a high-quality ($Q_T \sim 2000$) superconducting *LC* oscillator (i.e., a tank circuit) tuned to the Rabi frequency, acting as a weakly coupled but sensitive antenna for the oscillations in magnetic flux; see Fig. 1 for the circuit diagram, and Fig. 2 for a micrograph. Since the Rabi frequency is at least two orders of magnitude smaller than the one of the external field (in resonance with the qubit level splitting), the latter is effectively decoupled from the readout circuit. In addition to simplicity, this method of *Rabi spectroscopy* enables a long coherence time of about 2.5 μs (corresponding to an effective qubit quality factor $Q_{Rabi} \sim 7000$), a record for this class of devices. In conclusion, our recent experiments on two coupled flux qubits [3] will be briefly discussed.

[1] E. Il'ichev *et al.*, *Phys. Rev. Lett. 91*, 097906 (2003)
[2] J.E. Mooij *et al.*, *Science 285*, 1036 (1999)
[3] A. Izmalkov *et al.*, *cond-mat/0312332* (2003)

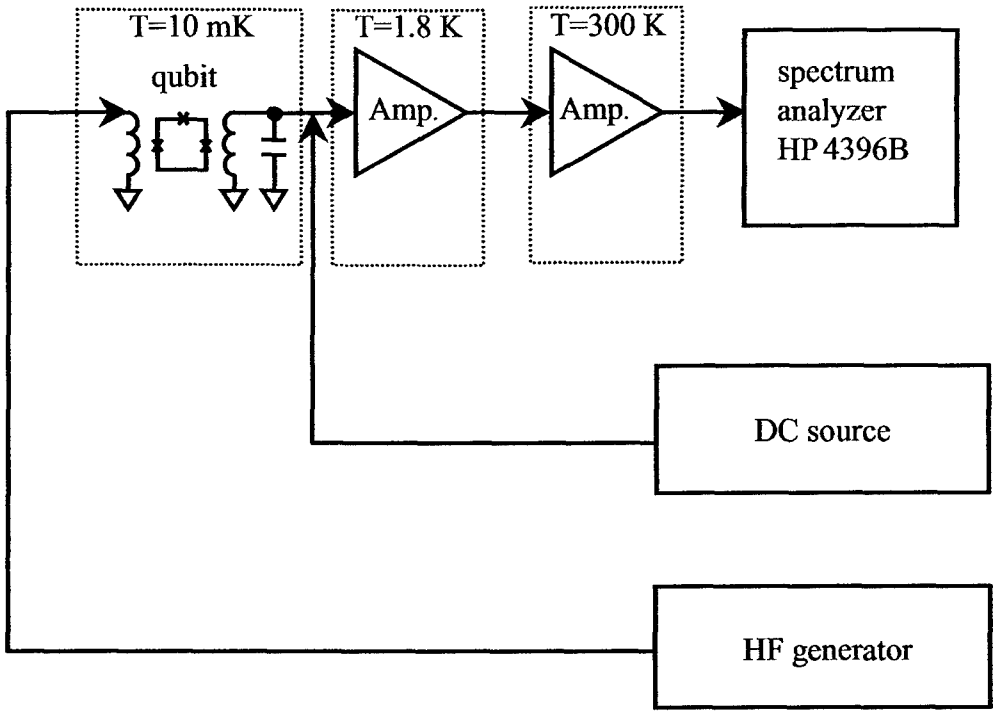

Fig. 1: Measurement setup. The flux qubit is inductively coupled to a tank circuit. The DC source applies a constant flux $\Phi_e \approx \Phi_0/2$. The HF generator drives the qubit through a separate coil at a frequency close to the level separation Δ/h = 868 MHz. The output voltage at the resonant frequency of the tank is measured as a function of HF power.

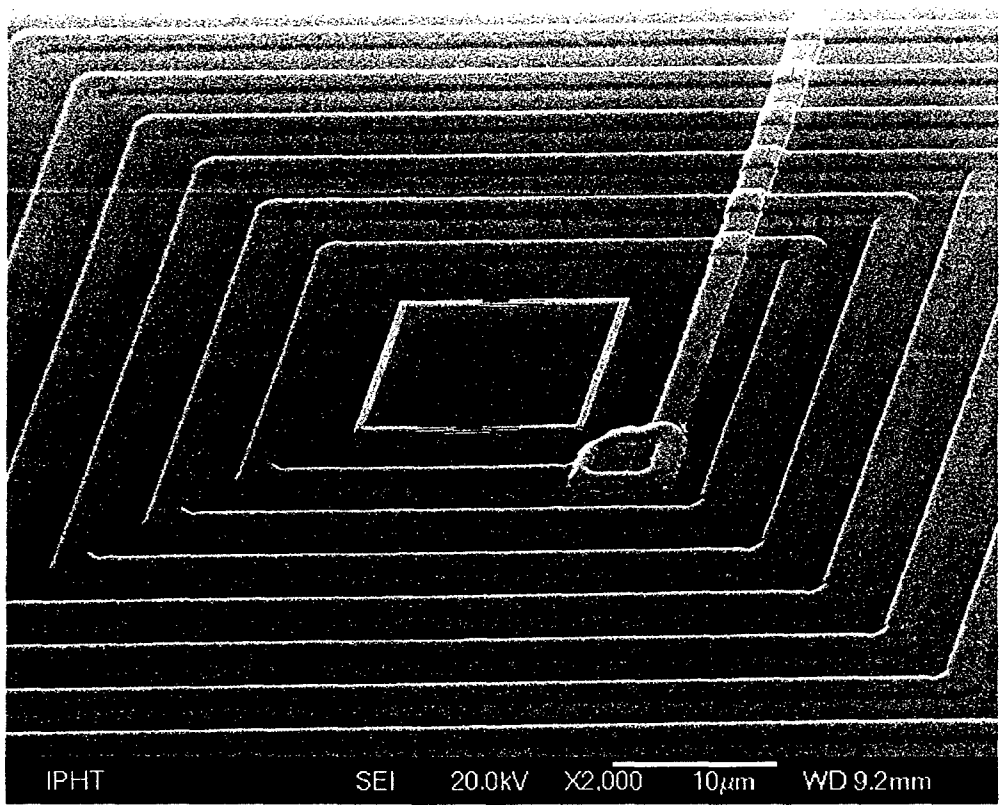

Fig. 2: The aluminum qubit inside the niobium pancake coil.

Josephson Junction Qubits with Symmetrized Couplings to a Resonant LC Bus

Stanford P. Yukon

Air Force Research Laboratory
Hanscom AFB, MA 01731 USA

We investigate the dynamics of a scalable quantum computer employing Josephson junction (JJ) prism qubits coupled to resonant LC buses. The basic qubit states are the symmetric ground $|0\rangle$ and antisymmetric excited $|1\rangle$ states of a two triangular cell JJ prism qubit. The physical qubits are paired into logical qubits that operate in a decoherence free subspace. The circulating currents, corresponding to the $|0\rangle$ and $|1\rangle$ physical qubit states, follow the perimeter of the qubit, and are symmetric with respect to the flux threading the two cells of the qubit. A coupled SQUID gradiometer that is antisymmetric with respect to the flux threading the two cells will not register any coupled flux until a Hadamard gate is carried out on the physical qubit, immediately prior to a measurement. The two basic states are then transformed into $\pm$ combination states that have antisymmetric 'figure 8' circulating currents whose flux is then measurable by the SQUID. The coupling of each qubit to an LC resonant bus is made by means of a loop that encircles both cells of the qubit symmetrically. This prevents the direct mutual inductance coupling of the bus to both antisymmetric microwave gate pulses and the measuring SQUID gradiometer.

One and two logical-qubit gates and bus transfers are carried out using bichromatic Molmer-Sorensen[1] gates. Since a resonant LC bus can only accommodate on the order of 50-100 logical qubits, the system can be enlarged by linking many buses together in an open network. Two adjacent buses may be linked by coupling each bus (one symmetrically and one antisymmetrically to prevent direct coupling) to a pair of physical 'transfer' qubits. A two qubit CN gate across two or more linked buses is accomplished by using one (two logical-qubit) Molmer-Sorensen gate per bus transfer, along with single qubit gates for the control and target qubits. Linking buses in this mannner thus allows for the construction of a quantum computer with the topology of a scalable open network.

[1] A. Sørensen and K. Mølmer, *Phys. Rev. 62*, 022311 (2000)

Quantum Macroscopic Coherence in Josephson Junction Arrays with Non Conventional Architectures

P. Sodano
Dipartimento di Fisica and Sezione I.N.F.N., Università di Perugia, Via A. Pascoli, Perugia, I-06123, Italy

Quite recently it has been evidenced that quantum states may support new kind of orders, which cannot be characterized by broken symmetries and, thus, cannot be described by the conventional Ginzburg-Landau theory [1]. Quantum orders may be viewed as the pertinent description of the pattern of the quantum entanglement in a quantum many-body ground-state. Quantum or topological orders have already been extensively used in the analysis of Fractional Quantum Hall systems [2], leading to an elegant explanation of their robust (against a weak but, otherwise, arbitrary perturbation) ground-state degeneracy and evidencing the intimate connection between the ground-state and the statistics of quasi-particles. The robustness of the ground-state degeneracy makes quantum ordered states very relevant candidates for the engineering of quantum devices naturally taming the intrinsic decoherence of other solid state devices [3]. Very recent studies hint to the new and exciting possibility that the topology of Josephson junction networks (JJN) may be crucial for inducing novel and unexpected macroscopic quantum phenomena [4] as well as for opening [5] to the possibility for an explicit realization of a quantum ordered state.

In this talk I shall focus the attention on the recently discovered possibility that JJN built on suitable graphs may support new and interesting quantum macroscopic states induced only by a pertinent engineering of the geometry and topology of the graph supporting the network [4]. In particular, I shall consider JJN built on comb-like graphs and star-graphs evidencing the fact that - already for this very simple graph topology - the array exhibits quantum macroscopic coherence at low temperatures. After discussing the theoretical possibility of a spatial Bose-Einstein condensation (BEC) of Cooper pairs for a JJN built on a comb-graph, I also shall discuss here a simple experiment which could enable to observe BEC in these systems .

A network of superconducting Josephson junctions is usually described by

$$H = -E_J \sum_{\langle i;j \rangle} \cos(\phi_i - \phi_j) + E_C \sum_i n_i^2 .$$

On each site i of the network there is a superconducting grain and the junctions are located between neighboring sites with Josephson energy E_J; $E_C = 2e^2/C_0$, where C_0 is the grain self-capacitance and e the electron charge, is the charging energy. ϕ_i is the phase of the superconducting order parameter at site labeled by i and its conjugate variable n_i ($[\phi_i, n_j] = \delta_{ij}$) describes the number of Cooper pairs in the i-th superconducting grain. The parameter E_J is related to the critical Josephson current $I^{(0)}$ by the relation $I^{(0)} = 2eE_J/\hbar$. The summation $\sum_{\langle i;j \rangle}$ runs over all the distinct nearest-neighbors pairs. By properly engineering the insulating support on which the superconducting grain are placed, one can realize star-shaped or comb-shaped networks: in Fig.1 a schematic description of a Josephson junction comb network is reported.

The computation of the Cooper pairs number for comb- [6] and star-network [7] yields that, below the critical temperature T_C at which BEC occurs, the critical Josephson current $I_c(T)$ of a junction far away from the backbone (center) of the comb (star) is given, in the limit $E_C \to 0$, by

$$\frac{I_c(T)}{I^{(0)}} \approx \frac{T}{T_c}$$

where $I^{(0)}$ is the critical current of the same Josephson junction for $T > T_c$ (see inset of Fig.1). This suggests that the measurement of the critical current of a suitably chosen junction should enable to detect the effect of the topology induced BEC in graph-shaped network.

[1] X. G. Wen, Phys. Lett. A , 175 (2002); Phys. Rev. B , 165113 (2003).
[2] X. G. Wen and Q. Niu, Phys. Rev. B , 9377 (1990).
[3] Y. Makhlin, G. Schön and A. Shnirman, Rev. Mod. Phys. , 357 (2001).
[4] R. Burioni, D. Cassi, I. Meccoli, M. Rasetti, S. Regina, P. Sodano, and A. Vezzani, Europhys. Lett. , 251 (2000).
[5] L. B. Ioffe and M. V. Feigel'man, Phys. Rev. B , 224503 (2002); B. Douçot, M. V. Feigel'man, and L. B. Ioffe, Phys. Rev. Lett. , 107003 (2003).
[6] G. Giusiano, F.P. Mancini, P. Sodano, and A. Trombettoni, Int. J. Mod. Phys. **B 18**, 691 (2004).
[7] I. Brunelli, G. Giusiano, F. P. Mancini, P. Sodano, and A. Trombettoni, J. Phys. **B 37**, S275 (2004).

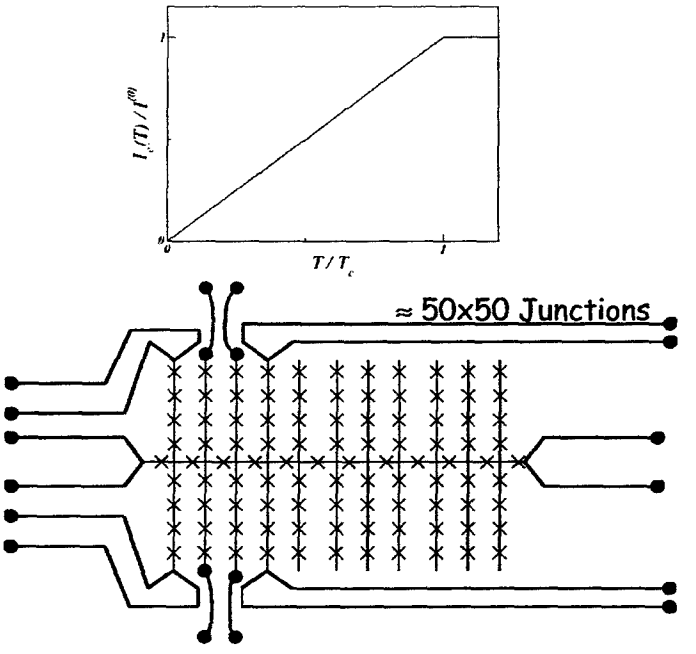

Fig.1. A schematic plot of a typical experimental setup with 50×50 Josephson junctions placed at the sites of the comb-shaped graph. Notice that superconducting grains belonging to neighbouring vertical fingers of the comb are *not* weakly coupled. Inset: Predicted Josephson critical current (in units of $I^{(0)}$) vs. T/T_c of a junction located far away from the horizontal backbone.

Properties of the Cooper pair shuttle

Rosario Fazio, Simone Montangero and Alesandro Romito
NEST-INFM & Scuola Normale Superiore I-56126, Pisa

Very recently, Gorelik *et al.* [1] proposed a very appealing setup, the Cooper pair shuttle, able to create and maintain phase coherence between two distant superconductors. It consists in a superconducting SET transistor where the metallic grain is driven in a periodic motion between the two electrods. The shuttling effect manifests in the fact that there is charge transport even though the grain, during is motion, is always in contact with only one of the elecrodes. Because of the superconducting electrodes, the shuttle does not only carry charge, as in the normal metal case, but it also establishes phase coherence between the superconductors. This is witnessed by the presence of a steady stste Josephson current.

We analyze how the presence of the environment affects the coherent transport, both in the average current and its moments, in the Cooper pair shuttle [2]. For the environment we consider the case when this is determined gate voltage fluctuations. The expression of the Josephson current depends on the phases of the superconducting electrodes, on the dynamical phases acquired during the motion of the central island and on the dephasing rates. Depending on the value of the dynamical and superconducting phases the critical current can be negative, i.e. the system can behave as a π-junction. An analysis of the critical current as a function of the dephasing rates reveals another interesting aspect: the Josephson current is a non-monotonous function of the damping the Josephson current can *increase* on increasing the coupling to the environment. The typical behaviour of the Josephson current as a function of the phases is shown in Fig.1

Cooper pair shuttling is a result of a non equilibrium steady state process. Therefore, to better characterize the transport, we analyzed supercurrent noise fluctuations. This should be contrasted with the standard Josephson effect, where the supercurrent is an equilibrium property of the system. Finally, we briefly discuss the finite frequency spectrum in the case of strong dephasing. Superimposed to the peak at the Josephson energy, there are oscillations of frequency of the order of period. The presence of these oscillations is related to the periodicity of the island motion. The modification of these fringes as a function of the phases is a signature of the coherence in the Cooper pair shuttle.

The full-counting statistics was analyzed by one of us in [3].

A possible experimental test of our results which does not require any mechanically moving part. The time dependence of the Josephson couplings can be regulated by a time dependent magnetic field and gate voltage, respectively. The setup consists of a superconducting nanocircuit in a uniform magnetic field. By substituting the Josephson junction by SQUID loops, it is possible to control the E_J by tuning the applied magnetic field piercing the loop. A configuration with three type of loops with different area, allows to achieve the require time dependence by means of a *uniform* magnetic field. This implementation has several advantages. It allows to control the coupling with the environment by simply varying the time dependence of the applied magnetic field. The time scale for the variation of the magnetic field should be controlled at the same level as it is done in the implementation of Josephson nanocircuits for quantum computation.

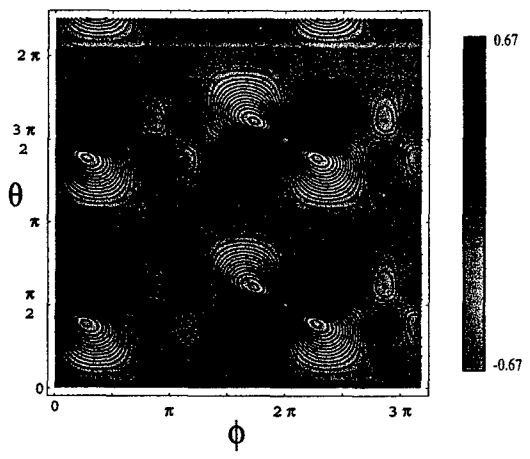

FIG. 1: Supercurrent (in units of e/T) as a function of the superconductor phase difference ϕ and of the phase accumulated during the contact to one of the electrodes θ.

In the limit in which the Josephson energy is much larger than the charging energy, the Cooper pair shuttle implements [4] a paradigm model for quantum chaos, the quantum kicked rotator. In this limit one can study dynamical localization and by further coupling the shuttle to a Cooper pair box it is possible to measure the dynamical fidelity as suggested in [5].

[1] L. Y. Gorelik, *et al.* Nature **411**, 454 (2001).
[2] A. Romito, F. Plastina and R. Fazio, Phys. Rev. **B 68**, R140502 (2003).
[3] A. Romito and Yu.V. Nazarov, cond-mat 0402412
[4] S. Montangero, A. Romito and R. Fazio, in preparation.
[5] S.A. Gardiner, J.I. Cirac and P. Zoller, Phys. Rev. Lett. **79**, 4790 (1997).

Dynamical suppression of discrete noise in Josephson qubits

G. Falci, A. D'Arrigo, A. Mastellone, and E. Paladino
Dipartimento di Metodologie Fisiche e Chimiche (DMFCI), Universitá di Catania. Viale A. Doria 6, 95125 Catania (Italy) & MATIS - Istituto Nazionale per la Fisica della Materia, Catania

Controlling the dynamics of a complex quantum system is at the heart of quantum information processing [1]. However in any real device the computational degrees of freedom entangle with the environment leading to decoherence [2]. Open-loop Bang-Bang (BB) quantum control techniques have been proposed as a way to achieve an effective decoupling from the environment [3, 4]. They may be operated by a sequence of very strong external pulses separated by a time Δt [3]. In the limit $\Delta t \to 0$ full decoupling [3, 4] of the unwanted interactions is achieved since the effective dynamics produced by them is averaged out by BB. The physics in this limit is a manifestation of the quantum Zeno effect [3, 5]. In practice Δt is finite especially if full-power pulses are generated. Thus decoupling is not perfect but the Zeno limit physics is still a good description if $\Delta t \ll \gamma^{-1}$, the typical time scale of the environment [3, 4]. If γ is large one may argue that BB chops noise and frequencies $\omega < 1/\Delta t < \gamma$ are averaged out. This optimistic scenario could foresee important applications to solid state coherent devices, where low-frequency noise [6] is one of the major problems for quantum state processing [7–9] and has been exploited in a series of recent papers [10–12].

Here we study environments of dissipative quantum bistable fluctuators [7], describing charge noise due impurities close to a solid-state qubit [7, 8, 13] which are responsible of a distictive phenomenology recently observed [14]. We consider a qubit ($\mathcal{H}_Q = -\frac{\epsilon}{2}\sigma_z - \frac{\Delta}{2}\sigma_x$) coupled to an impurity. The Hamiltonian has the general form [12]

$$\mathcal{H} = \mathcal{H}_Q - \frac{1}{2}\sigma_z \hat{E} + \mathcal{H}_E + \mathcal{V}(t) \tag{1}$$

where $\mathcal{H}_E$ describes an impurity level occupied by a localized electron, tunneling to a fermionic band whith switching rate γ. The charge in the impurity is coupled to the qubit, $\hat{E} = v\hat{n}_{imp}$, and operates as a stray random bias of amplitude v. Control is operated by $\mathcal{V}(t)$, representing a sequence of instantaneuos π-pulses about the $\hat{x}$ axis of the Bloch sphere. The evolution operator of the Hamiltonian (1) is $[\sigma_x \mathcal{S}]^{2N}$, where $\mathcal{S} = \exp(-i\mathcal{H}\Delta t)$ with $\mathcal{V}(t) = 0$ is the evolution between pulses. In order to take into account memory effects of the environment we denote with $\rho(t)$ the reduced density matrix (RDM) of the *qubit plus localized level* and use a standard master equation to find the map $\mathcal{E}_{\Delta t}[\rho(t)] = \rho(t+\Delta t) = e^{\mathcal{L}\Delta t}\rho(t)$. After $t = 2N\Delta t$ we get $\rho(t) \approx \left[\mathcal{P}\cdot e^{\mathcal{L}\Delta t}\right]^{2N}\rho(0)$ where $\mathcal{P}$ is the superoperator of the pulses. The RDM of the qubit $\rho^Q = \mathrm{Tr}_d[\rho(t)]$ is obtained by tracing out the localized level *at the end* of the protocol.

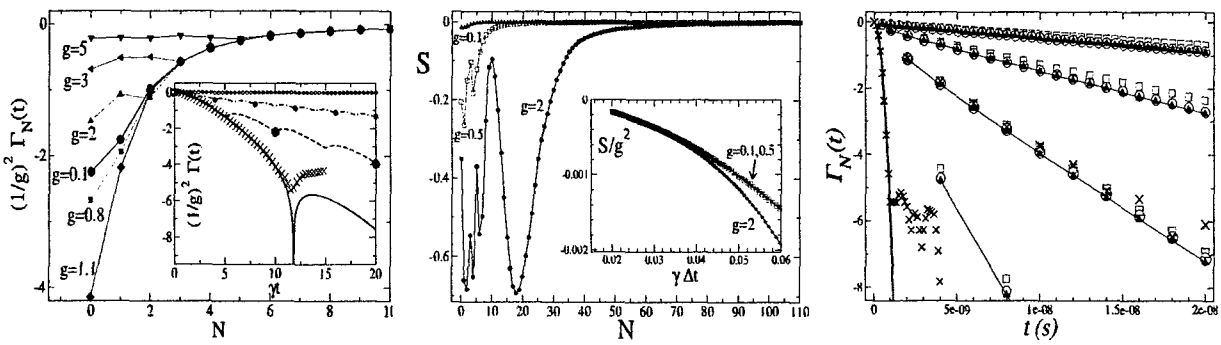

FIG. 1: **Left panel** - For fixed $t = 10\gamma^{-1}$ we plot $\Gamma_N(t)/g^2$ for BB procedures with N echoes. The parameter is $g \equiv v/\gamma$. A gaussian environment with the same power spectrum would give, for arbitrary g, the curve here labeled with $g = 0.1$. In the inset $\Gamma(t)$ for $g = 1.1$ without (thick line) and with pulses compared with results of the stochastic Schrödinger equation (crosses).
Central panel - We plot $S = \ln[\mathrm{Tr}(\rho^Q)^2]$ at fixed $t = 8\gamma^{-1}$ for protocols with N echo pair of pulses. Curves are parametrized by $g = (\Omega_1 - \Omega_0)/\gamma$. Here $\epsilon = \Delta$, $v/\Omega = 0.2$. In the inset it is shown that S scales as g^2 for $N \gg 1$.
Right panel - BB control of $1/f$ noise for $\Delta = 0$. The analytic $\Gamma_N(t)$ at $t = 2N\Delta t$ (symbols) is compared with the evolution with no pulses (thick solid line). Noise is generated with N_{fl} fluctuators with rates γ_i distributed from $10^4\,Hz$ to $10^{10}\,Hz$. Noise level $\propto v^2 N_{fl}$ is *fixed* at a value typical of experiments in charge qubits: it is realized with coupling $v = 9.23\cdot 10^9\,Hz$, for $q = 6$ (full triangles), 7 (circles) and 8 (squares), with $N_{fl} = 6\cdot 10^{17-2q}$. Crosses are stochastic Schrödinger simulations with 10^5 realizations of the $1/f$ process, for $q = 7$.

The major step of this program is the diagonalization of the 8×8 supermatrix $\left[\mathcal{P} \cdot e^{\mathcal{L}\Delta t}\right]^2$.

In some cases the calculation can be carried out analytically, as for $\Delta = 0$ [12]. We find that decoupling of this environment is sensitive to details of its dynamics. If pulses are not very frequent it shows a rich variety of behaviors, suggesting that BB may also be used for spectroscopy of a solid-state environment. An important parameter is $g = (\Omega_1 - \Omega_0)/\gamma$, where Ω_i are the splittings of the qubit when the fluctuator sits in state i, which quantifies the non-gaussianity of the environment [7]. Slow fluctuators ($g > 1$) are responsible for inhomogeneuos broadening and for a physics dominated by memory effects where decoherence depends strongly on details of the protocols. We study the decay of the coherences of the qubit, given by $\Gamma_N(t) = \ln \left| \frac{\rho_{ab}(t)+\rho_{cd}(t)}{\rho_{ab}(0)+\rho_{cd}(0)} \right|$ (Fig. 1 left). At any fixed $\bar{t} = 2N\Delta t$, $|\Gamma_N(\bar{t})|$ decreases monotonically when the pulse frequency $1/\Delta t$ increases, which shows that BB effectively suppresses RTN and in this regime $|\Gamma_N(\bar{t})| \sim g^2$ shows universal behavior. On other hand for $2N \ll \gamma t$ qualitative differences in the behavior are apparent for $g < 1$ and $g > 1$. The physics for $\Delta \neq 0$ is even richer. We study the degree of purity $S = \ln \mathrm{Tr}(\rho^Q)^2$, efficient decoupling corresponding to $S = 0$, i.e. localization in a "Zeno subspace" [5] which is a pure state. Results (Fig. 1 central) show that for frequent pulses $S \approx 0$, but decoupling of a slow fluctuator, $g > 1$, requires a very large N. Again we find universal behavior, $S \sim g^2$ (inset of Fig. 1 central). Instead for a smaller number of pulses it may happen, especially for $g > 1$ that S is not monotonic with N, including the possibility that the qubit decays *faster* than in absence of pulses [3], reminiscent of the *inverse* Zeno effect [5].

In order to treat $1/f$ noise we now extend our formalism to a "multi-mode" environment. We first generalize the results at $\Delta = 0$ of Ref. [3], to an arbitrary (non-gaussian) environment. For the evolution between two pulses at t_1 and t_2 we can use $[\mathcal{H}, \sigma_z] = 0$ and following the same steps of Ref. [3] we can write the evolution operator for a BB procedure at $t = 2N\Delta t$ as $\mathcal{S}_{2N}(t) = \left[e^{-i(\mathcal{H}_E + \frac{1}{2}\sigma_z \hat{E})\Delta t} e^{-i(\mathcal{H}_E - \frac{1}{2}\sigma_z \hat{E})\Delta t}\right]^N$. In the overall BB procedure σ_z is conserved, so we need only off diagonal entries of the RDM of the qubit, in the σ_z basis $\rho^Q_{\sigma\sigma'}(t) = \rho^Q_{\sigma\sigma'}(0)\, \mathrm{Tr}_E\left\{ \mathcal{S}_{2N}(t|\sigma)\, w_E\, \mathcal{S}^\dagger_{2N}(t|\sigma') \right\}$ where we assumed factorized initial conditions. Here $\mathcal{S}_{2N}(t|\sigma) = \langle \sigma | \mathcal{S}_{2N}(t) | \sigma \rangle$ expresses the conditional evolution of the environment under a well defined sequence of $\sigma = \pm 1$. The trace factorizes if the environment is made of noninteracting "modes", so we can apply this result to a set of noninteracting impurities originating $1/f$ noise. In particular the decay of the coherences is $\Gamma_N(t) = \sum_\eta \ln \left| \frac{\rho^{(\eta)}_{ab}(t)+\rho^{(\eta)}_{cd}(t)}{\rho_{ab}(0)+\rho_{cd}(0)} \right|$. Results in the right panel of Fig. 1 show that frequent pulses (curves with many symbols) drastically reduce decoherence. For noise levels typical of experiments with charge qubits (Fig. 1 right) the pulse rate for substantial recovery is practically independent on v. The situation may change if a broad distribution of the couplings v is considered [10]. The physics is richer for $\Delta \neq 0$ and possibly compensation of $1/f$ noise is non monotonic for increasing pulse frequency, as it happens for a single impurity.

---

[1] M. Nielsen and I. Chuang, *Quantum Computation and Quantum Communication*, Cambridge University Press, (2000).

[2] W. Zurek, Physics Today **44**, 36 (1991); G.M. Palma *et al.*, Proc. Roy. Soc. London A **452**, 567 (1996); U. Weiss, *Quantum Dissipative Systems*, World Scientific, Singapore (2001); H. Breuer and F. Petruccione, *The Theory of Open Quantum Systems*, Oxford University Press (2002).

[3] L. Viola and S. Lloyd, Phys. Rev. A **58**, 2733 (1998).

[4] L.Viola *et al.*, Phys. Rev. Lett. **82**, 2417 (1999); D. Vitali and P. Tombesi, Phys. Rev. A 59, 4178-4186 (1999).

[5] H. Nakazato *et al.*, Int. J. Mod. Phys. B 10, 247 (1996); P. Facchi and S. Pascazio, Phys. Rev. Lett. 89, 080401 (2002); E. Knill *et al.*, Phys. Rev. Lett., **84**, 2525 (2000); P. Zanardi, S. Lloyd, Phys. Rev. Lett., **90**, 067902 (2003); P. Facchi *et al.*, quant-ph/0303132; P. Facchi *et al.*, Phys. Rev. Lett. **86**, 2699 (2001).

[6] P. Dutta and P.M. Horn, Rev. Mod. Phys. **53**, 497 (1981); M.B. Weissmann, Rev. Mod. Phys. **60**, 537 (1988).

[7] E. Paladino *et al.*, Phys. Rev. Lett. **88**, 228304 (2002); E. Paladino *et al.*, Adv. Sol. State Phys., **43**, 747 (2003), cond-mat/0312411.

[8] G. Falci, E. Paladino, R. Fazio, in *Quantum Phenomena of Mesoscopic Systems*, B.L. Altshuler and V. Tognetti Eds., Proc. of the International School "Enrico Fermi", Varenna 2002, IOS Press (2003), cond-mat/0312550.

[9] A. Zorin *et al.*, Phys. Rev. B **53**, 13682 (1996); H. Muller *et al.*, Europhys. Lett. **55**, 253 (2001); Y. Nakamura *et al.*, Phys. Rev. Lett. **88**, 047901 (2002).

[10] E. Paladino *et al.* in *Macroscopic Quantum Coherence and Computing*, Kluwer (2003); E. Paladino *et al.*, Physica E, **18**, 29, (2003); Y.M. Galperin et al., cond-mat/0312490.

[11] H. Gutmann *et al.*, cond-mat/0308107; K. Shiokawa and D. Lidar, quant-ph/0211081; L. Faoro and L. Viola, quant-ph/0312159.

[12] G. Falci, A. D'Arrigo, A. Mastellone and E. Paladino, cond-mat 0312442.

[13] N.M. Zimmerman, J.L. Cobb and A.F. Clark, Phys. Rev. B **56**, 7675 (1997); R. Wakai and D. van Harlingen, Phys. Rev. Lett. **58**, 1687 (1987).

[14] Measurements were made by Chalmers Group (Goteborg) and by Quantronics Group (Saclay), priv. comm.

Optimal quantum machines by linear and non-linear optics

Fabio Sciarrino, and Francesco De Martini

Dipartimento di Fisica, Università di Roma La Sapienza

Istituto Nazionale per la Fisica della Materia

Since manipulations of qubits are constrained by the quantum mechanical rules, several classical information tasks can not be perfectly extended to the quantum world. The more relevant limitations in quantum information processing are the impossibility to perfectly clone any unknown qubit $|\phi>$ and to map it in its orthogonal state $|\phi^{\perp}>$. Even if these two processes are unrealizable in their exact forms, they can be optimally approximated by the so-called *universal quantum machines*: the optimal quantum cloning machine (UOQCM) and the universal-NOT (U-NOT) gate, which exhibit the minimum possible noise. Investigation of these optimal transformations is important since it reveals bounds on optimal manipulations of information with quantum systems.

The U-NOT gate and the UOQCM, have been contextually realized by adopting the process of stimulated emission generated by a single photon into an optical parametric amplifier [1]. We shall present how it is possible to implement the $1 \rightarrow 2$ UOQCM and the $1 \rightarrow 1$ U-NOT gate by slightly modifying the quantum state teleportation protocol [2]. In this case the UNOT gate is transferred in a different location, we deal hence with the teleportation of a quantum operation: the Tele-UNOT gate. A complete experimental realization of the protocol by a fully *linear* method will be discussed.

[1] F. De Martini, V.Buzek, F. Sciarrino, and C. Sias, *Nature (London)* 419, 815 (2002); F. De Martini, D. Pelliccia, and F. Sciarrino, *Phys. Rev. Lett.* 92, 067901(2004).

[2] M. Ricci, F. Sciarrino, C. Sias, and F. De Martini, *Phys. Rev. Lett.* 92, 047901 (2004); F. Sciarrino, C. Sias, M. Ricci, and F. De Martini, *Phys. Lett. A* 323, 34 (2004).

Monte Carlo method for a superconducting Cooper-pair-box charge qubit measured by a single-electron transistor

Hsi-Sheng Goan

Center for Quantum Computer Technology, University of New South Wales, Sydney, NSW 2052, Australia

A Monte Carlo method which allows one to follow each electron tunneling event has been successfully applied to simulate transport properties of a single-electron transistor (SET) or more complicated single electronics circuits. This method gives physical insight into the processes taking place in the simulated system, and macroscopic ensemble properties can be calculated using large ensembles of single electron tunneling events. But to our knowledge, it has not yet been formally applied to quantum measurement problems by a SET detector. Here, we provide such an investigation and derive the *quantum-jump* [1,2] stochastic master equation (or quantum trajectory equation) for a single superconducting Cooper-pair-box (SCB) charge qubit (generalization to other charge qubit case is simple) continuously measured by a SET [3]. We also show that the master equation for the "partially" reduced density matrix presented in Ref. [3] (referred to here as a "partial" course-grain description) can be obtained by taking a "partial" average on the stochastic master equation over the fine grained measurement records of the tunneling events in the SET.

If a measurement is made on the qubit system and the results are available, the state or density matrix is conditioned on the measurement results. If the subsequent system evolution after the measurement is concerned, the conditional, stochastic master equations derived here should be employed. A set of typical quantum trajectories (stochastic state evolutions) and its corresponding measurement record are shown in Fig. 1 to illustrate the conditional dynamics. We consider the case that the leading tunneling process in the SET are sequential transitions between two adjacent charge states N=0 and N+1=1 on the SET island. $dN_{L/R,c}$ represents the number (either zero or one) of electron tunneling events seen in the infinitesimal time dt through the left and right junctions of the SET, respectively. The subscript c indicates that the quantity to which it is attached is conditioned on previous measurement results. As expected, due to Coulomb blockade, the SET measurement record of the randomly distributed moments of detections shown in Fig. 1(i) and (j) is in the order of an exactly alternating $dN_{Lc}=1$ and $dN_{Rc}=1$ time sequence. The joint reduced density matrix operator of the SCB qubit and extra charge on the SET island can be written as $R_c=\rho_{N,c}|N\rangle\langle N|+\rho_{N+1,c}|N+1\rangle\langle N+1|$, where $\rho_{N/N+1,c}(t)$ is each a 2x2 operator in the qubit basis. The conditional qubit density matrix operator alone can be obtained by writing $\rho_c(t)=\mathrm{Tr}_N[R_c(t)]=\rho_{N,c}(t)+\rho_{N+1,c}(t)$. Figure 1(a)-(d) show the time evolution of the joint SCB-qubit and SET-island diagonal density matrix elements conditioned on the measurement results of Fig. 1(i) and (f). The conditional evolutions of the qubit alone shown in Fig. 1(e) and (f) can be obtained from the sum of the joint state evolutions of (a) and (b), or (c) and (d), respectively. The probabilities, $P_{0/1,c}=\mathrm{Tr}_{\mathrm{qb}}[\rho_{0/1,c}]=\rho^{00}_{0/1,c}+\rho^{11}_{0/1,c}$ of the SET island state alone in (g) and (h) can be

obtained by summing the evolutions in (a) and (c), or (b) and (d), respectively. Each quantum trajectory mimics a single history of the qubit state in a single run of the continuous measurement experiment. The conditional evolutions in (a)-(h) differ considerably from their ensemble average counterparts.

If only one measurement value is recorded in each run of experiments (e.g., the number of electrons N_R that have tunneled into the right lead or the drain in time t) and ensemble average properties (e.g, $P(N_R,t)$ the probability distribution of finding N_R in time t) are studied over many repeated experiments, the quantum trajectory approach presented here will give the same result as the master equation approach of the ``partially" reduced density matrix [3]. This is demonstrated in Fig. 2. However, the possible individual realizations of quantum trajectories and their corresponding measurement records (e.g, in Fig. 1) do provide insight into, and aid in the interpretation of the average properties.

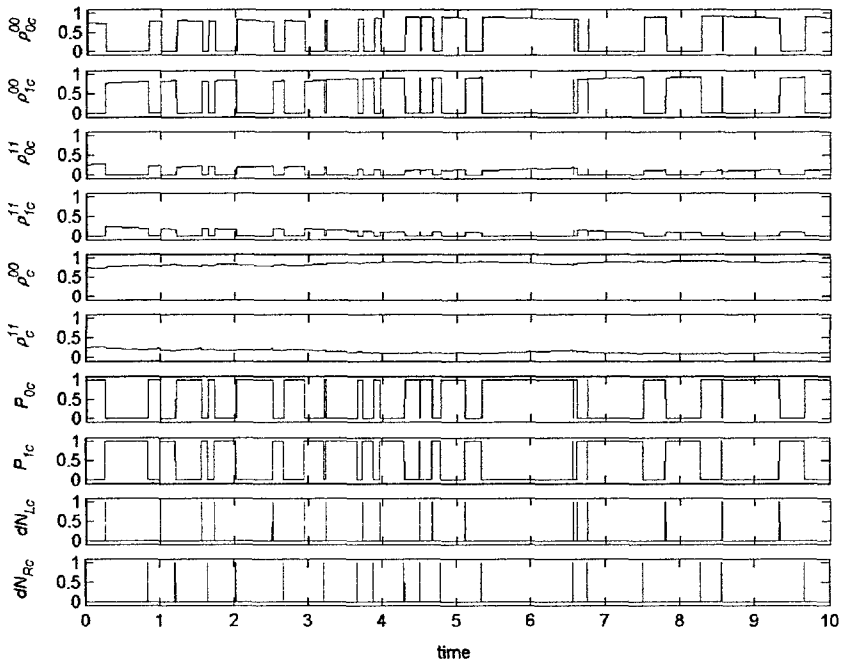

Figure 1. Conditional time evolution of the SCB charge qubit measured by the SET.

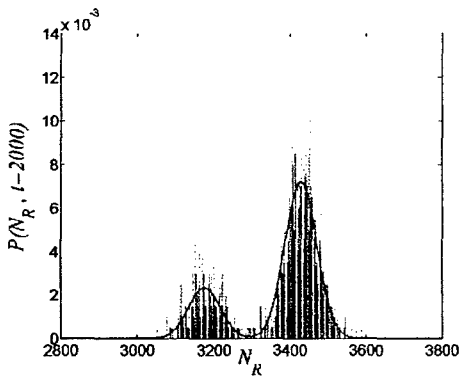

Figure 2. Probability distribution $P(N_R,t=2000)$. Our simulation of the normalized histogram, using 2000 quantum trajectories and their corresponding detection records, is already in good agreement with the plot in solid line, obtained from the Fourier analysis of the partially reduced density matrix method described in Ref.[3].

[1] H.-S. Goan et al., *Phys. Rev. B* **63**, 125326 (2001); Phys. Rev. B **64**, 235307 (2001).
[2] H.-S. Goan, *Quant. Info. Comp.* **3**, 121 (2003).
[3] Y. Makhlin, A. Shnirman and G. Schon, *Rev. Mod. Phys.* **73**, 357 (2001).

Entanglement in quantum critical spin systems in one and more dimensions

Tommaso Roscilde, Stephan Haas

Department of Physics and Astronomy, University of Southern California, Los Angeles, CA 90089-0484

Paola Verrucchi, Andrea Fubini

Dipartimento di Fisica dell'Universita' di Firenze and Istituto Nazionale di Fisica della Materia, UdR Firenze, Via G. Sansone 1, I-50019 Sesto Fiorentino (FI), Italy

Valerio Tognetti

Dipartimento di Fisica dell'Universita' di Firenze and Istituto Nazionale di Fisica della Materia, UdR Firenze, Via G. Sansone 1, I-50019 Sesto Fiorentino (FI), Italy
Istituto Nazionale di Fisica Nucleare, Sezione di Firenze, Via G. Sansone 1, I-50019 Sesto Fiorentino (FI), Italy

We present an extensive study of entanglement properties in easy-plane quantum spin systems with a quantum phase transition driven by a magnetic field applied in the easy plane. Making use of quantum Monte Carlo simulations, we are able to monitor the behavior of englement in the ground state and at finite temperature as a function of the applied field for different lattice geometries of the system. Our calculations focus on the entanglement of formation, quantified by the *one-tangle* [1] for the global entanglement of the system and by the *concurrence* [2] for the pairwise englement. For the case of a one-dimensional spin chain, we observe that the entanglement estimators are able to single out with high precision both the quantum critical point, through a minimum of the paiwise-to-global entanglement ratio, and the known occurrence of a factorized state below the critical field, through the vanishing of all entanglement estimators [3]. The vanishing of entanglement at a given field also persists at finite-temperature, so that the system displays a temperature-resistant *entanglement switch* effect. We then extend the same analysis to the case of a spin ladder and of a square lattice, and, thanks to the entanglement estimators, we find that the existence of a factorized state close to the quantum critical point is a general feature independent of the geometry.

[1] V. Coffman, J. Kundu, and W. K. Wootters, *Phys. Rev. A* 61, 053206 (2000).

[2] W. K. Wootters, *Phys. Rev. Lett.* 80, 2245 (1998).

[3] T. Roscilde, P. Verrucchi, A. Fubini, S. Haas, and V. Tognetti, cond-mat/0404403.

Phase second-harmonic-based Qubit

N. V. Klenov, V. K. Kornev

Department of Physics, Moscow State University, Moscow 119992, Russia

Introduction

The reported phase qubit is dc superconducting quantum interferometer (dc SQUID) containing two Josephson junctions, which are characterized by a second harmonic in their current-phase relations (CPRs):

$$I_j = I_{Cj}^{I} \sin(\varphi_j) + I_{Cj}^{II} \sin(2\varphi_j), \quad j = 1, 2, \qquad (1)$$

where I_{Cj}^{I} and I_{Cj}^{II} – amplitudes of the first and second harmonics respectively, φ_j - Josephson junction phase. This qubit was suggested first by Charlebois et al. [1] to be realized on the base of high-T_C superconductors. The advantages of this phase qubit, which is a "quiet" qubit, are the absence of a state-dependent spontaneous current in the loop and the uselessness of any bias magnetic flux [2].

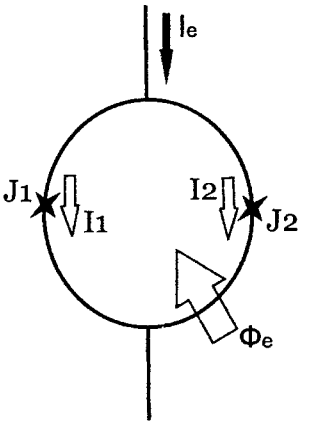

Qubit Design and Properties

The total Josephson energy of the interferometer is a function of three asymmetry parameters: the ratio of the first harmonic amplitudes of the junctions $\eta = I_{C2}^{I} / I_{C1}^{I}$ and the algebraic ratio of the second-to-first harmonic amplitudes in the current-phase relation for either of the two junctions $\alpha_{1,2} = I_{C1,2}^{II} / I_{C1,2}^{I}$. Normalized inductance of the qubit $l = 2\pi L I_0/\Phi_0$ ($\Phi_0 = h / 2e$ – magnetic flux quantum) must be as small as possible to eliminate any crosstalk between qubits. When one considers a small inductance of the qubit ($l << 1$), the total flux Φ through the loop approaches the applied magnetic flux Φ_e. In this case, the Josephson energy of the system at $I_{C1}^{I} = I_0$ is given by

$$\frac{E_J}{E_1} = -(\cos(\frac{\varphi}{2} + \theta) + \frac{1}{2}\alpha_1 \cos(\varphi + 2\theta) + \eta \cos(\frac{\varphi}{2} - \theta) + \frac{1}{2}\eta\alpha_2 \cos(\varphi - 2\theta)), \qquad (2)$$

where $\varphi = \varphi_1 - \varphi_2 = \varphi_e \equiv 2\pi \Phi_e/\Phi_0$; $\theta = (\varphi_1 + \varphi_2)/2$; $E_1 = \Phi_0 I_0 / 2\pi$ – characteristic energy.

When no external flux is applied (see the energy profile at $\varphi = 0$ in Fig. 1), the energy potential is always symmetric with respect to $\theta = (\varphi_1 + \varphi_2)/2$, even at strong asymmetry of the interferometer ($|\alpha_1 - \alpha_2| \sim 1$ or $|\eta - 1| \sim 1$). The left and right energy states are degenerate and form a basis of the qubit. This qubit is "quiet" because no external field and no bias current are required to form the qubit states. At the same time there is threshold value $\alpha^* = -0.6$ of the normalized amplitudes of second harmonic, that is critical for the phase qubit existence. If either α_1 or α_2 is larger then α^*, the interferometer energy does not show any double-well potential profile.

If external magnetic field is applied, the potential wells are lifted and the symmetry of the potential becomes broken at $\eta \neq 1$ and $\alpha_1 \neq \alpha_2$ (unequal junctions). But in the extreme case of inequality of the junctions ($\eta << 1$ or $\eta >> 1$) meaning transformation of the two-junction interferometer to a one-junction interferometer, the energy potential is symmetric again and the basis states are degenerate at any magnetic fields (at least up to $\varphi_e \approx 2\pi$).

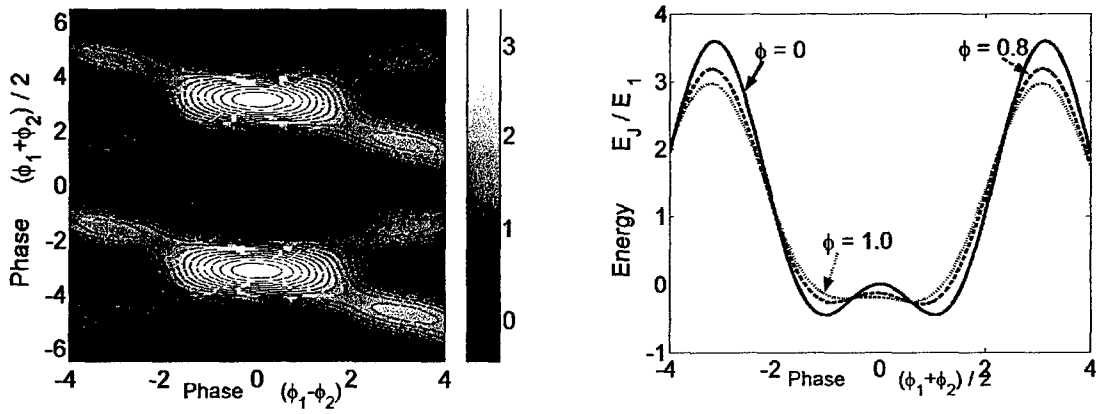

Fig. 1. Josephson energy of the qubit ($\alpha_1 = \alpha_2 = -1$, $\eta = 0.8$) versus Θ and $\varphi = \varphi_e$ (left) as well as one-dimensional profile (right) of the energy for different values of the normalized magnetic flux φ_e applied.

Evaluation of the Second Harmonic Amplitude

There is an experimental evidence that the second harmonic can reveal itself by formation of an additional side peak in the dependence of the dc SQUID critical current on applied magnetic field $I_C(H)$ [3]-[4]. The second harmonic impact on the dependence $I_C(\Phi_e)$ has been studied in detail numerically for different values of the normalized interferometer inductance l by means of computational solution of the simultaneous equations (1) and equation for the junction phase relation

$$\varphi_1 - \varphi_2 = \varphi_e - (l_1 i_1 - l_2 i_2) \qquad (3)$$

to find a maximum value of the superconducting transport current through the interferometer $i_e = i_1 + i_2$ as a function of the applied magnetic flux φ_e (here $i_e = I_e / I_0$, $i_{1,2} = I_{1,2} / I_0$, $l_{1,2}$ - normalized arm inductances).

It has been found that at $I_{C1}^{I} \sim I_0$ and $I_{C1}^{II} = 0$ the additional side peak caused by I_{C2}^{II} decreases rapidly with inductance l of the interferometer and vanishes completely at $l \approx 0.8$ [5]. If $l \geq 1$, this peak can exist only at sufficiently small values of the first harmonic amplitude I_{C1}^{I}. The dc SQUID inductance l_{crit}, which is critical for the side peak existence in the dependence $I_C(\Phi_e)$, was calculated numerically as a function of both the first and second harmonic amplitudes.

The obtained results for the SQUID critical current dependence on applied magnetic field allow evaluation of the second harmonic amplitude from the side peak parameters. This is very important for realization and optimization of the reported "quiet" phase qubit.

Acknowledgement

This work was supported in part by NATO Program "SfP" under Grant SfP-973559, INTAS Program under Grant 01-0806, and ISTC Program under Grant 2369.

References

[1] S. A. Charlebois, T. Lindstrom, A. Ya. Tzalenchuk, M. H. S. Amin, A. Yu. Smirnov, A. Zagoskin, T. Claeson in *"European Conf. on Applied Superconductivity"*, (IOP Publ. Ltd, Italy, Sept. 2003).

[2] Y. Makhlin, G. Schon, A. Shnirman, *Reviews of modern physics,* Volume 73, No. 2 (2001).

[3] E. Il'ichev, V. Zakosarenko, R. P. J. Ijsselstejn, H. E. Hoenig, H. –G. Meyer, *Phys. Rev. B,* Vol. 59, No. 17 (1999).

[4] V. K. Kornev, I. I. Soloviev, N. V. Klenov, N. F. Pedersen, I. V. Borisenko, P. B. Mozhaev and G. A. Ovsyannikov, *IEEE Trans. on Applied Superconductivity*, Vol. 13, No.2, (2003).

[5] V. K. Kornev, N. V. Klenov, I. V. Borisenko, G. A. Ovsyannikov, N. F. Pedersen, in *"European Conf. on Applied Superconductivity", Italy, Sept. 2003,* (IOP Publ. Ltd, Italy, Sept. 2003).

Selective Spin Coupling Using a Single Exciton

Brendon Lovett*, Ahsan Nazir*, Andrew Briggs*, Sean Barrett† and Tim Spiller†

*Department of Materials, Oxford University, Oxford OX1 3PH, United Kingdom
†Quantum Information Processing Group, Hewlett Packard Laboratories, Filton Road, Stoke Gifford, Bristol BS34 8QZ, United Kingdom

We present a novel scheme for performing a conditional phase (CPHASE) gate between two spin qubits in adjacent semiconductor quantum dots through delocalized single exciton states [1]. The delocalized states are formed through the resonant energy transfer or Foerster mechanism, in which an exciton can transfer between two resonant dots via an intermediate virtual photon.

We therefore consider two resonant quantum dots, each containing a single excess conduction band electron whose spin embodies the qubit. Excitons may be selectively created depending on the spin state of the dot through the Pauli blocking effect, in which a single circularly polarized laser pulse is applied, resonant with the s-shell heavy-hole exciton creation energies. These excitons are necessarily created in the z-angular momentum states given by $|3/2^{hh}, -1/2^{e}\rangle$. and, as noted in Refs. [[3, 2]], such a polarized laser will only create an exciton on a quantum dot if its excess electron is in the spin state $|m_z = 1/2\rangle$, due to the Pauli exclusion principle.

Since the Foerster interaction is non-magnetic, the single exciton created from the $|11\rangle$ state is delocalized and has a different energy from the localized single excitons created from the $|10\rangle$ and $|01\rangle$ states (see Fig. 1). It is therefore possible to selectively create an exciton from the $|11\rangle$ state only, and by applying a 2π pulse, a phase of -1 may be picked up on this state, whilst the other states remain unchanged (see Fig. 2). This is the CPHASE gate which is a universal two qubit gate for quantum computing.

Following on from work in Refs. [3, 4], we also show that arbitrary single-qubit rotations may be realized to a high fidelity with current semiconductor and laser technology. Two distinct single qubit operations are required for this. First, a Z-rotation gate is achieved by again exciting single excitons selctively using Pauli blocking. Second, an X-rotation gate is achieved by performing Raman transitions between the two qubit states, through the light hole exciton (see Fig. 3).

References

[1] A. Nazir, *et al.*, *xxx.lanl.gov/quant-ph/0403225* (2004).

[2] M. Feng *et al.*, *Europhys. Lett. 66*, 14 (2004)

[3] E. Pazy *et al.*, *Europhys. Lett. 62*, 175 (2004)

[4] T. Calarco *et al.*, *Phys. Rev. A 68* 012310 (2003)

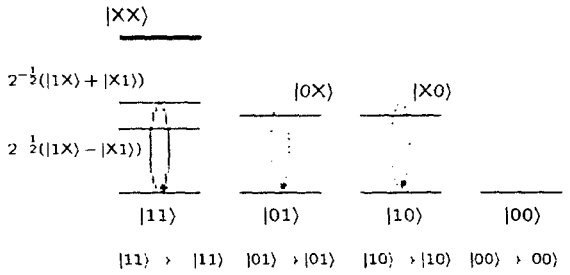

Figure 1: Schematic of the energy level structure of two resonantly coupled quantum dots, showing its dependence on the spin state of the excess electron on each dot.

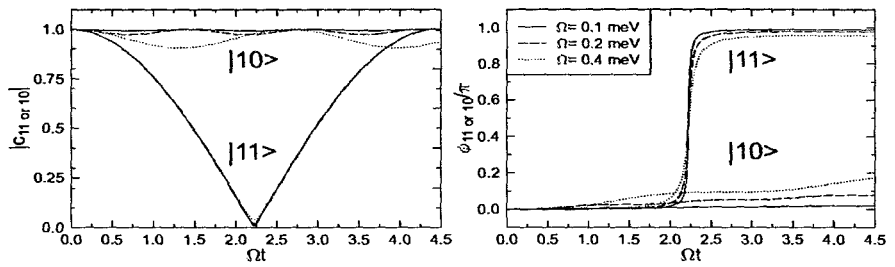

Figure 2: Amplitude (left) and phase (right) of states $|10\rangle$ and $|11\rangle$ during the CPHASE gate operation, with Foerster stragnth $V_{\mathrm{F}} = 0.85$ meV, biexciton binding energy $V_{\mathrm{XX}} = 5$ meV, and exciton creation energy $\omega_a = 2$ eV. Curves are shown for a variety of Rabi frequencies Ω.

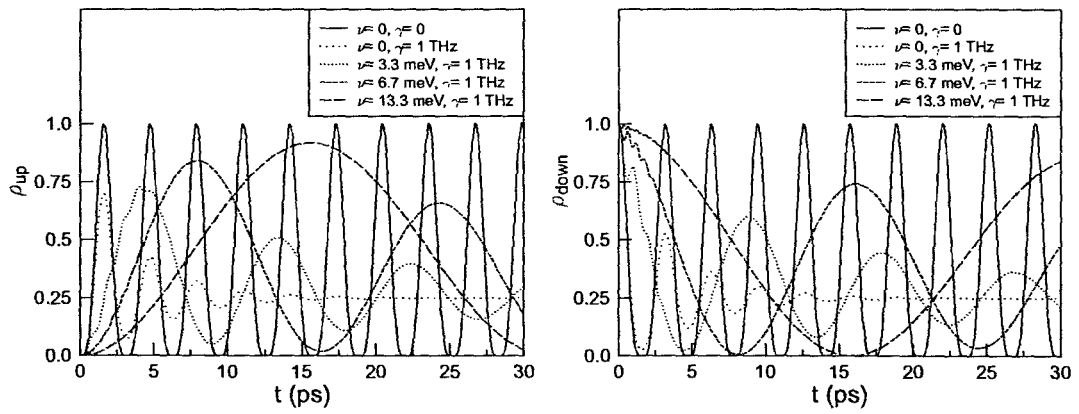

Figure 3: Population of the state of a single qubit during the proposed X-rotation gate induced by a two-laser Raman transition. Various values of the exciton decay rate γ and laser detuning ν are shown with $\omega_a = 2$ eV, and $\Omega = 1.33$ meV for both lasers.

On the Conversion of Ultracold Fermionic Atoms to Bosonic Molecules via Feshbach Resonances

Ehoud Pazy, Ami Vardi and Yehuda Band

Chemistry department, Ben-Gurion University of the Negev, Beer-Sheva 84105 Israel

Recently amazing progress has been made in the achievement of increasingly degenerate regimes of trapped atomic Fermi gases. After reaching the degenerate regime, experiments have dealt with mixtures of two hyperfine levels. This allows quite conveniently to adjust the effective interaction between atoms, employing a Feshbach resonance. At low temperatures the scattering between atoms is characterized by their s-wave scattering length. By slowly varying the magnetic field one can sweep through the magnetic Feshbach resonance. Starting with a weak attractive interaction between atoms of different hyperfine levels, i.e., small negative scattering length, making it more and more negative, and finally have it jump to a positive value at the other side of the resonance, corresponding to a repulsive interaction between atoms leading to a formation of diatomic molecules. Utilizing such magnetically tuned scattering resonances between two-component Fermi gases experimentalists have been able to produce, Bose-Einstein condensates of molecules formed by Fermionic atoms of ^{6}Li and ^{40}K as well as to probe the, theoretically predicted crossover from a Bose-Einstein condensate (BEC) to a Bardeen-Cooper-Schriefer (BCS) superfluid .

An interesting feature of a couple of such Feshbach sweep experiments [1,2] is that the experimental efficiency observed in the conversion of ultracold Fermi atomic gases of 40K and 6Li atoms into diatomic Bose gases was limited to 0.5. By constructing [3] the many-body state we show that the initial state preparation performed in such experiments involving two-component Fermi gases yields a mixture of even and odd parity pair-states, composed of two subsystems corresponding to two different spin states. Through the symmetry of the initial many-body state we are able to explain the 50% limited transfer efficiency in transforming atoms into molecules obtained in the above experiments as well as the fact that the Feshbach resonance sweep does not yield a swift heating of the remaining atomic Fermionic gas as was theoretically predicted [4].

In very low temperatures the Feshbach resonance is due to s-wave interactions, therefore the scattering atoms need to have a spatially symmetric wave function in order to create a molecule. In considering pairs of atoms in the initial state of the system, one from each spin state, half the atomic pairs are anti-symmetric spin-states and half are spin symmetric. More explicitly, the reduced two-particle density matrix obtained by tracing out all but one particle of one spin state and another particle of the other spin state contains 50% spin anti-symmetric spin-states, interacting via an s-wave (even parity spatial state), and 50% spin symmetric spin superposition which are effectively non-interacting at such low temperature. Thus when sweeping through the resonance sufficiently slow so that the Landau-Zener transition is traversed adiabatically it is clear that, since only even parity states can produce molecules through the Feshbach sweep, the conversion of ultracold Fermi gases into a diatomic Bose gas is limited to 0.5.

To obtain a transfer efficiency which is greater than 0.5, as is commonly achieved in current experiments, the odd parity spin-symmetric states must decorrelate before the constituent atoms can interact again via the Feshbach resonance. Therefore in achieving a higher efficiency the sweep rate was much slower, approaching ``close to thermal equilibrium'' conditions. Moreover in the relatively rapid sweep experiments [1,2] in which the Feshbach resonance sweep rate is sufficiently slow to pass adiabatically through the Landau Zener transition but faster than ``the collision rate'' in the gas,one expects a rapid heating of the Fermionic gas. However even though the Feshbach sweep produces holes in the Fermionic atomic sea, these holes can not be filled by the remaining atomic population, i.e., the population of atoms which have not been converted to molecules, since their composing atoms are non-interacting, due to their spatial symmetry which controls their interaction at ultra-low temperatures. This explains the experimental observation that the remaining atoms do not heat.

1. C. A. Regal, C. Ticknor, J. L. Bohn and D. S. Jin, Nature 424, 47 (2003).
2. K. E. Strecker, G.B. Partridge & R. G. Hulet, PRL 91, 080406 (2003).
3. E. Pazy, A. Vardi and Y. Band, submitted PRL.
4. E. Timmermans, PRL 87, 240403 (2001).

Linear-response conductance of the normal conducting single-electron pump

Roland Schäfer, Bernhard Limbach, Peter vom Stein, Christoph Wallisser

Forschungszentrum Karlsruhe, Institut für Festkörperphysik, Postfach 3640, D-76021 Karlsruhe, Germany

For single-electron devices the model Hamiltonian matches its experimental realization very closely. This has been proven most impressively for the normal-conducting single-electron transistor (SET) with the aid of Quantum-Monte-Carlo methods [1,2]. However, the lowest order perturbation theory, the so called sequential model, gives only a qualitative description in most practical cases. It ignores quantum fluctuations due to the coupling of charge states by the finite conductance of the tunneling contacts, which are fundamental constituents of the devices. Perturbation expansion (PE) has been suggested do deal with the impact of the coupling. Especially if the Coulomb blockade is lifted by lining up the energy of two neighboring charge states a situation arises which calls for sophisticated treatments. PE methods developed by Schöller and König [3,4] as well as by Grabert and Göppert [1,5] have been proven to describe the SET at the degeneracy point quantitatively up to $G = 1.5\ e^2/h$ [2,6]. Despite this success doubts on the applicability of PE in more general cases has occurred lately. Even for the SET, the validity range away from degeneracy is not clear. E.g. in the blockaded regime deviation between PE and experimental results are stronger than at the degeneracy point while the quantum Monte-Carlo data are in full accordance with the experiments. Furthermore, intermediate expressions of the PE calculation are burdened by cut-off parameters. In many expressions for the SET - including the mean charge on the transistor island and the conductance - these cut-offs cancel. But this happens to be somewhat fortunate, since no general rule is known which guarantees the cancellation. E. g. the occupation probability of the individual charge states contain the cut-off parameter explicitly.

To get more insight into the applicability of PE high quality conductance data on single-electron devices other than the SET are desirable. Here we present measurements of the linear response conductance of single-electron pumps (SEP). We have fabricated single-electron pumps with aluminum island and aluminum-oxide tunnel barriers in shadow evaporation technique. Usually single-electron pumps consists of a serial arrangement of three tunneling contacts forming two island; the electrostatic potential on each island can be adjusted via gate electrodes. However, in this simple layout only the serial conductance of the contacts can be measured and the distribution among the individual contacts remains unknown. To make the determination of the conductance of each contact possible, we replaced each outer contacts by two contacts. In the resulting device conductance parameters can be measured along different current paths. From a set of these parameters the individual conductances can be determined. In the final experiments the two outer contacts on the left and the right island are connected in parallel to the source and drain voltage source and act in the same manner as a single contact.

We report the measurements on three well characterized samples with varying asymmetry of the conductance between inner and outer tunneling contacts. In all cases the conductance is of the order of the conductance quantum e^2/h. This results in strong quantum fluctuations of the charge state, which manifest themselves - similar as in the case of the SET - by a logarithmic contribution to the linear-response conductance at low temperatures.

In addition in an easily accessible parameter regime we find a non-monotonic behavior of the conductance on temperature, which is correctly described by the sequential model. Phenomena of this kind are to be expected in all single-electron devices which are more complex than the SET. They can uncover internal characteristics unaccessible by other means - here e.g. the asymmetry of the conductance between the inner and outer tunneling contacts which is not directly measurable in the most natural SEP layout.

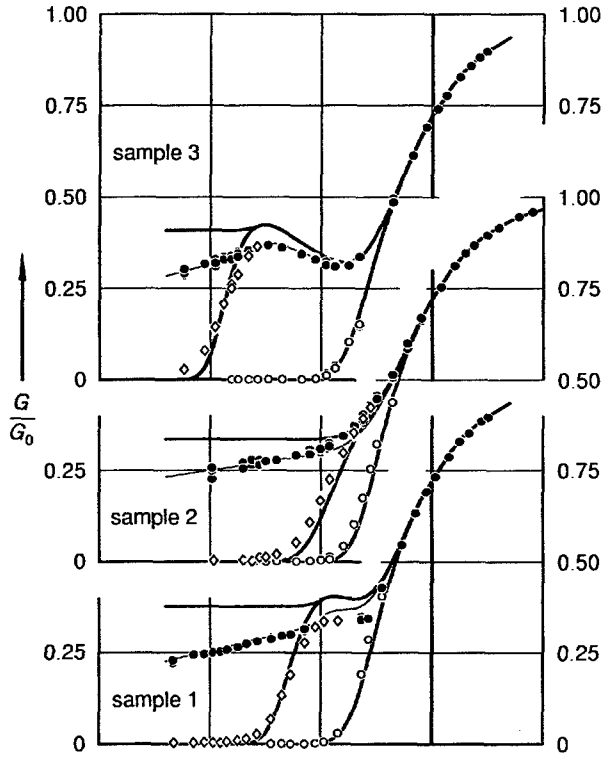

Linear response conductance of three SEP as a function of temperature. Shown are the minimal (o) and the maximal (●) conductance, as well as the conductance at a highly symmetric point of the SEP gate voltages (◊). The dashed lines are the result of an analytical solution of the sequential model obtained by restricting the model to four charge states. As solid lines the outcome of the full sequential model with independently determined sample parameters is shown. For the thin solid line a term of the form $\alpha \log(k_B T/E_\infty)$ has been added to the maximal conductance as calculated from the sequential model. Here α is a fitting parameter and E_∞ measures the capacitive coupling between the two SEP islands.

[1] G. Göppert, B. Hüpper, and H. Grabert, *Phys. Rev. B 62*, 9955 (2000)
[2] C. Wallisser, B. Limbach, P. vom Stein, R. Schäfer, C. Theis, G. Göppert, and H. Grabert, *Phys. Rev. B 66*, 125314 (2002)
[3] H. Schoeller, and G. Schön, *Phys. Rev. B 50*, 18436 (1994)
[4] J. König, H. Schoeller, and G. Schön, Phys. Rev. B 58, 7882 (1998)
[5] H. Grabert, *Phys. Rev. B 50*, 17364 (1994)
[6] P. Joyez, V. Bouchiat, D. Esteve, C. Urbina, and M. Devoret, *Phys. Rev. Lett. 79*, 1349 (1997)

Entanglement Assisted Metrology

P. Cappellaro, J. Emerson, N. Boulant, C. Ramanathan, S. Lloyd and D. Cory.

Nuclear Department, Massachusetts Institute of Technology - Cambridge, MA 02139

We present a new approach to the measurement of a single spin state, based on NMR techniques and inspired by the coherent control over many-body systems envisaged by Quantum Information Processing.

We propose to use the interaction of the spin of interest with an ensemble of spins (that we call Spin Amplifier) in order to enhance the signal from the single spin, up to the point where it is detectable by the usual inductive means. This method demands to control the polarization of about 10^6 spins, by inducing a coherent dynamics modulated by the interaction with a single spin.

The ensemble of spins forming the Amplifier is first prepared in a highly polarized state; it is then put in contact with the target spin (the spin we want to detect), which has already collapsed into one of the two states $|0\rangle$ or $|1\rangle$.

A simple quantum circuit, which illustrates how a collective measurement can provide knowledge of the single spin state, consists of a train of Controlled Not (CNot) gates between the target spin and each of the Amplifier spins: These gates effectively copy the state of the single spin onto the state of the Amplifier spins. At the end, the measurement of the total polarization in the Amplifier ($P \propto \Sigma_i \langle\psi|\sigma^i_z|\psi\rangle$) will indicate the state of the target spin. This first scheme demands that the ensemble spins are independently addressable, and the interaction with the single spin can only cause local perturbations on single spins.

Instead of demanding addressability of individual spin, we can develop equivalent schemes that connect better to the control we have on the physical system (and hence realizable in the near term), relying only on the collective behavior of the system and on entanglement among the Amplifier spins. With the creation of a macroscopic entangled state [1] (cat-state) in the Amplifier, the device acts as a collective single spin and thus is globally affected by a sole interaction with the target spin.

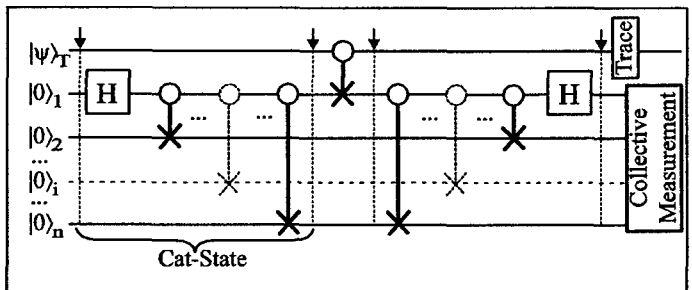

FIG. 1: Entanglement Scheme

We have implemented this scheme (Fig. 1) on a small QIP NMR liquid system, where the single spin is actually a macroscopic ensemble of spins (thus detectable), but they are measured only indirectly, through the scheme proposed.

In the experiment, the target spins are the single Proton spins of a ^{13}C labeled Alanine molecule ensemble (CH_3-C**H**(NH_2)-COOH), while the 3 Carbons compose the Amplifier. The spins interact via the scalar (J-)coupling $\Sigma_{i,j}\sigma_z^i\sigma_z^j$.

Before applying the circuit of Fig. 1, we first put the Proton spin into the identity state and prepare the Carbons in the pseudo-pure state $|000\rangle$ [2]. The state of the Proton is a superposition of the two decohered states $|0\rangle\langle 0|$ and $|1\rangle\langle 1|$: We can therefore effectively perform two experiments in parallel, and read out the outcomes from just one spectrum, where the lines are separated by the Carbon-Proton coupling splitting.

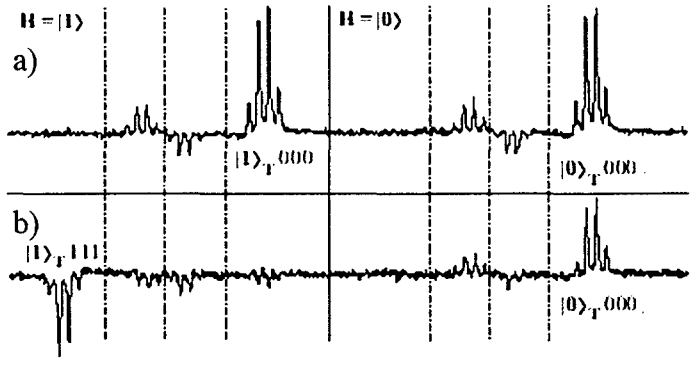

FIG. 2: Experimental Results:
a) Initial State: Pseudo-pure state of the 3 Carbons.
b) Final state: The polarization of the Carbons coupled to the target spin in state $|1\rangle$ (left) has been inverted, while it is unchanged for spins coupled to target spin in the $|0\rangle$ state (right).

The experimental results show that the polarization of the three Carbons is inverted conditionally on the state of the Proton, giving indirect measurement of its state.
Extending this scheme to larger systems with a much smaller target to Amplifier spins ratio, to obtain sensitivity enhancement, is experimentally challenging, yet we can relax some of the requirements.
The signature of a successful scheme is that it produces observable contrast in a measurement of the collective magnetization of the Amplifier. We define the contrast as $C = (P_0-P_1)/ P(0)$, P_0 and P_1 being respectively the polarizations for the target spin in the state $|0\rangle$ or $|1\rangle$ and initial polarization $P(0)$. The previous schemes provide the maximum contrast $C = 2$. Allowing for a lower, but still observable, contrast, we can envisage schemes that do not require control over individual spins. Furthermore, it is not necessary to restrict to the preparation of a cat-state, a wider class of entangled states is equally useful. Multiple Quantum Coherence [3] methods in NMR offer techniques for creating the wanted entangled states.
To further simplify the experimental task and avoid the need of applying the inverse of a rather complex map, we can borrow ideas of Quantum Chaos. It has been shown that the Fidelity between an initial state evolved under a unitary chaotic operator and the same state evolved under a perturbed version of the same operator decays exponentially with the number of repetitions of the map, for strong enough perturbations [4],[5]. If we apply the perturbation conditionally on the state of the target spin, the two possible resultant states will have an exponentially decreasing overlap. However, the expectation value of the polarization is a much weaker measurement than the Fidelity and therefore we expect this rate to simply bound the contrast growth rate.
In conclusion, we show that it is possible to transfer polarization from a target spin to an ensemble of spins, through the creation of a highly entangled state with RF pulses and the coupling between the target spin and its closest neighbors. The methods proposed open the possibility to a new class of devices, where quantum effects, such as entanglement, are used to make a transition from microscopic to macroscopic properties.

[1] A. Legget and A. Garg, Physical Review Letters 54 (9), 857 (1985).
[2] D. Cory, R. Laflamme, E. Knill, L. Viola, T. Havel, N. Boulant, and G. Boutis, Fortschr. Phys. 48, 875 (2000).
[3] M. Munowitz, A. Pines, and M. Mehring, J. Chem. Phys. 86, 3172 (1987).
[4] P. Jacquod, P. Silvestrov, and C. Beenakker, Phys. Rev. E 64, 055203 (2001).
[5] Y. S. Weinstein, J. V. Emerson, S. Lloyd, D. Cory, quant-ph/0210063, (2002)

Revealing anisotropy in a Paul trap through Berry phase

M. Scala, B. Militello, A. Messina

INFM, MIUR and Dipartimento di Scienze Fisiche ed Astronomiche, via Archirafi 36, I-90123 Palermo, Italy

When an ion confined in an *anisotropic* bidimensional Paul trap is subjected to a laser beam oriented along an arbitrary direction, the interaction between its electronic and vibrational degrees of freedom is described by a time-dependent hamiltonian model as a consequence of the lack of geometrical symmetry. Appropriately choosing the laser frequency, the hamiltonian model turns out to be sinusoidally oscillating at the difference between the proper frequencies of the centre of mass of the ion. Thus, if the anisotropy of the trap is sufficiently small, the evolution of the system can be considered as adiabatic. In the context of this physical situation, we have calculated the Berry phase acquired in a cycle by the instantaneous eigenstates of the trapped ion hamiltonian. Suitably choosing both the initial condition and a physical observable we succeed to forecast physical effects directly traceable back to the accumulated Berry phase. In particular we indeed bring to light that the mean value of the chosen observable after a cycle is the negative of that calculated at the same instant of time in the case of isotropic traps. This effect demonstrates that and how the Berry phase can be exploited to evidence the existence of a weak anisotropy in a Paul trap.

Amplifying Quantum Signals with a Josephson Bifurcation Amplifier

I. Siddiqi, R. Vijay, E. Boaknin, M. Metcalfe, C. Rigetti, F. Pierre, C.M. Wilson, L. Frunzio, and M.H. Devoret

Department of Applied Physics, Yale University
15 Prospect Street, New Haven, CT 06520-8284

Quantum measurements of solid-state systems, such as the readout of superconducting quantum bits, challenge conventional low-noise amplification techniques. Ideally, the amplifier for a quantum measurement should minimally perturb the measured system while maintaining sufficient sensitivity to overcome the noise of subsequent elements in the amplification chain. Additionally, the characteristic drift of materials properties in solid-state systems necessitates a fast acquisition rate to permit measurements in rapid succession. To meet these inherently conflicting requirements, we propose to harness the sensitivity of a dynamical system - a single RF-driven Josephson tunnel junction - tuned near a bifurcation point.

The superconducting tunnel junction is the only electronic dipolar circuit element with a non-dissipative nonlinearity which remains unchanged at arbitrary low temperatures. As the key component of present superconducting amplifiers, it is known to exhibit a high degree of stability. Moreover, all available degrees of freedom in the dynamical system participate in information transfer and none contribute to unnecessary dissipation resulting in excess noise.

The operation of our Josephson bifurcation amplifier is represented schematically in Fig. 1. The central element is a Josephson junction whose critical current I_0 is modulated by the input signal using an application-specific coupling scheme (input port), such as a SQUID loop or a SSET. The junction is driven with an sinusoidal signal $i_{RF}\sin(\omega t)$ fed from a transmission line through a directional coupler (drive port). In the underdamped regime, when the drive frequency ω is detuned form the natural oscillation frequency ω_p and when the drive current $I_{B'} < i_{RF} < I_B << I_0$, the system has two possible oscillation states which differ in amplitude and phase [1-2]. Starting in the lower amplitude state, at the bifurcation point $i_{RF} = I_B$ the system becomes infinitely sensitive, in absence of thermal and quantum fluctuations, to variations in I_0. The energy stored in the oscillation can always be made larger than thermal fluctuations by increasing the scale of I_0, thus preserving sensitivity at finite temperature. The reflected component of the drive signal, measured through another transmission line connected to the coupler (output port), is a convenient signature of the junction oscillation state which carries with it information about the input signal. The reflected signal phase ϕ is plotted in Fig 2. as a function of the drive current i_{RF}, with the two oscillation states of the junction being labeled "0" and "1".

This arrangement minimizes the back-action of the amplifier since the only fluctuations felt at its input port arise from the load impedance of the follower amplifier, which is physically separated from the junction via a transmission line of arbitrary length and can therefore be thermalized efficiently to base temperature.

We present an experiment that demonstrates the principle of bifurcation amplification, and we show that the sensitivity obtained is in good agreement with a

well established theory of dynamical transitions, thus making it relevant for stringent tests of superconducting qubits and gates.

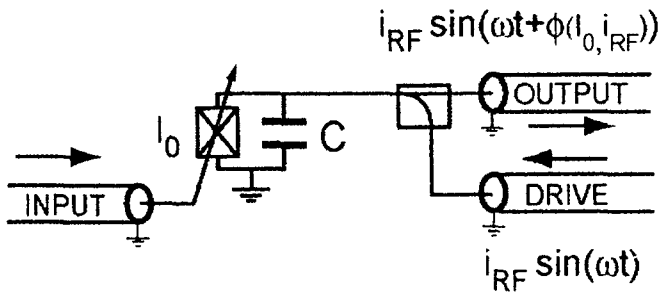

Figure 1: Schematic diagram of the Josephson bifurcation amplifier. A junction with critical current I_0 coupled to the input port is driven by an RF signal. In the vicinity of the dynamical bifurcation point, the phase of the resulting oscillation depends critically on the input signal and manifests itself in the reflected signal phase ϕ.

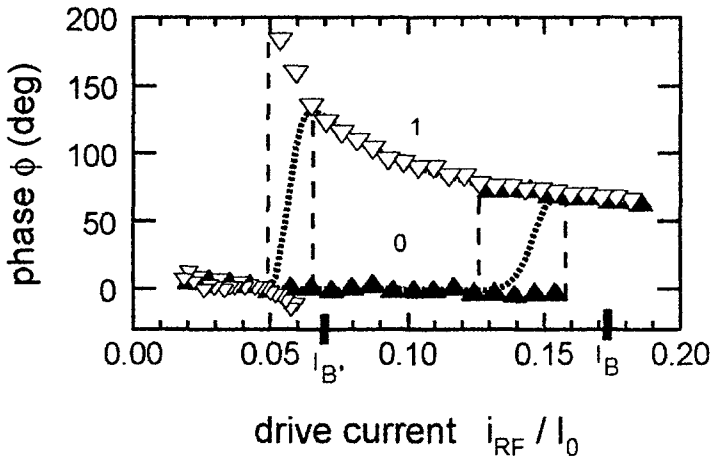

Figure 2: Reflected signal phase ϕ as a function of drive current i_{RF}/I_0. I_0=1.172μA; $(\omega_p-\omega)/\omega$=0.122. Symbols denote the mode of ϕ with up and down triangles corresponding to increasing and decreasing current, respectively. The dotted line is $<\phi>$. The calculated bifurcation points, $I_{B'}$ and I_B, are marked on the horizontal axis. The 0 and 1 phase states are reminiscent of the superconducting and dissipative states of the DC current biased junction.

References

[1] M.I. Dykman and M.A. Krivoglaz, *Physica A* 104, 480 (1980).

[2] I. Siddiqi, R. Vijay, F. Pierre, C.M. Wilson, L. Frunzio, M. Metcalfe, C. Rigetti, R.J. Schoelkopf, M.H. Devoret, D. Vion, and D.E. Esteve, *arXiv:cond-mat/0312553 v1*, (2003).

Coherent Dynamics of a flux-qubit coupled to a harmonic oscillator

P. Bertet[1], I. Chiorescu[1*], K. Semba[2], Y. Nakamura[3] C. J. P. M. Harmans[1], J. E. Mooij[1]

[1] *Quantum Transport Group, Kavli Institute of Nanosciences, Delft University of Technology, Lorentzweg 1,2628CJ, Delft, The Netherlands*
[2] *NTT Basic Research Laboratories, Atsugi-shi, Kanagawa 243-0198, Japan*
[3] *NEC Fundamental Research Laboratories, 34 Miyukigaoka, Tsukuba, Ibaraki 305-8501, Japan*
* *Present address : Department of Physics and Astronomy, Michigan State University, East Lansing, MI-48824, USA*

Superconducting circuits containing Josephson junctions are very promising candidates for the implementation of solid-state quantum bits or qubits [1]. Complex single-qubit operations have already been reported [2,3], as well as coherent dynamics of two coupled qubits [4] and realization of a quantum gate [5]. Coupling a qubit to a harmonic oscillator is interesting from a fundamental point of view to generate and study non-classical states of the oscillator, and is relevant in quantum information as well, since coupling many qubits via a harmonic oscillator has been proposed [6]. Here we present recent measurements demonstrating the coupling of a flux-qubit to the plasma mode of the DC Squid which at the same time is used to measure the qubit state. This coupling is manifested by the appearance of two side-band resonances around the bare qubit peak. By performing two-pulse experiments, we demonstrate that these additional resonances are indeed excitations of the coupled system. We also observe Rabi oscillations between the coupled |qubit,Squid> states, thus demonstrating entanglement between the states of two superconducting circuits. We use the qubit to measure intrinsic properties of the plasma mode : temperature, relaxation time. Conversely, we also measure the qubit's state via the plasma mode. These results indicate that complex manipulation of entangled states similar to cavity QED or trapped-ions experiments is within reach with superconducting circuits.

[1] J.E. Mooij et al., Science **285**, 1036 (1999)

[2] D. Vion et al., Science **296**, 896 (2002)

[3] I. Chiorescu, Y. Nakamura, C. J. P. M. Harmans, and J. E. Mooij, Science 10.1126/science.1081045 (2003).

[4] Y. A. Pashkin et al., Nature **421,** 823 (2003)

[5] T. Yamamoto, Y. Pashkin, O. Astafiev, Y. Nakamura, J. S. Tsai, Nature **425,** 941 (2003)

[6] Y. Makhlin, G. Schön & A. Shnirman, Nature **398**, 305 (1999)

Quantum tunneling phenomena in ultra-thin superconducting wires

M.Zgirski, K.-P.Riikonen, T. Holmqvist, M. Savolainen, V. Touboltsev and K. Arutyunov

University of Jyväskylä, Nanoscience Centre, Department of Physics, PB 35, 40014, Jyväskylä, Finland

A superconducting wire can be considered as quasi-one dimensional (1D) if its characteristic transverse dimension $\sqrt{\sigma}$ (σ being the cross section) is smaller than the coherence length $\xi(T)$. The shape of the bottom part of the resistive transition R(T) of a 1D superconducting strip is described by the model of phase slips activation. If the wire is infinitely long, then there is always a finite probability that a 'small' part of the sample is instantly driven normal: locally the modulus of the order parameter $|\Delta|$ goes to zero and its phase φ 'slips' by 2π.

Free energy of a current-carrying 1D superconductor is described by so called 'tilted washboard' potential (Fig.1). The black circle denotes a thermodynamically metastable state of a macroscopically coherent superconductor. The system can relax to a state of lower energy. There are two possible ways for a superconductor to decrease its energy. First, due to thermal excitation it can 'jump' over the energy barrier ΔF to a new potential minimum [1]: solid arrow in Fig. 1. Second, the system can tunnel through the energy barrier [2]: dotted arrow in Fig. 1. In the limit of infinitely small supercurrent the height of the barrier ΔF is the energy difference between normal and superconducting states of a system of the smallest possible size $\Omega = \xi \cdot \sigma$: $\Delta F = B_c^2 \cdot \Omega$, B_c being the critical magnetic field. Corresponding decrease of energy is accompanied by the change in phase by 2π (Fig. 1). It can be shown [1], that in case of thermally activated phase slips the effective resistance $R(T) \sim \exp(-\Delta F / k_B T)$. For a not too long wire $L \geq \xi(T)$ (only single phase slip event can happen at a time) with normal state resistance R_N the quantum tunneling contribution is [2]: $R(T) / R_N = (\xi / L) \cdot (\tau_0 \cdot \Gamma_{QPS})$, where $\tau_0 \sim h / \Delta$ is the duration of a phase slippage, and $\Gamma_{QPS} = B \exp(-S_{QPS})$ is the rate of quantum phase slip events, where $B \approx (S_{QPS} / \tau_0) \cdot (L / \xi)$, $S_{QPS} = A \cdot (R_Q / R_N) \cdot (L / \xi)$, $A \sim 1$, $R_Q = h / 4e^2 = 6.47\ k\Omega$.

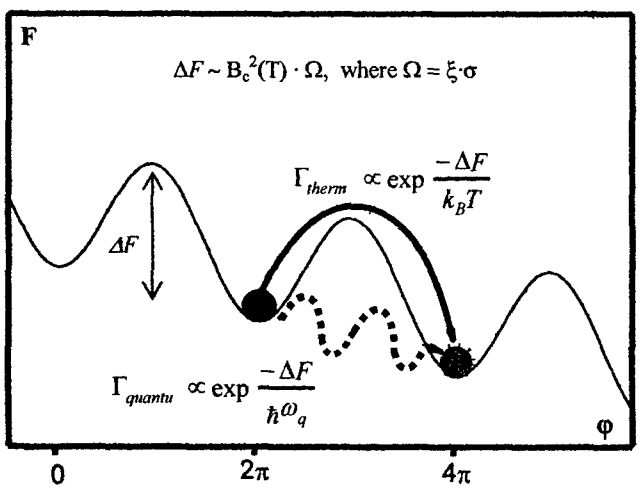

Fig. 1. Dependence of the free energy F vs. superconducting phase φ of a 1D current-carrying superconductor. The system (represented by a circle) can change its quantum state in two ways: by thermally activated phase slips (solid arrow), or by quantum tunneling (dotted arrow). Γ stands for the rates of the corresponding processes.

Several experimental attempts have been made to detect the QPS mechanism in narrow superconducting channels: ultra-thin In and Pb-In wires [3] and Mo-Ge film evaporated on top of a carbon nanotube [4]. The results are very intriguing, but the matter is far from being settled. The motivation of this work was to study the manifestation of the QPS mechanism in the *same* superconducting wire as a function of its cross section.

We have developed a method of progressive reduction of transverse dimensions of e-beam lift-off fabricated nanostructures by ion-beam sputtering [5]. The method enables galvanomagnetic measurements of the same sample in between the sessions of etching. Sputtering can be considered as an erosion of the surface due to bombardment of primary ions. The method is very promising, for it lets us directly follow changes in superconductive transition in a 1D superconductor along with successive reduction of its cross section. AFM control revealed that sputtering makes the sample surface smoother and more homogenous, eliminating inevitable imperfections while original lift-off process. For not too narrow Al wires the shape of R(T) transition can be perfectly fitted by the thermal activation model [1]. While for the wires that after few sputtering sessions have reached the effective diameter $\sqrt{\sigma} < 35$ nm a low temperature 'foot' develops, which can be associated with the QPS phenomena (Fig. 2).

This work has been supported by the EU Commission "ULTRA-1D" project NMP4-CT-2003-505457 "Experimental and theoretical investigation of electron transport in ultra-narrow 1-dimensional nanostructures".

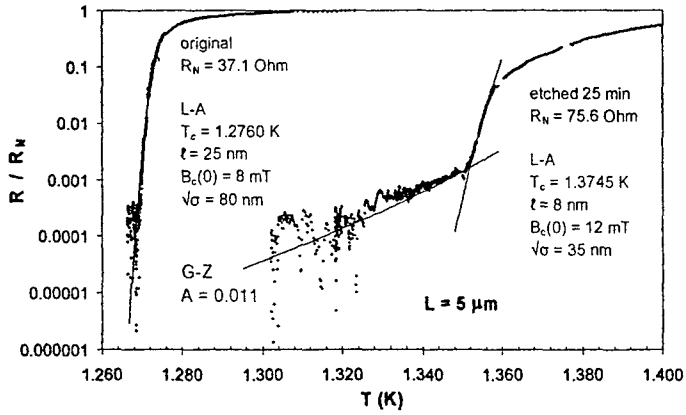

Fig. 2. Resistive transition R(T) of a 5 μm long *same* Al wire before sputtering (left curve) and after (right). High-temperature part of the transition can be described by the thermal PS activation mechanism (solid lines), while for the thinner wire the bottom 'foot' can be fitted by the QPS model.

[1] J. S. Langer, V. Ambegaokar, Phys. Rev. 164, 498 (1967); D.E. McCumber, B.I. Halperin, Phys. Rev. B 1, 1054 (1970)

[2] A. Zaikin, D. Golubev, A. van Otterlo, and G. T. Zimanyi, PRL 78, 1552 (1997); A. Zaikin, D. Golubev, A. van Otterlo, and G. T. Zimanyi, Uspexi Fiz. Nauk 168, 244 (1998); D. Golubev and A. Zaikin, Phys. Rev. B 64, 014504 (2001)

[3] N. Giordano and E. R. Schuler, Phys. Rev. Lett. 63, 2417 (1989); N. Giordano, Phys. Rev. B 41, 6350 (1990); Phys. Rev. B 43, 160 (1991); Physica B 203, 460 (1994)

[4] A. Bezryadin, C. N. Lau and M. Tinkham, Nature 404, 971 (2000); C. N. Lau, *et. al.*, Phys. Rev. Lett. 87, 217003 (2001)

[5] M. Savolainen, *et. al.*, to be published in Appl. Phys. A (2004), cond-mat/0311383

Modelling the current resolution of a specific Josephson junction system

Joachim Sjöstrand, Hans Hansson, Anders Karlhede

Department of Physics, Stockholm University
AlbaNova University Center, SE-10691 Stockholm, Sweden

Jochen Walter, David Haviland

Nanostructure group, Royal Institute of Technology
AlbaNova University Center, SE-10691 Stockholm, Sweden

In this paper we study a Josephson junction (JJ) (kept at cryo-temperature T) when connected to an external current source I(t), via a twisted pair with impedance Z_{tw}. See Fig 1(a). The generic features of such systems have been studied extensively by e.g. Kautz and Martinis [1]. Here however we are interested in the quantitative behaviour of our specific system. We study the probability distribution P of switching of the JJ, as a function of the current pulse from the source. Due to quantum effects and various noise sources, such as resistive leads at finite temperatures, this distribution will have a finite width. In a qubit system, such as the Quantronium [2], it is necessary that this width is small in order to clearly distinguish between different quantum states, and eventually realise the single shot measurement. Here we will compare simulated and measured values of this width.

To numerically calculate the function P, we: (i) model the junction with an ideal element in parallell with a capacitor C_J. (ii) for the current pulse we use a technique referred to as pulse and hold [3], with a fast switching pulse (with magnitude I_p and duration τ_p) followed by a longer hold pulse. (iii) We model Z_{tw} with a resistor R_1 in parallell with another resistor R_2 and a capacitor C_2 (the impedance corresponding to this setup is called Z_{RRC}, see Fig 1(b). Z_{RRC} is fitted to match Z_{tw} as closely as possible (see Fig. 2(a), (b) for the real and imaginary part of the measured impedance (solid line) and the model Z_{RRC} (dashed line). (iv) The thermal noise from Z_{tw} we model with the noise currents $I_{n1,2} = NvT_n/R_{1,2} \cdot A$ where N is a Gaussian distributed random number and A is a constant.

Applying Kirchoff's rules and the Josephson relations to the circuit in Fig 1(a) with the model impedance in Fig 1(b) we find a third order differential equation for the phase over the junction. This description is valid here since $E_J >> E_C$ ($E_C \tilde{} 0.5$ K, $E_J \tilde{} 6.3$ K).

The width ΔI of P we define as $\Delta I = \alpha^{-1}(r)$, where $r = \alpha(\Delta I) = |P(I_{sw}+\Delta I/2) - P(I_{sw}-\Delta I/2)|$ is the discriminating powe and I_{sw} is the switching current, $P(I_{sw})=1/2$.

In Fig. 3(a) we plot $\Delta I/I_{sw}$, and in Fig. 3(b) we plot ΔI as a function of τ_p. The stars connected with solid lines are measured data with $0.025 = T = 0.7$ K (we do not bother of identifying the temperature for the curves), and the stars connected with dashed lines are simulated data with $T_n = 0.03$, 0.7 and 4.0 K.

For $\tau_p = 10$ μs, the simulated data agrees well with the measured ones if $T_n = 0.03$ K. For $\tau_p = 0.1$ μs the $\Delta I/I_{sw}$ values agree for $T_n = 4$ K whereas the ΔI values do not agree at all. Increasing T_n further will (most likely) not increase ΔI in any considerable way. A more

thorough analysis indicates that the big difference in the ΔI values for τ_p=0.1 μs is at least not due to the simplification of the impedance.

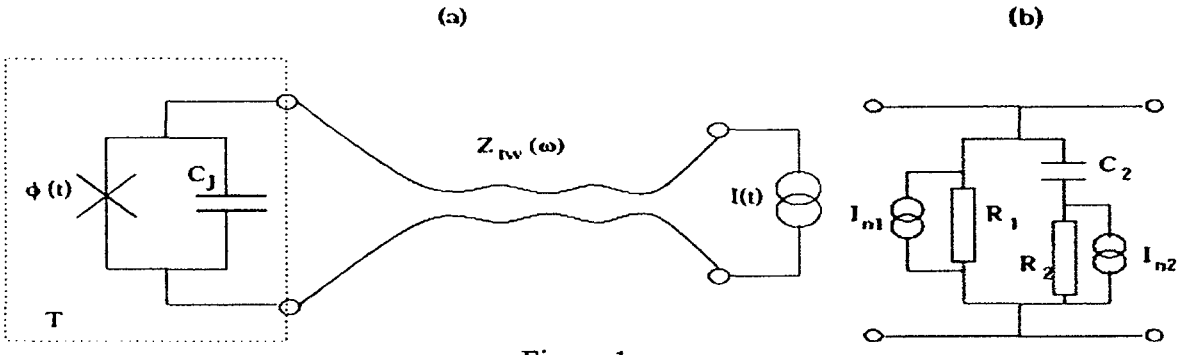

Figure 1

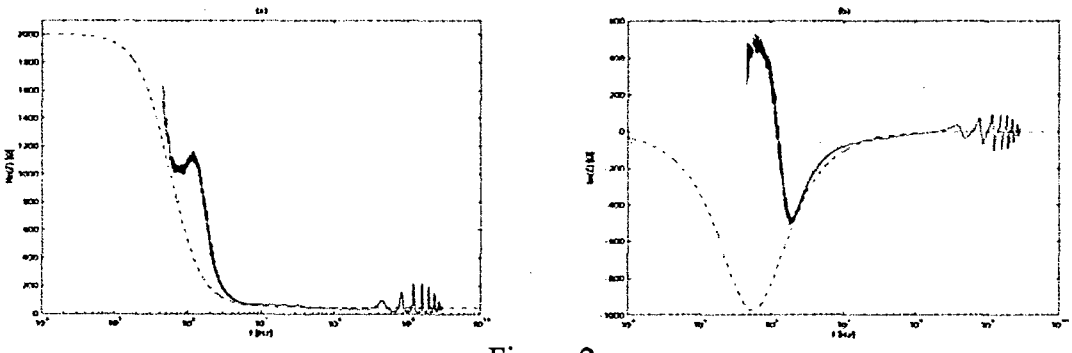

Figure 2

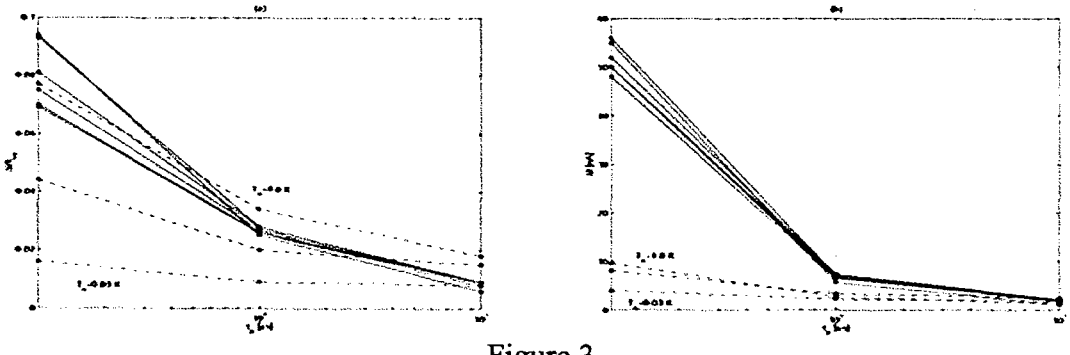

Figure 3

[1] R. L. Kautz and J. M. Martinis, Phys. Rev. B 42, 9903 (1990).

[2] D. Vion, A. Assime, A. Cottet, P. Joyez, H. Pothier, C. Urbina, D. Esteve and M. H. Devoret, *Science* 296, 886 (2002)

[3] J. Walter, S. Corlevi, D. B. Haviland, cond-mat/0403467

Binary detection of small switching currents

Jochen Walter, Silvia Corlevi and David B. Haviland

Nanostructure Physics, Royal Institute of Technology (KTH)
AlbaNova University Center, SE-106 91 Stockholm, Sweden

Several quantum-control experiments based on Josephson junctions measure the switching current to determine the quantum state of the circuit [1][2]. Some of these experiments rely on a pulsed readout where a rectangular current pulse is applied to the circuit and the voltage is measured to determine switching. The sample is typically mounted in a cryostat and small currents have to charge the capacitance of the measurement leads, delaying the signal at the readout stage. Hence, a switching in the very last instance of the pulse cannot build up enough voltage needed to trigger a detector. Here we present a method to circumvent this problem. A pulse of the order of the switching current, called the switch pulse, is immediately followed by a hold level of smaller amplitude. Its purpose is to latch the state of the circuit for the time that is needed until the readout is finished. With this hold level, a late switch can be detected and switching ambiguities are excluded.

After switching, the new stable operating point of the circuit is defined by the intersection of the sample IV and the loadline, set by the bias resistor R_b. The choice of the bias resistor depends on two things. On the one hand, the operating point should be at a voltage as low as possible, yet large enough to distinguish switch from no-switch. In this case, the power dissipated in the junction is minimal since a current through the device is minimal. On the other hand, a latching behaviour is only obtained if the slope of the loadline, which is $-1/R_b$, is smaller than the negative differential resistance of the junction IV.

The experimental setup is shown in figure 1. An arbitrary waveform generator (AWG) together with an attenuator and a bias resistor form the bias circuit. It is connected to the sample via twisted pair cables. High frequency noise is filtered at room temperature with a 15MHz low-pass MiniCircuit filter. The sample is placed in a dilution refrigerator with a base temperature of 25mK. The detection of the response voltage from the sample is done after the bias resistor. While the sample stays in the superconducting state, the main portion of the applied voltage is dropped across R_b and only a small voltage is registered. If the sample switches to the normal state with a high quasi-particle resistance (much larger than the bias resistor), the main voltage drop is across the sample and a larger voltage than in the no-switch case is detected. An event counter with a threshold voltage set between the switch and no-switch signal counts the switching events. Since the minimum threshold that can be programmed into the counter is 50mV, the signals, which are below the gap of about 400μV have to be amplified. A home-built pre-amplifier with a gain of 500 is responsible for this task. Finally, a fast digital sampling oscilloscope (DSO) with large memory can record complete measurement traces of 10^4 pulses and therefore offers the possibility of doing correlation analysis.

The experiments were carried out on SQUID junctions, see inset of fig. 1. The SQUID allows us to perform measurements in a wide range of switching currents, from the maximum switching current to zero, by applying a magnetic field to the SQUID.

Thus, the ratio of the two important energies of this system, which are the Josephson energy E_J and the charging energy E_C, can be continuously varied.

In a typical experiment a total of $N_t=10^4$ identical pulses, each separated by a wait time τ_W, are applied to the sample. The hold level is set that it never switches the sample. This level is maintained throughout the whole experiment. The amplitude of the switch pulse is initially at a level that no pulse causes a switch. It is then continuously increased until all N_t pulses switch the sample. The switching probability is obtained from $P=N/N_t$, where N is the number of switches. From the width of this switching distribution, the resolution ΔI of such a detector is obtained. We study the normalized resolution, $\Delta I/I$, where I is the current value at P=0.5. For small switching currents of the order of 12nA, we find a resolution of less than 10% for switching pulses of 100ns duration. For longer pulses or pulses with higher switching currents, the resolution decreases even further.

After each switch, the system needs time to relax to its initial state. Therefore, the wait time has to be chosen long enough in order that a pulse won't influence the outcome of a following pulse. We made a correlation analysis where we calculate the auto-correlation of a pulse-sequence as a function of the wait time, while the switching probability is held constant at P=0.5, see fig. 2. We find a substantial auto-correlation for wait times shorter than 40μs. A long decay time of the auto-correlation function might be explained by excessive heating due to quasi particle tunnelling in the junction when it switches above the gap voltage. However, since in our case we keep the voltage below the gap, only small currents discharge the capacitance of the leads. Therefore it is possible that the junction does not always retrap before a new pulse is applied.

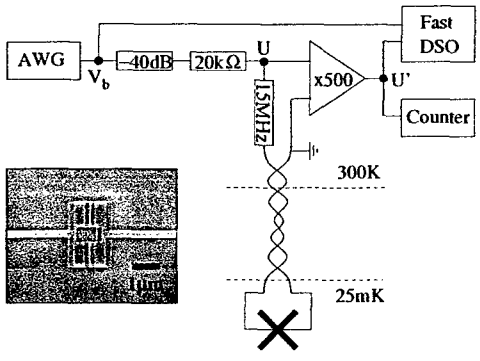

FIG. 1

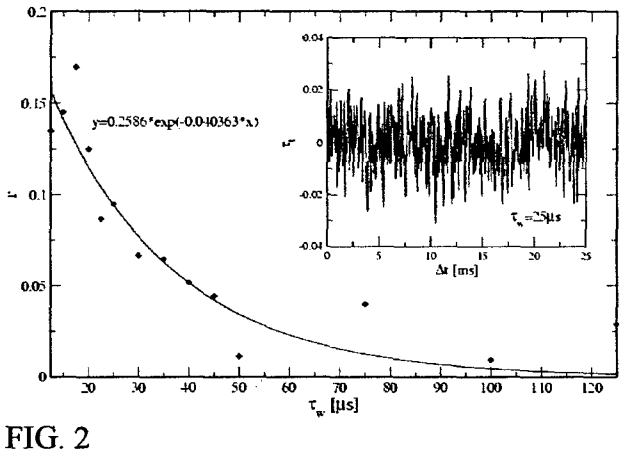

FIG. 2

[1] D. Vion, A. Aassime, A. Cottet, P. Joyez, H. Pothier, C. Urbina, D. Esteve, and M. H. Devoret, *Science 296*, 886 (2002)

[2] I. Chiorescu, Y. Nakamura, C. J. P. M. Harmans, and J. E. Mooij, *Science 299*, 1869 (2003)

Cooper pair transistor in a high impedance environment

S. Corlevi, W. Guichard and D.B. Haviland

Nanostructure Physics, Royal Institute of Technology
Albanova, 106 91 Stockholm, Sweden

We are conducting an experimental study on the effect of high impedance environment on a Cooper pair transistor (CPT). The CPT consists of two small-capacitance Josephson tunnel junctions in series with a gate electrode coupled through a capacitance C_g to a central island. In small-capacitance CPT the charging energy $E_{C\Sigma} = e^2 / 2C_\Sigma$, where $C_\Sigma \sim 2C_J + C_g$ is the total capacitance of the island, becomes relevant at low temperature, and charging effects influence the transport properties. In order to observe Coulomb blockade in a single Josephson junction and also in a CPT, care must be taken to isolate the junctions from their high frequency electromagnetic environment. The classical Josephson effect, realized in the low impedance environment ($\mathrm{Re}[Z(\omega)] < R_Q = h/4e^2 \sim 6.45$ kΩ), is suppressed in the high impedance environment where there are large quantum fluctuations of the phase. In a high impedance environment, the current voltage (I-V) curve of the CPT does not present a supercurrent feature, but a Coulomb blockade feature, and a region of negative differential resistance which is the signature of coherent tunnelling of Cooper pairs [1]. In order to observe the Coulomb blockade of Cooper pair in a CPT, the main requirement on the environment is that its impedance ($\mathrm{Re}[Z(\omega)]$) shunting the CPT must be much larger than the quantum resistance R_Q. In previous works [2], the impedance of the leads was increased by using small chromium resistors with a resistance of 50 kΩ, located on the chip close to the junctions. In our experiments, as in those of Watanabe [3], the high impedance of the leads is obtained by biasing the CPT with four SQUID arrays. The SQUID geometry allows the tuning *in situ* of the leads impedance over several orders of magnitude (10^4 Ω<$\mathrm{Re}[Z(\omega=0)]$<10^8 Ω), providing different electromagnetic environments to the CPT. Note that the junctions defining the CPT do not have a SQUID geometry, and thus are unaffected by the relatively small magnetic fields (the flux $\Phi=\Phi_0/2$ at 5 mT, where $\Phi_0=h/2e = 2\times10^{-15}$ Wb is the flux quantum) needed to tune the SQUIDs.

Measurements were performed in a dilution refrigerator with a base temperature of 15mK. No low temperature filtering is implemented in the cryostat. However, when the arrays are in the high impedance state, they act as good filters for electromagnetic fluctuations guided to the sample via the leads. The I-V characteristics of the CPT are measured in a four point configuration (Fig. 1). One pair of SQUID leads are used to apply a symmetric bias and measure the current, the other pair to measure the voltage across the CPT. Each array has 70 SQUIDs, with an area of 0.03 μm^2 per junction. The CPT junctions are designed to have an area of 0.01 μm^2 each. CPTs with different ratio $E_J/E_{C\Sigma}$ have been measured.

In several experiments performed in a low impedance environment [4,5], it has been shown how the *2e*-periodicity of the supercurrent in the gate induced charge is suppressed by non-equilibrium quasiparticles. In order to study this effect in a high impedance environment, we fixed the bias voltage across the SQUID arrays at a value of 50 μV and measured the current and voltage of the transistor as function of V_g. The

tunneling of charges in and out the island results in an oscillating behaviour of both the current and voltage across the transistor (Fig 2). It is interesting to notice how the character of the oscillations changes as the impedance of the environment is increased. In fact, as the magnetic field reduces the coupling energy of the SQUID arrays (increasing their impedance), the V_g dependence changes from *e*-periodic to *2e*-periodic. The change in periodicity is observed in both current and voltage oscillations. This suggests that non-equilibrium quasiparticles present in the system and responsible for the *e*-periodicity, can be suppressed by high impedance leads.

Figure 1

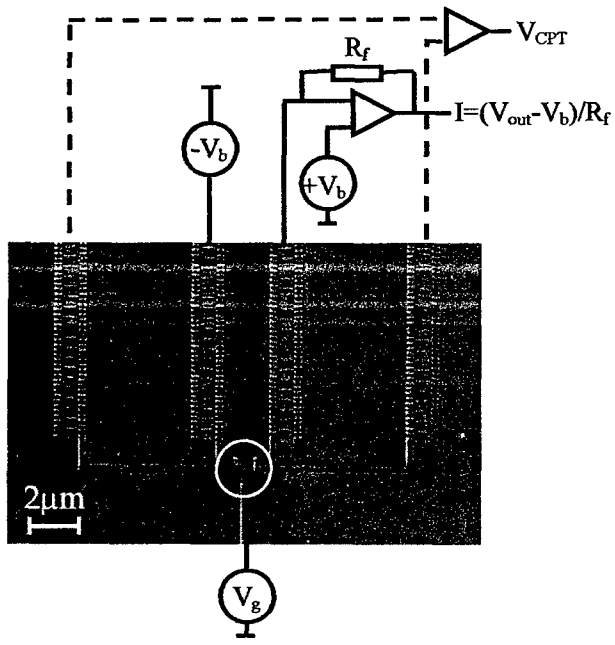

Figure 2

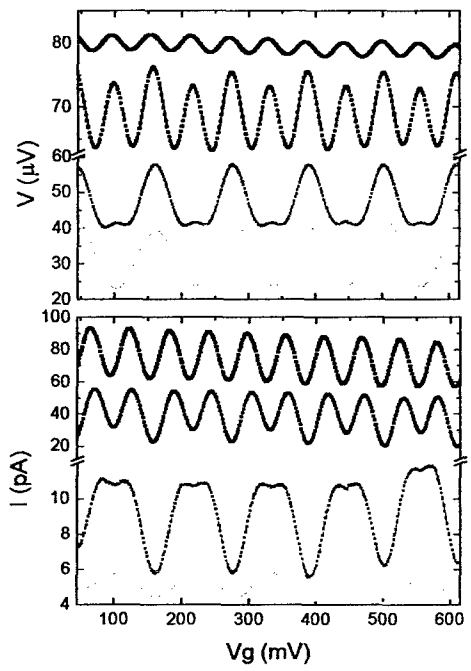

Fig 1: A SEM micrograph of the CPT biased by 4 SQUID arrays and measurement scheme.

Fig 2: Voltage and current modulation as function of Vg for different Re[Z(ω)]. From top to bottom: 55 kΩ, 450 kΩ, 10 MΩ, 20 MΩ. For this CPT $E_J/E_{C\Sigma}=0.62$.

[1] K.K. Likharev and A.B. Zorin, *J. Low. Temp. Phys. 59*, 347 (1985)

[2] L.S. Kuzmin, Yu. V. Nazarov, D.B. Haviland, P. Delsing and T. Claeson, *Phys. Rev. Lett. 67*, 1161 (1991)

[3] M. Watanabe, *Phys. Rev. B 69*, 94509 (2004)

[4] P. Joyez, *Ph.D. thesis*, (University Paris 6, France, 1995)

[5] J. Aumentado, M.W. Keller, J.M. Martinis and M.H. Devoret, *Phys. Rev. Lett. 92*, 66802 (2004)

Quantum dots for single photon and photon pair technology.

R. M. Stevenson[1], R. J. Young[1,2], P. See[1], R. M. Thompson[1,2], B. E. Kardynal, I. Farrer[2], P. Atkinson[2], D. A. Ritchie[2], and A. J. Shields[1].

[1]*Toshiba Research Europe Limited,*
260 Cambridge Science Park, Milton Road, Cambridge, CB4 0WE, UK.

[2]*Cavendish Laboratory,*
University of Cambridge, Madingley Road, Cambridge, CB3 0HE, UK.

Quantum dots have emerged as a popular platform for developing single photon emitting devices, an essential component in many areas of quantum information technology. Much progress has already been made, with the separate realisation of electrically driven [1], and quite efficient [2] devices. These demonstrations rely on the unique Coulomb energy for each exciton complex. Usually the radiative decay of the neutral single exciton is spectrally filtered to output only a single photon per cycle.

Further consideration raises an interesting question; what of the other exciton complexes formed during the decay of the initially excited exciton state? The initial state is not unique, due to the probabilistic nature of carrier capture, and thus radiative decay can occur via a multi photon cascade. It is also possible that non-radiative (dark) initial exciton states can be formed when the spins of the component electron and heavy hole have the same sign. These processes clearly must have an impact on operation, and device design must embrace any advantages that exist. Thus, we present time integrated and time resolved micro-photoluminescence experiments that reveal the broader properties of single photon and multi-photon emission from InAs quantum dots.

The dots studied here are fabricated by growing a single layer of InAs at the critical thickness for island formation in a GaAs matrix, so that an areal density of less than $1\mu^{-2}$ is achieved. These dots are thought to be rather small in size, and show relatively few emission lines in the spectra, due to the lack of a confined excited exciton state. We characterise the radiative decay of the biexciton state, and show reduced jitter for single photon emission of biexciton photons, and correlation with the linear polarisation of the subsequent exciton photon. The correlation is shown to exist due to the lifting of the degeneracy of the intermediate optically active exciton level, attributed to in-plane asymmetry of the electron and hole wavefunctions. The choice of polarisation for each linearly polarised pair of photons, is shown to be a random for each emission cycle, and we discuss how this might be used to implement optical quantum key generation [3].

We also observe evidence for non-radiative processes, including scattering between optically active exciton sub-levels, and the formation of very long lived optically inactive states. The latter is inferred from the lifetimes of predominantly optically inactive mixed states [4], created by in-plane magnetic fields. This is important for single photon emitters, where dark states can block emission for whole periods, and increase jitter by subsequent excitation into higher order exciton states.

[1] Z. Yuan *et al*, *Science* 295, 102, (2002).
[2] M. Pelton *et al*, *Phys. Rev. Lett.* 89, 233602, (2002).
[3] R. M. Stevenson *et al*, *Phys. Rev. B.* 66, 081302R (2002).
[4] R. M. Stevenson *et al*, *Physica E*, 21, 381 (2004).

Phonon-induced decay of the electron spin in quantum dots

Vitaly N. Golovach, Alexander Khaetskii, and Daniel Loss

Department of Physics and Astronomy, University of Basel, Klingelbergstrasse 82, CH-4056 Basel, Switzerland

Phase coherence of spin in quantum dots is of central importance for spin-based quantum computation in the solid state [1,2]. Sufficiently long coherence times are needed for implementing quantum algorithms and error correction schemes. If the qubit is operated as a classical bit, its decay time is given by the spin relaxation time T_1, which is the time of a spin-flip process. For quantum computation, however, the spin decoherence time T_2 — the lifetime of a coherent superposition of spin up and spin down states — must be sufficiently long. In semiconductor quantum dots, the spin coherence is limited by the dot *intrinsic* degrees of freedom, such as phonons, spins of nuclei, excitations on the Fermi surface (*e.g.* in metallic gates), fluctuating impurity states nearby the dot, electromagnetic fields, etc. It is well known (and experimentally verified) that the T_1 time of spin in quantum dots is extremely long, extending up to 100 μs. The decoherence time T_2, in its turn, is limited by both spin-flip and dephasing processes, and can be much smaller than T_1, although its upper bound is $T_2 \leq 2T_1$. Knowledge of the mechanisms of spin relaxation and decoherence in quantum dots can allow one to find regimes with the least spin decay.

In our work [3], we study spin relaxation and decoherence in a GaAs quantum dot due to spin-orbit interaction. We derive an effective Hamiltonian which couples the electron spin to phonons or any other fluctuation of the dot potential. We show that the spin decoherence time T_2 is as large as the spin relaxation time T_1, under realistic conditions. For the Dresselhaus and Rashba spin-orbit couplings, we find that, in leading order, the effective magnetic field can have only fluctuations transverse to the applied magnetic field. As a result, $T_2=2T_1$ for arbitrarily large Zeeman splittings, in contrast to the naively expected case $T_2 \ll T_1$. We show that the spin decay is drastically suppressed for certain magnetic field directions and values of the Rashba coupling constant. Finally, for the spin coupling to acoustic phonons, we show that $T_2=2T_1$ for all spin-orbit mechanisms in leading order in the electron-phonon interaction.

[1] D. Loss and D.P. DiVincenzo, Phys. Rev. A **57**, 120 (1998); cond-mat/9701055.

[2] D.D. Awschalom, D. Loss, and N. Samarth, eds., *Semiconductor Spintronics and Quantum Computing* (Springer, New York, 2002).

[3] V.N. Golovach, A. Khaetskii, and D. Loss, cond-mat/0310655.

Single-shot read-out of an electron spin qubit

R. Hanson, J.M. Elzerman, L.H. Willems van Beveren, L.M.K. Vandersypen and L.P. Kouwenhoven

Kavli Institute of Nanoscience Delft and ERATO Mesoscopic Correlation Project, P.O. Box 5046, 2600 GA Delft, The Netherlands

The spin of a single electron, confined in a semiconductor quantum dot, provides a natural two-level system suitable as a qubit in a quantum computer [1]. We demonstrate here recent experimental progress towards realization of an electron-spin based quantum computer: isolation of a single electron, identification of the two-level spin system and single-shot read-out of the spin state of a single electron.

Our device, defined electrostatically in a GaAs/AlGaAs heterostructure, consists of two coupled quantum dots in close proximity to a quantum point contact (QPC). Using this QPC as a charge detector, we show that we can deplete the two dots to contain just a single electron each [2]. Even in this few-electron regime, the resonant current through the two dots in series is still measurable.

By applying an in-plane magnetic field and performing large-bias tunneling spectroscopy, we can directly measure the Zeeman splitting of the orbital ground state, thereby identifying the spin qubit two-level system [3]. Furthermore, we show that the quantum dot can be operated as an electrically tunable spin filter. The polarization of the filter is opposite for electrons tunneling to the one- and two-electron ground state, and is estimated to be very close to 100% in magnitude [4].

To use this system as a spin qubit, an essential ingredient is a read-out device, i.e. a way to measure the orientation of a single electron spin. We use the Zeeman energy difference between the two spin orientations to achieve spin-to-charge conversion; spin "up" has a low energy and is trapped on the dot, whereas spin "down" has a higher energy and can escape to the leads. By measuring the charge dynamics, using the nearby QPC with a bandwidth of ~100 kHz, we are able to perform single-shot read-out of the spin. We use this method to determine the relaxation time of the spin qubit, and find $T_1 = 0.85$ ms for an in-plane magnetic field of 8 T.

[1] D. Loss and D.P. DiVincenzo, *Phys. Rev. A 57*, 120 (1998); L.M.K. Vandersypen *et al.*, in *Quantum Computing and Quantum Bits in Mesoscopic Systems* (Kluwer Academic, New York, 2003), *quant-ph/0207059.*

[2] J.M. Elzerman *et al.*, Phys. Rev. B. **67**, 161308(R) (2003).

[3] R. Hanson *et al.*, Phys. Rev. Lett. **91**, 196802 (2003).

[4] R. Hanson *et al.*, cond-mat/ 0311414.

ELECTRONIC CORRELATIONS IN TRANSPORT THROUGH MOLECULES

B. R. Bułka[1], T. Kostyrko[2], P. Stefański[1], W. Babiaczyk[1], S. Lipiński[2]

[1]*Institute of Molecular Physics, Polish Academy of Sciences, 60-179 Poznań, ul. M. Smoluchowskiego 17, Poland*

[2]*Institute of Physics, A. Mickiewicz University, 61-6146 Poznań, ul. Umultowska 85, Poland*

Research of low dimensional organic conductors, polymers and magnetic metallic nanostructures has a long tradition in our institute. We also perform theoretical studies of such systems. Recently our interests are focused on electronic transport through nanostructures and single molecules. In these systems electronic correlations and interference processes play an important role, leading in some cases to the Kondo and the Fano resonance. Magnetic systems are every promising for their potential applications in electronics. Interplay between the charge and the spin degree of freedom is a relevant aspect in our research. These problems will be presented for the coherent transport through simple models of molecules (for a single atom, a two-atomic molecule and a carbon nanotube). Magnetoresistance is an important quantity for operating magnetoelectronics devices, therefore its features will be presented in detail. The magnetoresistance is positive for uncorrelated electron transport; however, correlations can influence the magnetoresistance changing its value and even its sign. The problem of correlations and many-body effects will be also discussed for strong non-equilibrium electronic transport through molecules.

Macroscopic Quantum Superposition States, Squeezing and Entanglement in SQUID Rings

M.J. Everitt, T.D. Clark and P.B. Stiffell
Centre for Physical Eectronics and Quantum technology, School of Science and Technology, University of Sussex, Brighton, Sussex BN1 9QT, U.K.

J.F. Ralph
Department of Electrical and Electronic Engineering, University of Liverpool, Brownlow Hill, Liverpool, L69 3GJ, U.K.

A. Vourdas
Department of Computing
University of Bradford, West Yorkshire BD7 1DP, U.K

In this paper we consider the behaviour of a quantum regime SQUID ring (here, one Josephson weak link enclosed by a thick superconducting ring) from the viewpoint of generating superpositions of macroscopically distinct states and in the squeezing of coherent states [1,2]. We show that because of the Josephson coupling term in the SQUID ring Hamiltonian both are possible. On this basis we consider that the SQUID ring constitutes a strong contender for application in future quantum circuit technologies. In order to make our calculations correspond to a more realistic situation we also consider the effect on the SQUID ring of a dissipative (decohering) external environment, taking the standard open systems approach commonly used in the field of Quantum Optics. We show that even with such a decohering environment in place it is still possible to utilise SQUID ring for creating superpositions and squeezing provided the dissipation is not too great.
As another example of applying the techniques familiar to the field of quantum optics, we consider the problem of entangling a SQUID ring coupled inductively to an electromagnetic field oscillator mode. We demonstrate by solving the time dependent Schrödinger equation that we can create a state of maximal entanglement between them. We show that this state can be generated and controlled through the application of a time dependent external magnetic flux bias applied to the ring. When this flux is adiabatically ramped through an avoided crossing we are able to create a reasonably good approximation to a maximally entangled state. However, we find that this state of entanglement can be enhanced considerably by using a non-adiabatic flux pulse. We extend these calculations to include the effects of dissipative environments coupled to the SQUID ring. We demonstrate that even including such decohering environments it is possible to maintain a sufficient degree of entanglement over time scales that would be required for quantum technologies.

[1] J. R. Friedman, V. Patel, W. Chen, S. K. Tolpygo, and J. E. Lukens, Nature (London) **406**, 43 (2000).
[2] M. J. Everitt, T. D. Clark, P. B. Stiffell, A. Vourdas, J. F. Ralph, R. J. Prance, and H. Prance, "Superconducting analogs of quantum optical phenomena: Macroscopic quantum superpositions and squeezing in a superconducting quantum-interference device ring", Phys. Rev. A Scheduled Issue **69**(4) (1 Apr 2004).

Frequency Down Conversion and Entanglement between Electromagnetic Field Modes via a Mesoscopic SQUID Ring

P.B. Stiffell, M.J. Everitt and T.D. Clark
Centre for Physical Electronics and Quantum technology,
School of Science and Technology, University of Sussex, Brighton,
Sussex BN1 9QT, U.K.

J.F. Ralph
Department of Electrical and Electronics Engineering,
University of Liverpool, Brownlow Hill, Liverpool L69 3GJ, U.K.

A. Vourdas
Department of Computing
University of Bradford, West Yorkshire BD7 1DP, U.K

In this work, and by analogy with Quantum Optics, we discuss the highly non-perturbative properties of SQUID rings (here, a Josephson weak link enclosed by a thick superconducting ring) in the quantum regime. In particular, we investigate the possibility of frequency down conversion, via a quantum mechanical SQUID ring, between quantised electromagnetic field oscillator modes. We show that because of these non-perturbative properties (essentially due to the cosinusoidal Josephson coupling term in the SQUID ring potential) that multi-photon down conversion can take place between an input photon and output photons at sub-integers of the input frequency. In addition, these output photons are created in an entangled state with the degree of entanglement adjustable through the static magnetic flux applied to the SQUID ring. Given that it appears from these calculations that the number of output photon states can be large, we consider the application of such entangled photons in quantum technologies.

Photon-induced entanglement of quantum currents in distant mesoscopic SQUID rings

A. Vourdas, D.I. Tsomokos, C.C. Chong.

Department of Computing, School of Informatics, University of Bradford, Bradford, BD7 1DP, England.

SQUID rings irradiated with nonclassical electromagnetic fields, are studied. The Josephson current is, in this case, a quantum mechanical operator, whose expectation value with respect to the density matrix describing the external electromagnetic field yields the experimentally observed current.

Two mesoscopic SQUID rings A and B, which are far from each other, are considered. A source of two-mode nonclassical microwaves irradiates the two rings with correlated photons. Classically correlated (separable) and quantum mechanically correlated (entangled) microwaves are considered, and their effect on the Josephson currents is quantified, using the external field approximation. Results for different examples that involve microwaves in number states and coherent states are derived. It is shown that the quantum currents and the quantum statistics of the electron pairs tunneling through the distant Josephson junctions in the two rings are correlated.

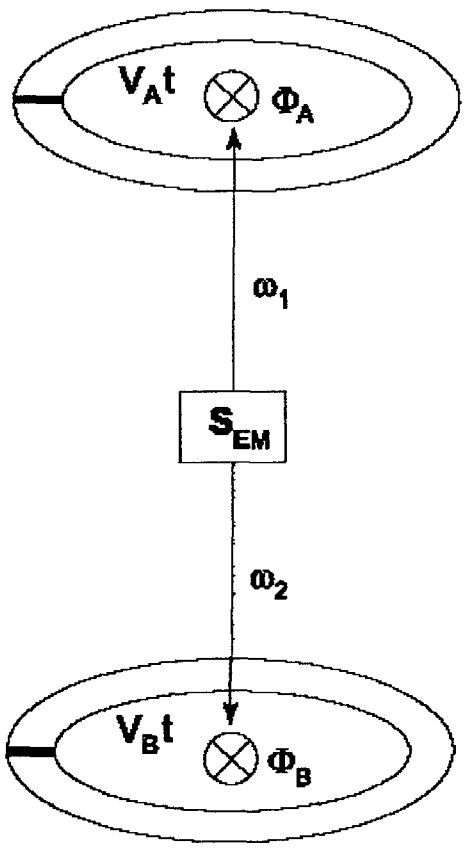

Time evolution of two distant SQUID rings irradiated with entangled electromagnetic fields

A. Konstadopoulou[1], R. Migliore[2], Z.Ahmad Zukarnain[1], A. Messina[2], A. Vourdas[1].

[1] *Department of Computing, University of Bradford, Bradford BD7 1DP UK.*

[2] *Dipartmento di Scienze Fisiche ed Astronomiche, via Archirafi 36, Palermo 90123, Italy.*

A system comprising of two squid rings irradiated with entangled electromagnetic fields is considered. The Hamiltonian describing the system is:

$$H=\frac{\Delta}{2}\sigma_Z^A+\frac{\Delta}{2}\sigma_Z^B+\omega_1(\alpha_1^+\alpha_1+\frac{1}{2})+\omega_2(\alpha_2^+\alpha_2+\frac{1}{2})+\lambda_A\sigma_x^A(\alpha_1+\alpha_1^+)+\lambda_B\sigma_x^B(\alpha_2+\alpha_2^+)$$

The time evolution of this system is studied numerically. Both separable and entangled electromagnetic fields are considered and their effects on the currents is calculated. It is shown that the currents in the two Squid rings are correlated.

Application of The Impedance Measurement Technique for Investigation of Quantum Properties of Superconducting Structures.

E. Il'ichev[1], A.Yu. Smirnov[2] M. Grajcar[3] A. Izmalkov[1], 4 D. Born[1], Th. Wagner[1], W. Krech[4], H.-G. Meyer[1], and A. Zagoskin[2].

[1]*Institute for Physical High Technology, P.O. Box 100239, D-07702 Jena, Germany*
[2]*D-Wave Systems Inc., 320-1985 W. Broadway, Vancouver, B.C., V6J 4Y3, Canada*
[3]*Department of Solid State Physics, Comenius University, SK-84248 Bratislava, Slovakia*
[4]*Friedrich Schiller University, Institute of Solid State Physics, D-07743 Jena, Germany*

We implement the impedance measurement technique (IMT) for characterization of interferometer-type superconducting qubits. In the framework of this method, the interferometer loop is inductively coupled to a superconducting high-quality tank circuit. Conclusive information about qubits is obtained from the read-out of the tank properties. We show that the IMT is a powerful tool to study quantum properties of superconducting structures.

Reentrant behavior associated with the Berezinskii Kosterlitz Thouless transition in Josephson junction arrays and the role of dissipation.

L. Capriotti,[1] A. Cuccoli, [2,3] A. Fubini, [2,3] V. Tognetti, [2,3] and R. Vaia[4,3]

[1]*Kavli Institute for Theoretical Physics, University of California, Santa Barbara, CA 93106, USA*
[2]*Dipartimento di Fisica dell'Università di Firenze - via G. Sansone 1, I-50019 Sesto Fiorentino (FI), Italy*
[3]*Istituto Nazionale per la Fisica della Materia - U.d.R. Firenze - via G. Sansone 1,I-50019 Sesto Fiorentino (FI), Italy*
[4]*Istituto di Fisica Applicata 'Nello Carrara' del Consiglio Nazionale delle Ricerche, via Madonna del Piano, I-50019 Sesto Fiorentino (FI), Italy*

The phase diagram of a 2D Josephson junction array with large substrate resistance, described by a quantum XY model, is studied by means of Fourier path-integral Monte Carlo. A genuine Berezinskii-Kosterlitz-Thouless transition is found up to a threshold value g* of the quantum coupling, beyond which no phase coherence is established. Slightly below g* the phase stiffness shows a reentrant behavior with temperature, in connection with a low-temperature disappearance of the superconducting phase, driven by strong nonlinear quantum fluctuations. The presence of dissipation, due to the shunt resistences, reduces the region where this reentrance appears. However it is persisting for significant dissipations and eventually vanishes for the decreasing of the shunt resistences when the quantum fluctuations are strongly reduced by the dissipation, ects.

Persistent currents in a superconductor/normal loop

M. D. Kim and J. Hong
School of Physics, Seoul National University, Seoul 151-742, Korea

We study the persistent currents of normal/superconducting loop modulated by the phase shift, η, of electron wave functions due to the Andreev reflection process at the boundaries. When the energy splitting E is smaller than the pair potential Δ, the persistent currents show the periodicity of the superconducting unit flux quantum, $\Phi_0/2$, regardless of the length of the normal and the superconducting sector, while it is so only in the limiting case of thin normal segment in previous studies. In the limit $E << \Delta$, the persistent currents take the Josephson type formula, $I \propto \sqrt{\Delta}\sin(\pi/2 - 2\eta)$.

Quantum Order in Josephson Junction Arrays

G. Cristofano[1], V. Marotta[1], A. Naddeo[2], P. Sodano[3]

[1]*Dipartimento di Scienze Fisiche, Università di Napoli "Federico II" and INFN, Sezione di Napoli, Via Cinthia - C. U. Monte S. Angelo – 80126 Napoli, Italy*
[2]*Dipartimento di Scienze Fisiche, Università di Napoli "Federico II" and Coherentia - INFM, Unità di Napoli, Via Cinthia - C. U. Monte S. Angelo – 80126 Napoli, Italy*
[3]*Dipartimento di Fisica, Università di Perugia and INFN, Sezione di Perugia, Via A. Pascoli – 06123 Perugia, Italy*

Quantum order is a desirable property of Josephson junction networks since it may allow for their use as devices for quantum computation. There have been by now several proposals [1]. In this contribution we show that fully frustrated Josephson networks may support quantum order [2]. In order to meet such a request we analyze the fully frustrated XY (FFXY) model on a square lattice with $U(1)\otimes Z_2$ symmetry [3] within a twisted conformal field theory (CFT) framework [4]. In particular we show that its ground state is degenerate, the different states being accessible by adiabatic flux change techniques. Such a degeneracy is shown to be strictly related to the presence in the spectrum of quasiparticles with non abelian statistics and can be lifted non perturbatively through vortices tunneling, so giving rise to a highly entangled state.

[1] L. B. Ioffe, V. B. Geshkenbein, M. V. Feigelman, A. L. Fauchère and G. Blatter, *Nature 398*, 679 (1999); G. Blatter, V. B. Geshkenbein and L. B. Ioffe, *Phys. Rev. B 63*, 174511 (2001); L. B. Ioffe and M. V. Feigelman, *Phys. Rev. B 66*, 224503 (2002); B. Doucot, M. V. Feigelman and L. B. Ioffe, *Phys. Rev. Lett. 90*, 100501 (2003).
[2] G. Cristofano, V. Marotta, A. Naddeo and P. Sodano, submitted to *Phys. Rev. Lett.*.
[3] O. Foda, *Nucl. Phys. B 300*, 611 (1988).
[4] G. Cristofano, V. Marotta, A. Naddeo and P. Sodano, Napoli DSF-T-04/2004, INFN-NA-04/2004 preprint.

Distilling Angular Momentum Schrödinger Cats in Trapped Ions

B. Militello, and A. Messina

INFM, MIUR and Dipartimento di Scienze Fisiche ed Astronomiche dell'Università di Palermo,
Via Archirafi, 36, I-90123 Palermo. Italy

A quantum system (S) in interaction with a repeatedly measured one (M) undergoes a non-unitary time evolution pushing it into some specific subspaces. It is assumed that the measured system is found in the initial state at each step, and that both the M-S interaction and its duration between two measurement acts are the same during all the process. Such three ingredients (measured state, interaction, interaction duration) give raise to a "selection rule" determining what states of S decay (the "residual" states) and what states are decay-preserved (the "distilled" states).

On the basis of this strategy, we report a method for distilling the vibrational state of a trapped ion centre of mass in order to obtain angular momentum eigenstates and angular momentum Schrödinger cat superpositions.

Dynamics of single-electron charge and spin in semiconductor quantum dots

Toshimasa Fujisawa[a,b)]

[a]*NTT Basic Research Laboratories, NTT Corporation,*
3-1 Morinosato-Wakamiya, Atsugi, 243-0198, Japan.
[b]*Tokyo Institute of Technology.*

The quantum dynamics in solid-state nanostructures has attracted much attention for building blocks of quantum computing. We present some recent results on coherency, dissipation and dephasing of charge and spin degrees of freedom in semiconductor quantum dots.

First, we discuss coherency of charge states in a double quantum dot. Consider a two-level system consisting of two charge state, in which an excess electron occupies an energy state in one or the other dot. When these two states are coupled by a tunneling barrier, one can induce coherent charge oscillations by means of non-adiabatic excitation with a high-speed voltage pulse. We have successfully observed clear coherent charge oscillations. The charge qubit can be manipulated arbitrarily by tailoring the pulse waveform. The experiments indicate the potential application for quantum information processing.

Second, we discuss about dissipation of spin degree of freedom in a quantum dot. Electron spin in quantum dots is expected to have a long decoherence time. We investigate the energy relaxation time from an excited state to the ground state in one- and two-electron quantum dots. We find that the relaxation time from spin-triplet state to spin-singlet state in a two-electron quantum dot can be longer than hundreds of microseconds. The long spin relaxation time is advantageous for spin based information storage.

Control of nuclear spins by quantum Hall edge channels

S. Komiyama and T.Machida[a, +]

Department of Basic Science, University of Tokyo, 3-8-1 Komaba, Meguro-ku, Tokyo, Japan

[a] PRESTO, Japan Science and Technology Corporation (JST), 3-8-1Komaba, Meguro-ku, Tokyo, Japan

Extremely weak interaction of nuclear spins to their environments yields, on one hand, their exceedingly long de-coherence time, but on the other hand, makes their control and detection a nontrivial task. Contriving ingenious means of controlling/detecting nuclear spins is thus an important experimental challenge for exploring the implementation of spintronics, quantum information processing or quantum computation in solid state devices. We show here that spin-split edge channels in the integer quantum Hall effect (IQHE) devices provide a unique tool to (i) polarize, (ii) unitary-transform, and (iii) detect nuclear spins. The number of manipulated nuclear spins is small, on the order of 10^9.

The one-electron energy of a finite two-dimensional electron gas (2DEG) system is quantized into discrete Landau levels (LLs) in strong magnetic fields, where each orbital LL is spin split into spin-up and spin-down Zeeman sub-levels. Due to confining potential, the LLs increase their energies as a boundary of the 2DEG layer is approached and form respective edge channels along the boundary at the Fermi level. By selectively transmitting different edge channels by means of cross-gate biasing technique, one can unequally populate the spin-up edge channel and the spin-down edge channel of the lowest orbital LL in a GaAs/AlGaAs Hall bar device in the ν=2 IQHE regime. Over-populated edge channel (either with spin-up or spin-down) can be chosen by the polarity of the source-drain voltage applied to the device. When the up-spin channel is over populated, for instance, spin-up electrons undergo spin-flip transition to empty states of the spin-down edge channel. Due to the hyperfine interaction [1] this process is accompanied by the down-to-up spin-flop transition in the nuclear spin system, leading to the development of strong dynamic nuclear polarization (DNP) in the region only along the edge channels. The DNP, in turn, induces an effective magnetic field for the electron spin system, again, via the hyperfine interaction. This leads to a change of the resistance of the device, through which the DNP is sensitively detected. By passing radio-frequency (rf) currents through a fine metal strip placed near the edge channels locally generate rf-magnetic fields in the region of DNP. Nuclear magnetic resonance (NMR) as well as the Rabi oscillation of initialized nuclear spins are electrically detected

(through the resistance) [2,3]. Free-induction decay as well as the spin-echo experiments have been made, suggesting T_2 = 80 μs. In addition, by externally modifying the confining potential via side-gate-biasing technique, the edge channels are shifted side-wise over a 120nm distance, thereby locally probing the spatial profile of the DNP. DNP proved to spread roughly over a 20 nm-wide region (twice the magnetic length). The number of manipulated nuclear spins is suggested to be on the order of 10^9. The spin-split edge channels are thus a powerful tool to (i) efficiently initialize, (ii) unitary-transform, and (iii) sensitively detect nuclear spins.

The work is supported in part by Precursory Research for Embryonic Science and Technology (PRESTO) of Japan Science and Technology Corporation (JST), and by Grant-in-Aid for Specially Promoted Research from the Japan Ministry of Education, Culture, Sports, Science and Technology.

[+]Present address: *Institute of Industrial Science, Ce308, University of Tokyo, 4-6-1 Komaba, Meguro-ku, Tokyo, Japan*

[1] B.E.Kane, L.N.Pfeiffer, and K.W.West, Phys. Rev. B 46 (1992) 7264.

[2] T.Machida, T.Yamazaki, and S. Komiyama, Appl. Phys. Lett. 80 (2002) 4178.

[3] T. Machida, T. Yamazaki, K. Ikushima, and S. Komiyama, Appl. Phys. Lett. 82 (2003) 409.

NMR-like control of a quantum bit superconducting circuit

E. Collin, G. Ithier, P. Joyez, D. Vion, and D. Esteve

CEA-SACLAY, Orme des merisiers, 91191 Gif sur Yvette Cedex, France.
** E-mail: vion@drecam.saclay.cea.fr*

The Quantronium [1] is a superconducting quantum bit circuit (Fig. 1) based on small Josephson junctions in which decoupling from the external circuit ensures a long coherence time. The state of the qubit is manipulated using resonant microwave pulses, or adiabatic pulses on the control parameters of the circuit Hamiltonian. We demonstrate here that NMR methods can be efficiently used for manipulating the qubit and probing decoherence mechanisms [2].

First, we have shown that arbitrary transformations can be implemented by combining microwave pulses. Two pulse sequences with different phases, that implement rotations around orthogonal axes, have been performed. The overall agreement with theory shows that rotations combine as expected (Fig; 2). We have addressed the issue of transformation robustness using the composite pulses developed in NMR. We have shown in particular that the CORPSE sequence efficiently compensates for of resonance effects.

In order to investigate decoherence mechanisms acting in the quantronium, we have developed new methods to probe quantum coherence. In particular, we have used two pulse experiments with a temporary change of the working point during the time delay between the two pulses, and implemented echo experiments (see Fig 3).

We have also measured decoherence during driven evolution in presence of microwaves. We have measured the decay of Rabi oscillations, and of the spin-locking polarisation following the usual spin-locking protocol in NMR (see Fig 3). We find that the decay time of Rabi oscillations and of the spin-locking polarisation can be longer than during free evolution coherence time.

These driven regime and spin echo experiments rise the question of increasing the effective coherence time; which is a central issue for qubits.

[1] D. Vion et al., Science 296 (2002).
[2] E. Collin et al., cond-mat/0404503

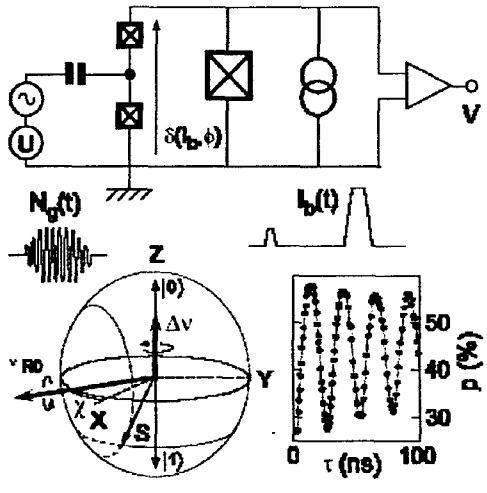

Fig 1: top: circuit diagram of the quantronium. The Hamiltonian is controlled by two parameters: the charge coupled to the box island between the two small junctions, and the phase across their series combination. The qubit state is manipulated by applying resonant microwave pulses, or adiabatic pulses on the control parameters. The oscillations of the switching probability of the readout junction reveal the Rabi oscillations of the qubit state.

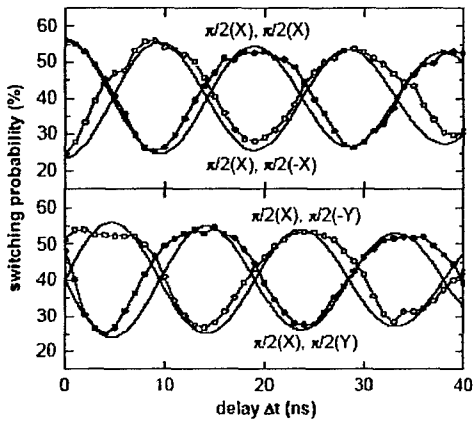

Fig.2: Switching probability after two $\pi/2$ pulses with different phases, corresponding to different rotation axes. The Ramsey patterns are shifted as predicted for each phase combination. This experiment proves that rotations can be combined in order to implement any qubit transformation.

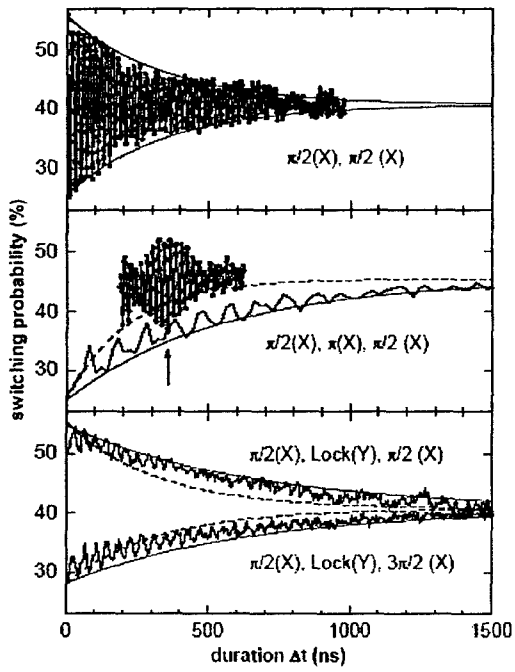

Fig. 3: Top : switching probability (dots) after a Ramsey $\{\pi/2(X), \pi/2(X)\}$ sequence as a function of the time delay between pulses. Fits of the envelope (time constant 350 ns). Middle: example of echo measured in a $\{\pi/2(X), \pi(X), \pi/2(X)\}$ sequence. Thin line: echo signal at the nominal minimum position. bold line: exponential fit of the envelope (550 ns time constant). dashed line: fit of the lower envelope of the Ramsey pattern measured in the same conditions (220 ns time constant). Bottom: switching probability after two spin-locking sequences, as a function of the sequence duration. Thick lines: exponential fits of the envelopes, with time constant 650 ns. The dashed lines show a fit of the envelope of the Ramsey pattern measured in the same conditions (time constant : 320 ns).

Analysis of decoherence in a quantum bit superconducting circuit

E. Collin, G. Ithier, P. Joyez, D. Vion*, and D. Esteve.

CEA-SACLAY, Orme des merisiers, 91191 Gif sur Yvette Cedex, France.
** E-mail: vion@drecam.saclay.cea.fr*

The Quantronium [1] is a superconducting Josephson quantum bit (Fig. 1) whose quantum state can be arbitrarily transformed by combining quasi-resonant microwave pulses and adiabatic pulses [2] on two control parameters of the circuit Hamiltonian: an electric charge N_g and a phase δ.

The coherence time T_2 of this qubit during its free evolution was measured by several different pulse sequences, and at different working points (Fig. 2) where the dominant contribution to decoherence is the external charge or phase noise at first or second order. The coherence time during driven evolution was also measured as a function of the detuning between the microwave frequency and the qubit frequency (Fig. 3). All these data are analyzed using a generalized Bloch-Redfield model.

[1] D. Vion et al., Science 296 (2002).
[2] E. Collin et al., cond-mat/0404503.

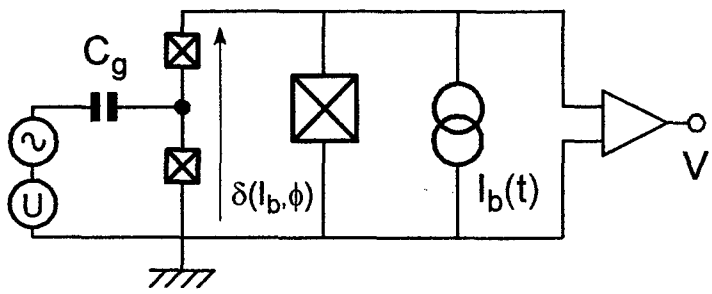

Fig 1: Circuit diagram of a qubit prototype: the quantronium. The qubit state is manipulated by applying quasi-resonant microwave pulses on $N_g=CgU/(2e)$, and adiabatic pulses on N_g or I_b. The state is read out by pulsing I_b to the critical current of the large Josephson junction.

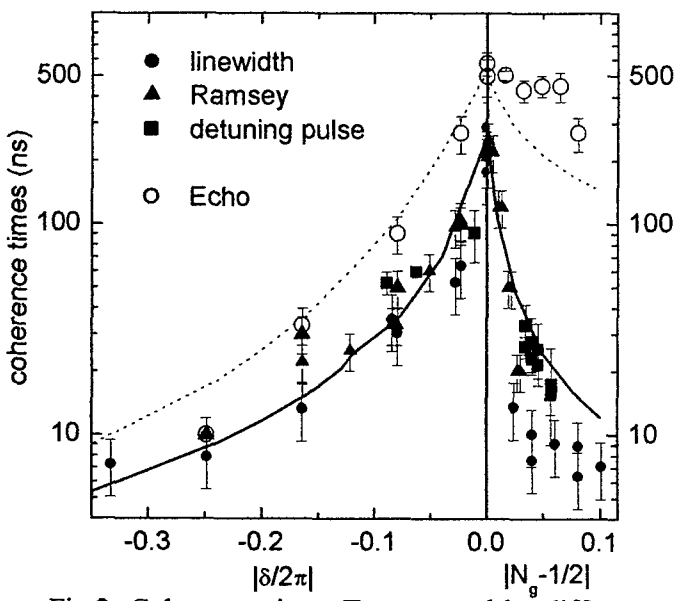

Fig.2: Coherence times T_2 measured by different techniques as a function of the phase or charge shift from the optimal working point (δ =0 ; N_g=1/2). Lines correspond to the model.

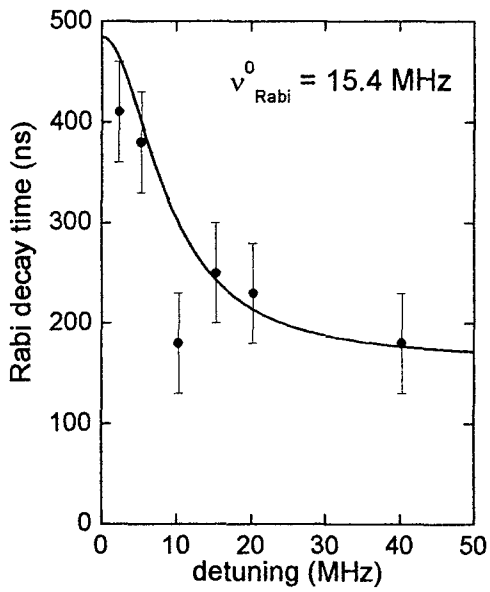

Fig.3: Coherence times during microwave driven Rabi oscillations as a function of the detuning. Line corresponds to the model.

Improvements to Josephson Phase Qubits

R. W. Simmonds, K. B. Cooper*, D. A. Hite, R. McDermott*, S. Nam, M. Steffen*, D. P. Pappas, J. M. Martinis*

National Institute of Standards and Technology, Division 817, 325 Broadway st. Boulder, CO 80305 USA
**Department of Physics, Broida Hall, Building 572, University of California, Santa Barbara, CA USA 93106-9530*

Although Josephson junction quantum bits show great promise for quantum computing, the origin of dominant decoherence mechanisms remains unknown. All superconducting qubit experiments thus far have shown relatively low (coherence) amplitude and short relaxation times (for Rabi oscillations). Recently, we have improved the operation of a Josephson Junction based "phase" qubit by incorporating it into a superconducting loop. This has allowed us to further decouple the qubit from its environment and has eliminated quasiparticle heating effects. A new detection scheme based on an asymmetric d.c. SQUID allows detection of the quantum states with high efficiency and a controllable back action. This new device has revealed previously unknown two state microwave resonators within the qubit Josephson junction itself.[1] It seems likely that all Josephson junction based qubits are suffering from these material defects as well. Although two-level systems are known to exist in amorphous materials[2], these individual two-level microwave resonators within Josephson tunnel barriers have remained hidden for over forty years. As major sources of decoherence, they play a vital role in understanding the full effective Hamiltonian of Josephson tunnel junctions.

At certain bias points, strong coupling to these resonators destroys the coherence of the qubit. Although previous reports have focused on the characteristic decay time of coherent oscillations, our data demonstrates that decoherence from these spurious resonators primarily affects the amplitude of the oscillations. We have constructed a model for the microscopic resonators, where we consider two-level states in the barrier with large tunneling matrix elements corresponding to a microwave frequency. These two level systems couple to the qubit by producing critical current fluctuations in the tunnel barrier. If we assume that the two states of the resonator correspond to ON and OFF configurations of individual conduction channels in the tunnel barrier, then their strength can be estimated from the current-voltage characteristics of the junction. Essentially, low subgap currents indicate weaker resonators and improved qubit performance. This suggests that the quality of the Josephson junction determines the density and size of these resonators and therefore the quality of the qubit.

State-of-the-art Josephson junctions employing superconducting (Al or Nb) electrodes and native oxide tunnel barriers typically are fabricated using sputter deposition onto thermally oxidized Si wafers for microelectronics fabrication. For most applications, such as SQUID technologies, there has never been a necessity to further improve the crystalline quality of the junctions to correspondingly improve the device performance. We believe that these spurious resonators originate from bulk or interface defects and inhomogeneous or non-uniform oxidation during tunnel barrier formation. In this work, we detail recent efforts to engineer Josephson junctions with increasingly improved

crystalline quality and smoother interfaces, and to correlate the microstructure of the junctions with low frequency transport measurements and quantum measurements of phase qubits. Our data, thus far, indicates a strong correlation between improved "smoothness" of the superconductor-insulator interface and junction performance. By creating tunnel junctions from sputtered trilayers, as opposed to a two-step "ion-milled" process, we have reduced the size of subgap currents and have shown improved coherence of fabricated phase qubits.

We will discuss the details of samples grown using two techniques, sputtered trilayers and evaporated trilayers. Sputtered trilayers are a simple to fabricate and are currently the preferred method for qubit fabrication. The evaporated trilayers, on the other hand, are grown using a truly unique method, and while in its preliminary stages, this growth technique may someday replace sputtered trilayers for qubit applications. In order to prepare the evaporated trilayers, we have grown tunnel junctions using an atomically flat metallic seed layer of Al on Si(111)-(7 × 7) substrates. The seed layers were deposited at 120 K and subsequently annealed at 425 K to achieve ultra smooth, epitaxial films. The Josephson trilayer was completed through the homoepitaxy of Al deposited on the seed layer at room temperature, oxidized in a conventional manner and then capped with the Al counterelectrode *in situ* under ultra high vacuum conditions. These evaporated trilayers were fabricated into tunnel junction devices of various diameters and transport measurements were made at ~ 30 mK. *I-V* characteristics for samples with various degrees of crystalline quality have been compared, and we conclude that there is a strong correlation between the morphology of oxidized base electrodes that are smooth and the lowering of subgap currents. This is an important step in addressing the origin of spurious resonators ubiquitously found in our Josephson phase qubits.

In order to eliminate the effect of these resonances completely, further materials research is being investigated. We have made more epitaxial trilayers, added impurities to the superconducting leads, as well as used various oxidation methods. We will present our preliminary results. Furthermore, simple changes have been made in order to investigate the ways in which these resonators can influence junction performance. We have changed the area of the qubit junction, the inductance of the superconducting loop, and the mutual inductance to its bias coil. We have confirmed that a reduction in area does reduce the number of resonators within the frequency range of operation, but each resonator has an increased strength. We have measured the distribution of these resonators in terms of their strength and their number density over the measurable frequency range. This data helps to further characterize junction quality. We have also developed a mathematical model of these resonators which agrees well with experimental data. This model provides insight both into the possible physical origins of the resonances, as well as into refocusing schemes to eliminate their effects on the qubit.

[1] R. W. Simmonds, K. M. Lang, D. A. Hite, D. P. Pappas, and John M. Martinis, *cond-mat/0402470* (2004)

[2] W. A. Phillips, *Rep. Prog. Phys.*50, 1657 (1987)

Non-hysteretic positioner for nano-lithography and cryogenic *in situ* adjustable nano-junctions

Benjamin Thomsen and Jesper Mygind*, Department of Physics, B309, Technical University of Denmark, DK-2800 Kongens Lyngby, Denmark.
*email: myg@fysik.dtu.dk

Here we describe a novel motor, which is capable of non-hysteretic (reversible) positioning of a sample in three orthogonal directions (x, y, and z) with nanometer resolution both at room temperature and at cryogenic temperatures. The motor can translate the sample ± 1.5mm in the x-y plane and ± 2mm in the z-direction and within this range park the sample at any position in firm contact with the motor body (zero voltage on the piezo stacks).

The motor is integrated with a small specially designed head, which except for modifications necessary for cryogenic operation assembles a standard insert for Scanning Probe Microscopy (SPM). The SPM head faces the sample stage and consists of a conventional piezoelectric x-y-z tube scanner carrying either an STM tip (STM-head) or an AFM cantilever (AFM-head). With the sample parked in fixed position by the x-y-z motor the SPM head allows for fine positioning and scanning with atomic precision. A new millikelvin AFM head is under construction. It utilizes single mode glass fibers both for supplying the laser beam focused onto the cantilever, and for transmitting the reflected beam back to the room temperature detection system.

The x-y translation of the sample is facilitated by two sets (A and B) of piezo stacks ("legs") glued onto a thick brass plate. The legs are placed evenly (60 degrees) in a circle with diameter approx. 20mm (see Fig. 1). Each leg consists of three 5mm by 5mm piezo stacks ("legs"), each with four x-shear plates glued in series with four y-shear plates and a multilayer z-stack. On top and bottom of each leg is glued a 5mm by 5mm Al2O3 plate. After gluing the six legs are optically polished to obtain same length. The operational relies on the well known louse principle, modifyed to a 6 leg configuration, where in every step 3 legs are lifted fully free from the polished quartz or sapphire surface before they are jointly moved to the new position. The z translation utilizes a similar working principle that enables a linear motion.

The motor can be used as a coarse positioning device, which with a (large) number of (up to a) micrometer long x-y-z steps rapidly brings the selected region of the sample in first contact with the probe tip in the SPM head. Contact is registered as either the first small tunnel current in the STM head or the small change in the deflection of the laser beam focused on the cantilever in the AFM head. Maintaining the contact the motor then parks the sample with zero voltage on the motor piezos. Here the galvanic contacts to the wires leading to the motor piezos may be disconnected, so that the electrical noise from the high-tension amplifiers cannot induce mechanical disturbances in the sample position. After having parked the sample x-y-z scanner tube unit regulates the position of the STM tip or AFM cantilever. Actually, one may use very small x-y-z steps in the motor to adjust the tip-sample distance so that also

the off-set voltages applied to the tube scanner are near zero. Recent experimental results will be reported on.

Presently we are investigating the creep of the motor piezos and the tube scanner at low temperatures. For the non-scanning applications eg. nano-lithography and nano-junction fabrication it is necessary to have a linear dependence of the tip position on the piezo voltage. However, noise in the "feed back" optical loop used is estimated to induce a 1-10 nanometer fluctuation in the spatial resolution. In many cases this limits the accuracy and for better precision one has to "live with" the creep in the piezos. The optical servo system will be briefly described.

Together the motor and the SPM head form an instrument, which enables atomic resolution both in the scanning modes and at fixed positions. This allows for a wide spectrum of applications, such as nano-lithography and studies involving *in situ* adjustable junctions. A particular advantage of cryogenic operation is that thermal fluctuations in the piezo-electrical materials are very small. The disadvantage is that the piezo-electrical constants at e.g. 4.2K are reduced to about 20% of the room temperature values. The motor mounted with an SPM head is very compact and fits into the 34mm diameter bore of a standard (Oxford) millikelvin 3He/4He cooler placed in the center of a 10 tesla superconducting magnet.

The motor and the SPM head are jointly run by a computer (with an A/D interface input/output card) in conjunction with a standard SPM controller (Veeco, Digital Instruments). Depending on the controller and the software one may utilize all the standard modes of operation, eg. tapping mode.